Plastoglobules - a new destination for recombinant proteins produced in transplastomic plants and characterization of plastidial At-SOUL heme binding protein

A dissertation submitted to the
UNIVERSITY OF NEUCHATEL
For the degree of
Doctor of Natural Sciences

presented by

Shanmugabalaji VENKATASALAM

Laboratory of Plant Physiology, Institute of Biology
University of Neuchâtel

Thesis committee

Prof. Felix Kessler, Thesis director
Prof. Jean-Marc Neuhaus
Prof. Sacha Baginsky
Prof. Stefan Hörtensteiner

2012

Keywords: chloroplast, plastoglobule, plastoglobulin, plastid transformation, molecular farming, HIVp24, HCV core protein, *Nicotiana tabacum,* SOUL heme binding protein, tetrapyrrole

Université de Neuchâtel

FACULTE DES SCIENCES
Secrétariat-Décanat de la faculté
Rue Emile-Argand 11
CH-2000 Neuchâtel

IMPRIMATUR POUR LA THESE

Plastoglobules – a new destination for recombinant proteins produced in transplastomic plants and characterization of plastidial At-SOUL heme binding protein

Shanmugabalaji VENKATASALAM

UNIVERSITE DE NEUCHATEL

FACULTE DES SCIENCES

La Faculté des sciences de l'Université de Neuchâtel,
sur le rapport des membres du jury

Prof. Felix Kessler, UniNe, directeur de thèse
Prof. Jean-Marc Neuhaus, UniNe
Prof. Stefan Hörtensteiner, Université de Zürich
Prof. Sacha Baginsky, Martin-Luther Universität, Halle-Wittenberg, D

autorise l'impression de la présente thèse.

Neuchâtel, le 7 août 2012

Le doyen :
P. Kropf

Content

Contents……1

Abstract……5

Abbreviations……...7

1 Introduction……..11

1.1 Plastids are vital organelles of plants……..…...11
1.1.1 Distribution of plastids……..…11
1.1.2 Chloroplast biogenesis……..11
1.1.3 Structure and compartmentalization of chloroplast……..12
1.2 Plastoglobules – the lipoprotein particles in plastids……13
1.2.1 Plastoglobule……..…...13
1.2.2 Plastoglobulins……...14
1.2.3 Metabolic enzymes in plastoglobules……....16
1.2.4 A member of plastoglobule proteins have unknown functions……...17
1.3 Molecular farming - plastid transformation……18
1.3.1 Recombinant protein expression in plants……18
1.3.2 Recombinant fusion proteins target to plant lipid and protein bodies……18
1.3.3 Chloroplasts as bioreactors for biopharmaceuticals……....19
1.3.4 Advantages of transplastomic plants……..…19
1.3.5 The HIVp24 protein and HCV core protein as antigens……..…20
1.4 SOUL-heme binding proteins……...20
1.4.1 The significance and regulation of tetrapyrrole metabolism in plants……20
1.4.2 Heme biosynthesis in plants……23
1.4.3 Structure and biochemical chacterization of SOUL-heme binding proteins……25
1.5 Aim of the thesis……..26

2 Results……27

2.1 Plastoglobules - a new destination for recombinant proteins produced in transplastomic plants……..27

2.1.1 PGL35 (FBN1a) is highly conserved in higher plants……...27

2.1.2 Chloroplast expression constructs…….....27

2.1.3 Introduction of transgenes into the tobacco plastid genome……...29

2.1.4 RFLP and homoplasmy analysis of transplastomic plants……...29

2.1.5 Expression and accumulation of the recombinant fusion protein in transplastomic tobacco…….32

2.1.6 Over expression of the recombinant fusion proteins leads to enlargement of the plastoglobules…….....35

2.1.7 Localization of the Streptavidin-PGL35-HIVp24 fusion protein in transplastomic chloroplasts……..…….37

2.1.8 Targeting of the Streptavidin-PGL35-HIVp24 fusion proteinto Plastoglobules……..37

2.1.9 Purification of HIVp24 using streptavidin-biotin affinity chromatography followed by TEV elution……..40

2.2 Characterization of plastidial At-SOUL heme binding proteins……..…….42

2.2.1 Homologs and putative topology of At-SOUL heme binding proteins.....42

2.2.2 Localization of AtSOUL4 heme binding protein……..42

2.2.3 Heme binding to AtSOUL4 *in vitro* and *in vivo*……..……...48

2.2.4 *In-vitro* phosphorylation of AtSOUL4……...51

2.2.5 Reverse genetic study of plastid SOUL heme binding proteins……...54

2.2.6 AtSOUL4 is present both as a monomer and in very large complexes…..54

2.2.7 Lipidomics analysis of *soul4* mutant and wild type……...60

2.2.8 Involvement of the plastidic AtSOUL proteins in photomorphogenesis?...60

2.2.9 *soul5-1* mutant is hypersensitive to red and far red light……..66

3 Discussion……69

3.1 A PGL35 fusion protein targets to plastoglobules and thylakoids in transplastomic tobacco chloroplasts……69

3.1.1 Transplastomic tobacco is a suitable system to target recombinant proteins in plastoglobules and thylakoid membranes……69

3.1.2 Overexpression of PGL35 leads to enlargement of the plastoglobules.....70

3.1.3 Recombinant protein targeting to plastoglobules depends on hydrophobicity and isoelectric point……71

3.1.4 Recombinant HIVp24 purified from the fusion proteinto near homogeneity……...73

3.1.5 Future respective for improvement of the plastoglobule targeting System……....73

3.2 Unraveling the functions of plastidial SOUL heme-binding protein…….……74

3.2.1 AtSOUL4 is located in plastoglobules…….……74

3.2.2 Heme specifically binds to the AtSOUL4 heme-binding protein……...…74

3.2.3 AtSOUL4 heme binding protein is phosphorylated by CKII and stromal protein extract…….....75

3.2.4 AtSOUL4 is present in lipid droplets but not involved in lipid metabolism.75

3.2.3 Putative model for potential function of plastidial AtSOUL4 Heme binding protein……..…..…76

4 Materials and Methods……..……..79

4.1 Materials……..…79

4.1.1 Biological material…….…....79

4.1.2 Oligonucleotides……....79

4.1.3 cDNA clones…….……....80

4.1.4 Chemicals……..…..81

4.1.5 Antibodies……..……...81

4.1.6 Plasmids……..……....81

4.2 Methods…….…...…..81

4.2.1 Physiological methods…….……..…..…81

4.2.2 Cloning methods……82

4.2.3 DNA constructs……..83
4.2.4 Chloroplast isolation and in vitro import reactions……...…85
4.2.5 Generation of affinity-purified antibodies……...….86
4.2.6 Transient transformation of *N. benthiamiana* leaves by agroinfiltration.....86
4.2.7 Stable transformation of *A. thaliana* and tobacco chloroplasts……..…87
4.2.8 PCR analysis of plants…….……..87
4.2.9 Southern and Northern blot analyses……..……88
4.2.10 Western blot analysis…….……88
4.2.11 Phosphorylation Assays……..……..89
4.2.12 Heme-binding assay……..…….……89
4.2.13 Blue Native PAGE……..…..90
4.2.14 Prenyllipid analysis……..……90
4.2.15 Arabidopsis crossing……..…….……90
4.2.16 Porphyrin analysis.....……...…….……90
4.2.17 Heme Extraction……...……...……91
4.2.18 Photomorphogenic conditions……..……91
4.2.19 Gradient floatation centrifugation of chloroplast membranes……..…….…91
4.2.20 Fluorometry and chlorophyll measurement……..……..…….91
4.2.21 Electron microscopy……..……..92
4.2.22 Immunofluorescence……..……92
4.2.23 Purification of HIVp24……..……...92

REFERENCES……95

ACKNOWLEDGEMENTS……..…..115

Abstract

Plastoglobules (PG) are lipid droplets existing in most types of plastids. Plastoglobulins (PGL) also known as fibrillins (FBN) are evolutionary conserved proteins present at the surface of PG, but to various extents also at the thylakoid membrane. PGLs are thought to have a structural function in PG, and it is known that almost the complete protein is required for PGLs to assemble on PG. Here, we report on the expression of the Arabidopsis plastoglobulin of 35kD (PGL35 or FBN1a) expressed as a mature protein fused to HIVp24 in transplastomic tobacco. A PGL35-HIVp24 fusion targeted in part to plastoglobules but a larger proportion was recovered in the thylakoid fraction. These findings suggest that PGL35-HIVp24 folds correctly after its synthesis inside the chloroplast and is then assembled not only on plastoglobules but also on thylakoid membranes. The fusion protein accumulated up to a 1% of the total protein and could be purified by biotin affinity chromatography of a total membrane extract. Targeting of PGL35 fusion proteins to plastoglobules has the potential to become an interesting expression system but it will be necessary to master the parameters that govern the partioning between plastoglobules and thylakoid membranes for this to become an effective technique. This study represents a step forward in this direction.

In addition to lipids and PGLs, the PG harbours other proteins: The PG proteome in Arabidopsis consist of about two dozen proteins including uncharacterized plastoglobule protein AtSOUL4, which has a predicted heme-binding motif. The Arabidopsis genome contains six proteins with a SOUL motif; two of them AtSOUL4 and AtSOUL5 are predicted to be plastid localized and AtSOUL5 was found in the thylakoid proteome. A SOUL homolog, AtSOUL1, is highly expressed and the *soul1* mutant is hypersensitive to red light. In addition, *C. reinhardtii* eyespot phosphoproteins contained SOUL3. However, due to the presence of SOUL-heme binding proteins in light perception systems and their implication in plant photomorphogenesis, the SOUL heme binding proteins may be involved in light signalling. The heterologously expressed recombinant AtSOUL4 protein binds to heme *in vitro* as well as *in vivo*. Moreover, AtPGL35 and AtSOUL4 fluorescent fusion proteins colocalized in chloroplasts. Furthermore, immunoblot analysis of chloroplast membrane fractions shows that AtSOUL4 localized at the plastoglobule. AtSOUL4 has a highly conserved CKII phosphorylation site in C-terminal. Moreover, *In vitro* phosphorylation studies revealed that AtSOUL4 is phosphorylated most likely by a stromal CKII like kinase. The double knock out of AtSOUL4 and AtSOUL5 revealed a conditional shade avoidance behavior, indicating that AtSOUL4 heme-binding protein might also be involved in the light signalling.

Abbreviations

aadA	Streptomycin/Spectinomycin adenylyl transferase Gene
ABA	Abscissic acid
ABC1	Activity of BC1 complex
ADRP	Adipocyte differentiation-related protein
AIDS	Acquired Immune Deficiency Syndrome
ALA	Aminolevulinic acid
At	Arabidopsis thaliana
ATP	Adenosine triphosphate
BN-PAGE	Blue native-polyacrylamide gel electrophoresis
bp	Base pairs
CaMV	Cauliflower mosaic virus
CAO	Chlorophyllide a oxygenase
CBP	Calmodulin binding peptide
CCD	Carotenoid cleavage dioxygenase
CFP	Cyan fluorescent protein
Chl	Chlorophyll
CHLH	Mg-chelatase H subunit
CKII	Casein Kinase II
cop	Constitutively photomorphogenic
CRD	Mg-proto IX monomethylester cyclase
Cre	Cyclization recombinase
CRY	Cryptochrome
CTAB	Cetyltrimethylammonium bromide
CTAPi	C-terminal Tandem affinity purification
det	Deetiolated
DIC	Differential interference contrast
DMPQ	2,3-dimethyl-6-phytyl-1,4-benzoquinone
DNA	Deoxyribonucleic acid
DTT	1,4-dithio-D-threitol
E. coli	Escherichia coli
EDTA	Ethylenediamine-N,N,N’,N’-tetraacetic acid
ELT	Esterase/lipase/thioesterase
EST	Expressed sequence tag
FC	Ferrochelatase

GFP	Green fluorescent protein
gun	genomes uncoupled
HCV	Hepatitis C virus
Hepes	4-(2-hydroxyethyl)-1-piperazineethanesulfonic acid
HIVp24	Human immunodeficiency virus core protein-p24
HO	Heme oxygenase
HPLC	High-performance liquid chromatography
hy	Long hypocotyl
IgG	Immunoglobulin G
IPTG	Isopropyl-β-D-1-thiogalactopyranoside
kb	Kilo base pairs
KDa	Kilo Dalton
LB	T-DNA left boarder or Luria-Bertani
Lhcb2	Chlorophyll a/b binding protein
LoxP	Locus of X-over P1 (Bacteriophage P1)
MES	2(N-Morpholino)ethanesulfonic acid
mRNA	Messenger RNA
MS	Murashige and Skoog
NDC1	NAD(P)H Dehydrogenase C1
Nef	Negative Regulatory Factor
Ni-NTA	Nickel-nitrilotriacetic acid
NMR	Nuclear magnetic resonance
p22HBP	Heme binding protein 22kDa
PAGE	Polyacrylamide gel electrophoresis
PC-8	Plastochromanol-8
PCR	Polymerase chain reaction
pFCC	Primary fluorescent chlorophyll catabolite
Pfr	Far red form of phytochrome
PG	Plastoglobules
PGL /FBN	Fibrillins
PHOT	Phototropins
phy	Phytochrome
PIF	Phytochrome Interacting Factor
PQ-9	Plastoquinone-9
Pr	Red form form of phytochrome
ProtA	Protein A
P*rrn*	Ribosome RNA operon promoter

PSI	Photosystem I
PSII	Photosystem II
PΦB	Phytochromobilin
RbcL	Large subunit of RubisCO
RFLP	Restriction fragment length polymorphism
RNA	Ribonucleic acid
ROS	Reactive oxygen species
RubisCO	Ribulose-1,5-bisphosphate carboxylase oxygenase
SDS	Sodium dodecyl sulfate
SDS-PAGE	SDS-polyacrylamide gel electrophoresis
Sec	General secretion pathway
Tat	Twin-arginine translocation pathway
T-DNA	Transfer DNA
TEM	Transmission electron microscopy
TEV	Tobacco etch virus
TIC	Translocon at the inner chloroplast membrane
TMV	Tobacco mosaic virus
TOC	Translocon at the outer chloroplast membrane
Toco-α	α-tocopherol
Toco-γ	γ-tocopherol
Tricine	N-tris(hydroxymethyl)methylglycine
Tris	Tris(hydroxymethyl)aminomethane
TSP	Total soluble protein
UHPLC-QTOFMS	HPLC-quadrupole time-of-flight mass spectrometer
UTR	Untranslated region
Vit-K	Vitamin-K
VTE1	Tocopherol cyclase
WT	Wild type
YEB	Yeast extract broth
YFP	Yellow fluorescent protein

Upper case, italic gene, wild type allele (e.g. *AtSOUL4*)

Lower case, italic mutant allele (e.g. *soul4-2*)

Upper case protein (e.g. AtSOUL4)

% (v/v) ml/100ml

% (w/v) g/100ml

1 INTRODUCTION

1.1 Plastids are the vital organelles of plants

1.1.1 Distribution of plastids

Plastids are a crucial group of plant cellular organelles distinguish from other eukaryotes. The plastid originated through endosymbiosis whereby a single-celled protist engulfed a free-living photosynthetic cyanobacterium (Reyes-Prieto et al., 2007). All plastids in a plant originate from small, undifferentiated plastids termed proplastids, which are found in dividing cells in meristems. The proplastids differentiate into specific plastid types depending on the environmental factors and tissue type. Chloroplasts are a major plastid type differentiating under light influence. Chloroplasts are the sites of photosynthesis and other important plant functions such as carbon, nitrogen, and sulphur assimilation and metabolism (Neuhaus and Emes, 2000). They produce fatty acids, aromatic and nonaromatic amino acids, purine and pyrimidine bases, isoprenoids and tetrapyrroles. The proplastids differentiate into other plastid type such as amyloplast leucoplasts, elaioplasts and chromoplasts depening on the tissue type and contents. Amyloplasts are mainly filled with starch in potato tubers (Waters and Pyke, 2004). Elaioplasts store lipids in oilseeds and tapetum (Piffanelli and Murphy, 1998). Chromoplasts contain red, orange, and yellow coloured pigments, isoprenoid carotenoids and xanthophylls present in flower petals and fruit (Weston and Pyke, 1999). Etioplasts are partially differentiated plastid present in cotyledon and leaves of dark-grown plants (Mustilli et al., 1999). They show a characteristic lattice-like semicrystalline structure known as the prolamellar body. The prolamellar body contains large amounts of thylakoid lipids, protochlorophyllide, bound to its reducing enzyme protochlorophyllide oxidoreductase (Armstrong et al., 1995; Vinti et al., 2005). Upon illumination, the prolamellar body transforms to the thylakoids with their photosynthetic machinery.

1.1.2 Chloroplast biogenesis

In plant development, light has a main role in the synthesis of chlorophyll as well as in chloroplast biogenesis, photomorphogenesis and the coordinate expression of many light-regulated nuclear- and chloroplast encoded genes (Chory, 1993; Bauer et al., 2001). Photoreceptors (phytochromes, phototropins and cryptochrome) activated by light. The main phytochromes such as phyA and phyB act during seedling photomorphogenesis (Quail,

2002; Tepperman et al., 2006). The cytosolic inactive phytochromes (Pr) is activated by light and converted into active Pfr form. This will transport into the nucleus to initiate signalling (Quail, 2002). The cryptochromes CRY1 and CRY2 absorbing in the blue-UVA range of the spectrum (Lin, 2000), the phototropins PHOT1 and PHOT2, which are involved in blue light mediated chloroplast relocation, stomatal opening and phototropism (Briggs and Christie, 2002). The light dependent signaling factors have been reported, such as constitutively photomorphogenic (cop) (Deng et al., 1991; Deng and Quail, 1992; Chamovitz et al., 1996; Suzuki et al., 2002) or de-etiolated (det) genes (Chory et al., 1989). HY5 acts as the positive regulator of photomorphogenesis under a broad spectrum of light (Chory, 1992). A recent study shows that PIF3 negatively regulates the expression of HEMA1 and GUN5 in dark (Shin et al., 2009). The hy1 mutant is unable to synthesize phytochromobilin (chromophore) resulting in the loss of phytochrome activity (Muramoto et al., 1999).

The biogenesis of chloroplasts needs considerable protein import from the cytosol. Most chloroplast proteins are imported through the TOC/TIC complex. The *AtTOC159* mutant is albino and seedling lethal. It has been shown that Toc159 is upregulated by light and confers substrate specificity for photosynthetic proteins (Bauer et al., 2000). The mechanism of protein import into the chloroplast via the TOC/TIC complex is very well documented (Kessler and Schnell, 2009). As most of the proteins needed for chloroplast function are encoded by nucleus, plastids have retrograde (from plastid to nucleus) signaling for tight coordination between the chloroplast and nuclear gene expression. Many factors have been suggested to be involved in the retrograde signaling. Chloroplast controls nuclear gene expression indirectly by metabolites, ROS and other cellular process (Pogson et al., 2008; Pfannschmidt, 2010). The genomes uncoupled (gun) mutants were isolated, in a genetic screen of seedlings treated with norflurazon and still expressing a nuclear encoded reporter gene under control of retrograde signaling (Susek et al., 1993). The *gun* genes may affect nuclear transcription via tetrapyrrole intermediates (Nott et al, 2006; Pfannschmidt, 2010).

1.1.3 Structure and compartmentalization of chloroplast

Chloroplasts are about 5-10μm in diameter and 3-4μm in thickness, present in each cell at numbers of 10 to more than 100 depending on the plant species (Lopez-Juez and Pyke, 2005). Chloroplasts are composed of stroma (aqueous matrix), thylakoids, starch granules and plastoglobules. The chloroplast is the organelle where photosynthesis occurs at photosystem I (PSI) and photosystem II (PSII). The photosynthetic apparatus is localised in the thylakoids. Thylakoid membranes are arranged in stacks, the grana, interconnected by

stromal lamellae. Photosynthetic protein-bound chlorophyll pigments are excited by light and initiate electron flow to ultimately generate ATP and NADPH. Photosynthesis allows plants to grow photoautrophically by harvesting light energy and CO_2 that is fixed by RubisCO to produce sugars. Chloroplast envelope and thylakoid membranes are rich in galactolipids, whereas the other plant membranes are mainly composed of phospholipids (Jarvis et al., 2000).

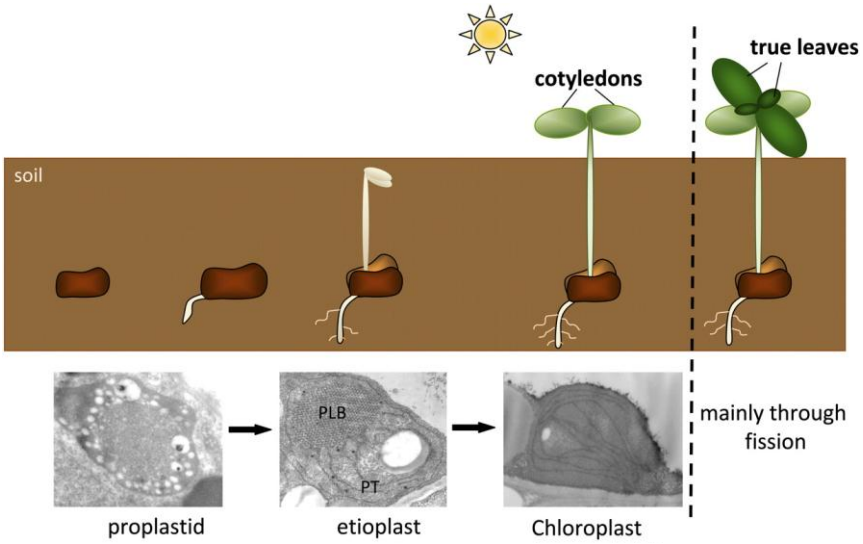

Figure 1.1. Chloroplast biogenesis and development in seedlings. PLB, Prolamellar body; PT, prothylakoids.

1.2 Plastoglobules - the lipoprotein particles in plastids

1.2.1 Plastoglobule

Plastoglobules are chloroplast lipid droplets that are contiguous with the thylakoid membranes (Kessler et al.,1999; Austin et al., 2006). Ultra structure microscopy study demonstrated that plastoglobules arise from a ‘‘blistering’’ of the stroma-side leaflet of the thylakoid membrane, predominantly along highly curved margins (Austin et al., 2006), and are hence a single lipid layer studded with proteins. The first PG protein was discovered in the carotenoid fibrils of red pepper chromoplasts (Deruere et al., 1994). Plastid-lipid associated proteins (PAPs) or plastoglobulins were also discovered in different plant species (Deruere et al., 1994; Pozueta-Romero et al., 1997; Kessler et al., 1999). Plastoglobules

contain within the outer polar lipid monolayer, neutral lipids such as plastoquinone, phylloquinone, α-tocopherol, fatty acid phytyl esters, triacylglycerol and carotenoids (Brehelin et al., 2007; Brehelin and Kessler, 2008). Plastoglobule size may vary depending on developmental stage and environmental conditions. A series of studies have reported an increase in plastoglobule size and number under biotic and abiotic stress conditions. However, plastoglobules have widely been considered passive lipid storage droplets.

The proteome of plastoglobules has around two dozen proteins (Vidi et al., 2006; Ytterberg et al., 2006; Lundquist et al., 2012). These fall into three categories: Plastoglobulins (PGL or FBN), plastid metabolic proteins and unclassified proteins. The most recent study based on quantitative comparative proteomics shows 23 of the 30 core proteins that were previously assigned to the PG (Vidi et al., 2006; Ytterberg et al., 2006). An additional seven proteins were newly identified and mostly low abundance proteins of the core PG proteome (Table. 1.1). PGs are thought to play major roles in chloroplast development, senescence, and stress defense (Nordby and Yelenosky, 1985; Locy et al., 1996; Rey et al., 2000; Oksanen et al., 2001; Gaude et al., 2007; Lichtenthaler, 2007). The sizes of the plastoglobules varied from 30 nm to 5 mm depending on the developmental and environmental conditions. Plastoglobules play a role in chloroplast to chromoplast transition particularly the formation of the colored carotenoids fibrils (Vishnevetsky et al., 1999). During senescence, the chlorophyll is broken down into phytol and chlorophyllide. The phototoxic chlorophyllide is rapidly catabolized (Hortensteiner, 2006) and the remaining toxic phytol incorporated into fatty acid phytyl esters in plastoglobules (Ischebeck et al., 2006; Gaude et al., 2007; Lippold et al., 2012). This clearly shows that accumulation of these thylakoid catabolites in plastoglobules may protect thylakoid membranes from toxic effects of the free phytol.

1.2.2 Plastoglobulins

The PGL (plastoglobulin) family in Arabidopsis consists of thirteen genes. Seven members were recovered in the plastoglobule proteome. However, it has now been demonstrated that plastoglobulin/FBNs partition to varying degrees between the thylakoid membrane and the plastoglobule depending on hydrophocity and isoelectric point (Lundquist et al., 2012). The role of PGLs is probably mainly to control the formation as well as structure and shape of the lipid bodies that have been proposed to "bud" from the thylakoid membrane (Austin et al., 2006). In view of the presence of PGL/FBNs at both PG and thylakoid membranes this may

Table.1.1 The PG core proteome by quantitative comparative proteomics

Accession No.	Protein Name		NadjSPC[a]	CV[b]	Percentage Mass PG Core[c]	PG/Thylakoid[d]	PG/Stroma[d]	Reference[e]			
								1	2	3	
				%							
AT4G04020	Fibrillin 1a (FBN1a)	PGL35 PGL30 PGL33 PGL40	0.100	15	16.1	34	176	×	×	×	Previously identified
AT3G23400	Fibrillin 4 (FBN4)		0.074	30	11.9	32	121	×	×	×	
AT4G22240	Fibrillin 1b (FBN1b)		0.059	12	9.6	40	713	×	×	×	
AT2G35490	Fibrillin 2 (FBN2)		0.044	4	7.1	59	1,188	×	×	×	
AT5G05200	ABC1K9		0.032	8	5.2	440	–[f]	×	×	×	
AT4G31390	ABC1K1		0.028	8	4.5	16	–	×	×	×	
AT1G79600	ABC1K3		0.027	23	4.3	11	–	×	×	×	
AT3G58010	Fibrillin 7a (FBN7a)	PGL34	0.022	44	3.5	15	146	×	×	×	
AT4G19170	Carotenoid dioxygenase 4 (CCD4)		0.021	25	3.3	18	42	×	×	×	
AT4G32770	Tocopherol cyclase (VTE1)		0.016	5	2.6	131	–	×	×	×	
AT1G54570	Diacylglycerol acyltransferase 3 (DGAT-3)		0.016	12	2.6	31	–	×	×	×	
AT5G08740	NAD(P)H dehydrogenase C1 (NDC1)		0.015	8	2.5	19	–	×	×	×	
AT2G42130	Fibrillin 7b (FBN7b)	PGL30	0.013	45	2.1	11	23	×	×	×	
AT1G32220	Flavin reductase-related 1		0.013	23	2.1	22	102	×	×	×	
AT4G13200	Unknown 1		0.012	17	1.9	11	–	×	×	×	
AT3G10130	SOUL domain protein		0.011	10	1.8	61	–	×	×	×	
AT2G46910	Fibrillin 8 (FBN8)	PGL31	0.011	12	1.8	29	434	×	×	×	
AT1G71810	ABC1K5		0.011	12	1.7	17	–	×	×	×	
AT1G78140	UbiE methyltransferase-related 1		0.009	43	1.5	48	–	×	×	×	
AT1G06690	Aldo/keto reductase		0.009	35	1.5	13	765	×	×	×	
AT2G34460	Flavin reductase-related 2		0.009	26	1.5	6	75	×	×	×	
AT2G41040	UbiE methyltransferase-related 2		0.009	17	1.5	72	–	×	×	×	
AT3G26840	Diacylglycerol acyltransferase 4 (DGAT 4)		0.009	14	1.4	–	–	×	×	×	
AT3G24190	ABC1K6		0.016	14	2.6	15	322			×	Newly identified
AT4G39730	PLAT/LH2–1		0.010	29	1.6	–	–			×	
AT3G43540	Unknown 2 (DUF1350)		0.008	42	1.3	14	80			×	
AT3G07700	ABC1K7		0.005	27	0.8	37	–			×	
AT1G73750	Unknown SAG		0.002	80	0.4	–	–			×	
AT3G27110	M48 protease		0.002	42	0.3	17	–			×	
AT5G41120	Esterase 1		0.002	30	0.3	–	–			×	
AT5G42650	Allene oxide synthase (AOS)								×		Removed
AT1G09340	Rap38/CSP41B								×		
AT1G26090	Anion-transporting ATPase								×		
AT1G28150	Unknown								×		
AT4G01150	Unknown								×		
AT3G63140	Rap41/CSP41A								×		
AT5G01730	WAVE3								×		
AT2G21330	FBPA-1							×	×		
AT4G38970	FBPA-2							×	×		
AT2G01140	FBPA-3							×	×		
AT3G26060	PrxQ							×			
AT1G52590	Unknown (DUF39)							×			
AT3G26070	Fibrillin (FBN3a)							×			

[a]Abundance of each PG core protein. [b]Coefficient of variation of the average NadjSPC across the three biological replicates. [c]Contribution of each proteinto protein mass of the PG core proteome as a percentage of total core proteome. [d]Abundance ratio based on NadjSPC in PG and other chloroplast compartments. [e]1, Vidi et al., (2006); 2, Ytterberg et al., (2006); 3, Lundquist et al., 2012 (Lundquist et al., 2012).

involve their coordinated action at the two compartments. Plastoglobules as well as PGL homologs are present throughout the plant kingdom (Lichtenthaler, 1968). Homologues of Arabidopsis PGL35 and PGL34 were notably also found in the tobacco EST (PozuetaRomero et al., 1997). It is therefore likely that homologues of Arabidopsis PGLs behave similarly in different species. Previous studies demonstrated that with the exception of a short C-terminal stretch the complete sequence of a PGL was necessary for proper plastoglobule targeting (Vidi et al., 2007). Comparably, adipophilin (also termed Adipocyte Differentiation-Related Protein, ADRP), which is one of the lipid body-associated proteins in mammalian cells, has no lipid-binding motif (hydrophobic domains or amphipathic α-helices) and discontinuous stretches of the protein are necessary for targeting to lipid bodies (Targett-Adams et al., 2003). It has been shown that the yellow fluorescent protein fused to PGL34 was expressed and properly targeted to plastoglobules in nuclear transgenic Arabidopsis plants using chloroplast fractionation (Vidi et al., 2007). The fact that PGL/FBN assembly onto either plastoglobules or thylakoid membranes depends on physical properties of the whole protein suggests that it is folded after import from the cytosol and then assembled. The plastoglobulin family is believed to have mostly structural functions. A recent report suggests that, they may also play a role in metabolite transport (Singh and McNellis, 2011). The plastoglobulins expression depends on abiotic and biotic stress (Brehelin and Kessler, 2008). The bell pepper and potato plastoglobulin accumulating during wounding, drought stress, various oxidative stress and high light (Pruvot et al., 1996; Gillet et al., 1998; Chen et al., 1998; Langenkamper et al., 2001). Arabidopsis plastoglobulin AtPGL35 is regulated by ABA (Yang et al., 2006). Furthermore, plastoglobulins accumulate in response to light and temperature stress related jasmonate biosynthesis (Youssef et al., 2010). Phosphorylated AtPGL30.4 was found in tomato, during defence response to *Pseudomonas syringae* pv (Jones et al., 2006), suggesting that plastoglobulin may also be kinase-regulated under stress. Together the six plastoglobulin core proteins constituted 53% of the PG proteome mass in Arabidopsis (Lundquist et al., 2012).

1.2.3 Metabolic enzymes in plastoglobules

Arabidopsis PG proteome contains known metabolic enzymes. The tocopherol cyclase (VTE1) involved in vitamin E synthesis (Porfirova et al., 2002). VTE1 catalyzes the conversion of 2,3-dimethyl-5-phytyl-1,4-hydroquinol (DMPQ) to γ-tocopherol. The carotenoid cleavage dioxygenase CCD4 with specificity for 8`-apo-β-caroten-8`-al in Arabidopsis, involved in the carotenoid metabolism (Huang et al., 2009). A recent report shows that

NAD(P)H Dehydrogenase C1 (NDC1) is necessary for phylloquinone synthesis (Eugeni-Piller et al., 2011).

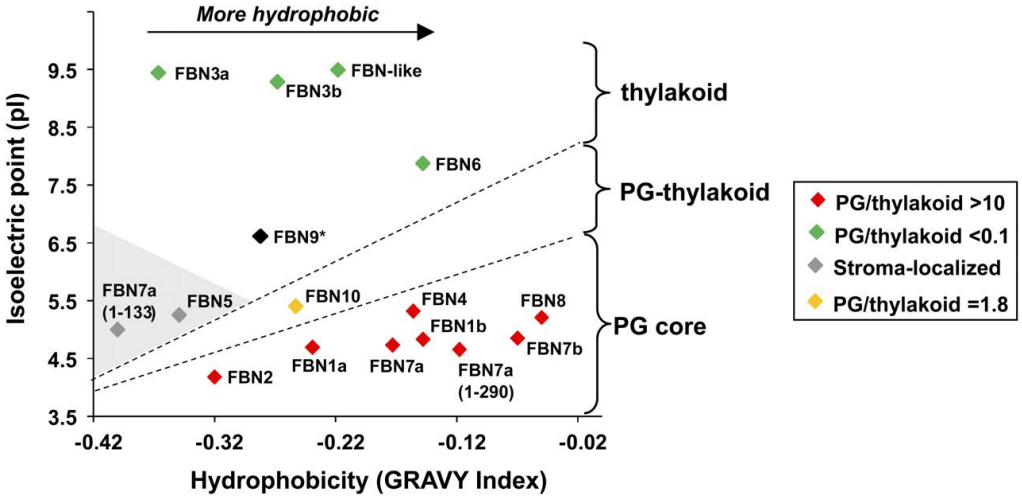

Figure 1.2 Fibrillin distribution correlates with pI and hydrophobicity. The pI and hydrophobicity (GRAVY index) were determined for 16 FBN protein products (the chloroplast transit peptide was removed) using the ProtParam tool at the ExPasy Web site (http://expasy.org/). The 16 proteins were grouped by subcellular localization and plotted by hydrophobicity (GRAVY index) and pI.

1.2.4 A member of plastoglobule proteins have unknown function

The second most abundant class of core proteins consisted of six ABC1 kinases. The ABC1K proteins were identified in *Saccharomyces cerevisiae* (Abc1p/Coq8p) and *E. coli* (UbiB) mainly involved in ubiquinone metabolism (Poon et al., 2000; Do et al., 2001). The role of possible targets of the PG-localized ABC1 like kinases proteins may be in prenyllipid/ubiquinone metabolism. The ELT1 and 2 (esterase/lipase/thioesterase) are required for phytyl ester synthesis (Lippold et al., 2012). The SOUL4 heme binding protein may be involved in heme metabolism in plastids.

1.3 Molecular farming - plastid transformation

1.3.1 Recombinant protein expression in plants

The potential of transgenic plants for cost-effective production of pharmaceutical molecules is now becoming apparent. Plants have the advantage over established fermentation systems (bacterial, yeast or animal cell cultures) to (i) be considerably cheaper, (ii) reduce the risk of pathogen contamination, (iii) be amenable to large scaling up and (iv) require only established farming procedures (Ma et al., 2005). Chloroplasts are an excellent organelle for protein accumulation because of their relatively large volume and numbers per cell, as well as the possibility of genetic transformation. They therefore represent the targeting destination of choice for many recombinant proteins in leaf crops, such as tobacco. Extraction and purification of recombinant proteins from leaf material contribute to a large extent to the production costs.

1.3.2 Recombinant fusion proteins target to plant lipid and protein bodies

Several strategies have recently been developed to target recombinant fusion proteins to plant protein bodies, for instance human immunoglobulin (IgG) α-chains (Obregon et al., 2006), elastin-like polypeptides (Conley et al., 2009), zeolin (de Virgilio et al., 2008) and hydrophobins (Joensuu et al., 2010). In each case, targeting to protein bodies was very useful to enhance the production yield and simplify the downstream processing of recombinant protein purification. The downstream purification process of recombinant protein from plants can involve demanding and time-consuming procedures, which may contribute substantially to the high cost of the final product. The oleosin technology is a method specific to plants where an oleosin fusion protein accumulates in seed oil bodies and can be purified using a simple extraction and centrifugation procedure followed by release of the target protein by proteolytic cleavage (Vanrooijen and Moloney, 1995; Boothe et al., 2010). The main advantage of oil bodies is the easy separation from other cellular components by floatation centrifugation. Plant seed oil bodies (oleosomes) are well-known as carrier for foreign proteins and have the potential of reducing the cost of downstream purification (Parmenter et al., 1995). Plastoglobules represent an analogous system present in the chloroplast. The low density of plastoglobules has the same advantage as oil bodies for rapid enrichment of the recombinant protein by floatation centrifugation. The yellow

fluorescent protein fused to PGL34 accumulated to 0.2% of the total leaf protein and was properly targeted to plastoglobules in transgenic *Arabidopsis* plants and successfully purified by floatation centrifugation (Vidi et al., 2007).

1.3.3 Chloroplasts as bioreactors for biopharmaceuticals

Transplastomic plants have advantages over conventional expression systems such as microbial and yeast fermentation or insect and mammalian cell cultures. High-level expression of pharmaceutical proteins in transplastomic plants is well established (De Cosa et al., 2001; Tregoning et al., 2003; Glenz et al., 2006; Zhou et al., 2008; Oey et al., 2009). Proteins have also been targeted to various intra-chloroplast compartments. Aprotinin, a bovine protease inhibitor, was targeted to the lumen of thylakoids of tobacco plastid transformants using a general secretion (Sec) or twin-arginine translocation (Tat) pathway signal peptides derived from nuclear genes which encode luminal proteins (Tissot et al., 2008). Plastid-encoded pre-Tic40 was properly processed and targeted and assembled into a functional complex at the inner membrane of the chloroplast (Singh et al., 2008). Zeolin with a plant secretory signal peptide was targeted to the thylakoid membrane upon chloroplast transformation (De Marchis et al., 2011). Recombinant disulfide-bond containing proteins can be expressed in transformed plastids when targeted to the lumen of thylakoids (Bally et al., 2008).

1.3.4 Advantages of transplastomic plants

Plastid transformation is of huge interest in molecular farming (Daniell et al., 2009; Bock and Warzecha, 2010). This technology has been employed to achieve high levels of protein expression in chloroplasts, due to high gene copy number and absence of epigenetic effects, transgene pyramiding and maternal chloroplast inheritance (Maliga, 2004; Bock, 2007; Maliga and Bock, 2011). Chloroplast genome transmission by pollen occurs at a very low frequency intobacco (Ruf et al., 2007). The CRY protein from *Bacillus thuringiensis* reached 45% of the total soluble protein (TSP) (De Cosa et al., 2001), tetanus toxin fragment C (TetC) of *Clostridium tetani* represented 25% TSP of the leaf tissue (Tregoning et al., 2003), HIVp24 from human immunodeficiency virus reached 40% TSP (Zhou et al., 2008) and a phage lytic protein reached the extremely high level of more than 70% TSP (Oey et al., 2009). Compared with other crop species, tobacco is the most established system for recombinant protein expression, because it is readily amenable to genetic engineering and has many additional advantages, such as high biomass yield, non-food and non-feed crop

properties, which minimize the risk of plant-made recombinant proteins entering the food supply (Menassa et al., 2001).

1.3.5 The HIVp24 protein and HCV core protein as antigens

Around 33 million HIV (human immunodeficiency virus) infected people were estimated worldwide in 2007 (WHO, 2009). The core protein p24 has 80% amino acids conserved among all HIV-1 genotypes (Hanke and McMichael, 2000). The HIV antigen p24 is expected to be a key component of any AIDS vaccine (Obregon et al., 2006). Hepatitis C virus (HCV) is estimated to infect 170 million people worldwide (Moradpour et al., 2007). The core protein is required for RNA packaging and viral assembly, and is the most highly conserved HCV protein exhibiting 78–90% amino acid identity between the six described HCV genotypes (Robertson et al.,1998). HCV core protein is a target of vaccine development for Hepatitis C disease (Elmowalid et al., 2007). A further advantage of plastids is the absence of protein glycosylation pathways, which makes them suitable for expression of the HCV core protein (Moradpour et al., 2007).

1.4 SOUL-heme binding proteins

1.4.1 The significance and regulation of tetrapyrrole metabolism in plants

Tetrapyrroles play crucial roles in photosynthesis, respiration and in various other biological processes. In plants, chlorophyll, heme, siroheme, and phytochromobilin are the main tetrapyrroles derived from a common biosynthetic pathway in plastids. Nevertheless, under some conditions these tetrapyrroles can also lead to severe photo-oxidative damage, and cell death. Therefore tetrapyrrole transport and metabolism needs to be highly regulated. In Arabidopsis, 2% of the proteins are tetrapyrrole binding proteins (Mochizuki et al., 2010). The 5-aminolevulinic acid (ALA) is the precursor for all tetrapyrroles pathway intermediates up to uroporphyrinogen III are common to the biosynthesis of tetrapyrroles. The pathway branches at this step to form siroheme. Uroporphyrinogen III is converted to protoporphyrinogen IX by decarboxylation and oxidation. The chlorophyll branch and heme branch depend on insertion of either $Mg2^{+}$ or $Fe2^{+}$ into protoporphyrin IX, by Mg-chelatase

and ferrochelatase, respectively. In the chlorophyll branch, Mg-protoporphyrin IX is converted to protochlorophyllide and subsequently into chlorophyllide *a*. Chlorophyllide *a* is converted into chlorophyll a by esterification by chlorophyll synthase. A part of the chlorophyll *a* is converted to chlorophyll *b* by chlorophyllide *a* oxygenase (CAO) by passing through the 'chlorophyll cycle' (Tanaka and Tanaka, 2007). Chl breakdown is a vital biological process for leaf senescence and fruit ripening. The Chl breakdown intermediates are potentially toxic to cells. In plastids, a series of enzymatic reactions convert Chl into linear colorless tetrapyrrole derivatives primary fluorescent Chl catabolites (pFCC). pFCC molecules are then exported to the vacuole and are finally broken down to monopyrrole molecules (Hörtensteiner, 2006; Hörtensteiner and Kräutler, 2011).

The tetrapyrrole pathway has complex and tight regulation at the transcriptional and post translational levels. The GUN4, HEMA1, CHLH, CRD1 (CHL27) and CAO are highly regulated during light and circadian signals at the transcriptional level (Papenbrock et al., 1999; Matsumoto et al., 2004; Stephenson, et al., 2008). Heme is the major feedback inhibitor of glutamyl tRNA reductase (Cornah et al., 2003). The potential regulatory protein FLU (Meskauskiene et al., 2001) binds to GluTR and represses ALA synthesis in dark. The Mg-chelatase activity is regulated by GUN4, which interacts with Mg-chelatase and stimulates Mg-chelatase in chloroplast membranes (Larkin et al., 2003; Adhikari et al., 2009). The chlorophyllide a oxygenase (CAO) is a well characterized example of post-translational regulation in response to over accumulation of chlorophyll *b* (Yamasato et al., 2005). The nucleus must monitor the plastid conditions to optimize gene expression. The plastid sends signals to the nucleus (retrograde signaling) in various ways and Mg-protoporphyrin IX, a tetrapyrrole metabolite has been reported to be one of the plastid signal molecules (Nott et al., 2006).

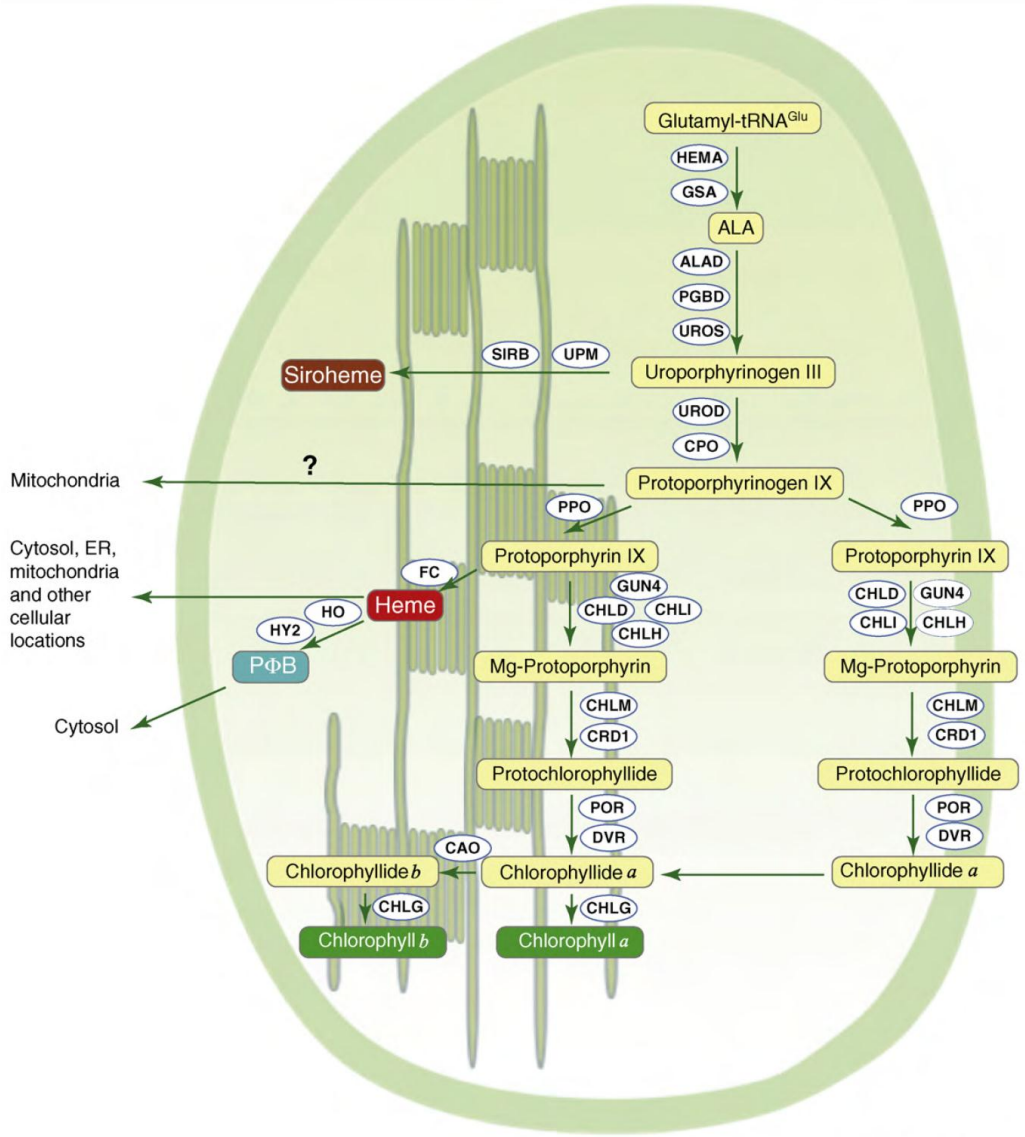

(Mochizuki et al., 2010)

Figure 1.3 Localization of tetrapyrrole synthesis in chloroplasts.
The sub-organellar localizations (stroma, envelope or thylakoids) of tetrapyrrole enzymes and biosynthetic intermediates in the chloroplast, most of the data are based on proteomic analyses.

1.4.2 Heme biosynthesis in plants

In the heme branch, ferrochelatase (FC) inserts Fe2+ into protoporphyrin IX to produce protoheme (heme b). In Arabidopsis, FC has two isoforms: FC1 and FC2 (Smith et al., 1994). FC2 is mainly expressed in photosynthetic tissues (Singh et al., 2002) and is thus likely involved in heme production for photosynthetic cytochromes and hemoproteins. The protoheme is noncovalently bound via coordination with Fe^{2+} atom by histidine and/or cysteine residues (Schneider et al., 2007). Heme oxygenase catalyzes the oxidation and ring opening of protoheme and produce the biliverdin IXα. There are four HO isoforms in Arabidopsis: HO1, HO2, HO3 and HO4 (Davis et al., 2001; Terry et al., 2002). The HO1 mutant *hy1* show a characteristic phytochrome-deficient long hypocotyl phenotype, showing that HO1 plays a major role in biliverdin IXα synthesis (Davis et al., 1999; Muramoto et al., 1999). In plants, biliverdin IXα is reduced to PΦB, which is the chromophore of the phytochrome family of photoreceptors, by PΦB synthase. In Arabidopsis, a single isoform of PΦB synthase (HY2) is involved in reduction of biliverdin IXα to PΦB (Kohchi et al., 2001). The primary product of PΦB synthase is 3*Z*-isomer of PΦB, then 3*Z*- PΦB convert into 3*E*-PΦB by isomerization (Terry et al., 2002). The 3E-PΦB can serve as functional precursor of the phytochrome chromophore. Phytochromobilin (PΦB) is exported to the cytosol and covalently attached to apophytochrome (PHYA-PHYE) forming holophytochrome (Terry, 1997). Phytochromes are a well-known family of red/far-red responsive photoreceptors. Absorption of red light triggers a isomerization of "Z" to 'E" PΦB, resulting in the far-red light absorbing form Pfr. This Pr-to-Pfr transition is associated with the rearrangement of the protein backbone (Rockwell et al., 2006). In mammals and yeast, heme acts in several important signaling roles, such as transcription (Guarente and Mason, 1983; Shan et al., 2004; Sun et al., 2004; von Gromoff et al., 2008), translation (Joshi et al., 1995), posttranslational protein modification (Chen et al., 1989), translocation (Lathrop and Timko, 1993), and ion-channel function (Tang et al., 2003). In Chlamydomonas Mg-Proto IX and heme act as signaling molecules on gene expression involved in the tricarboxylic acid cycle, heme-binding proteins, stress-response proteins, and protein folding and degradation (Voss et al., 2011).

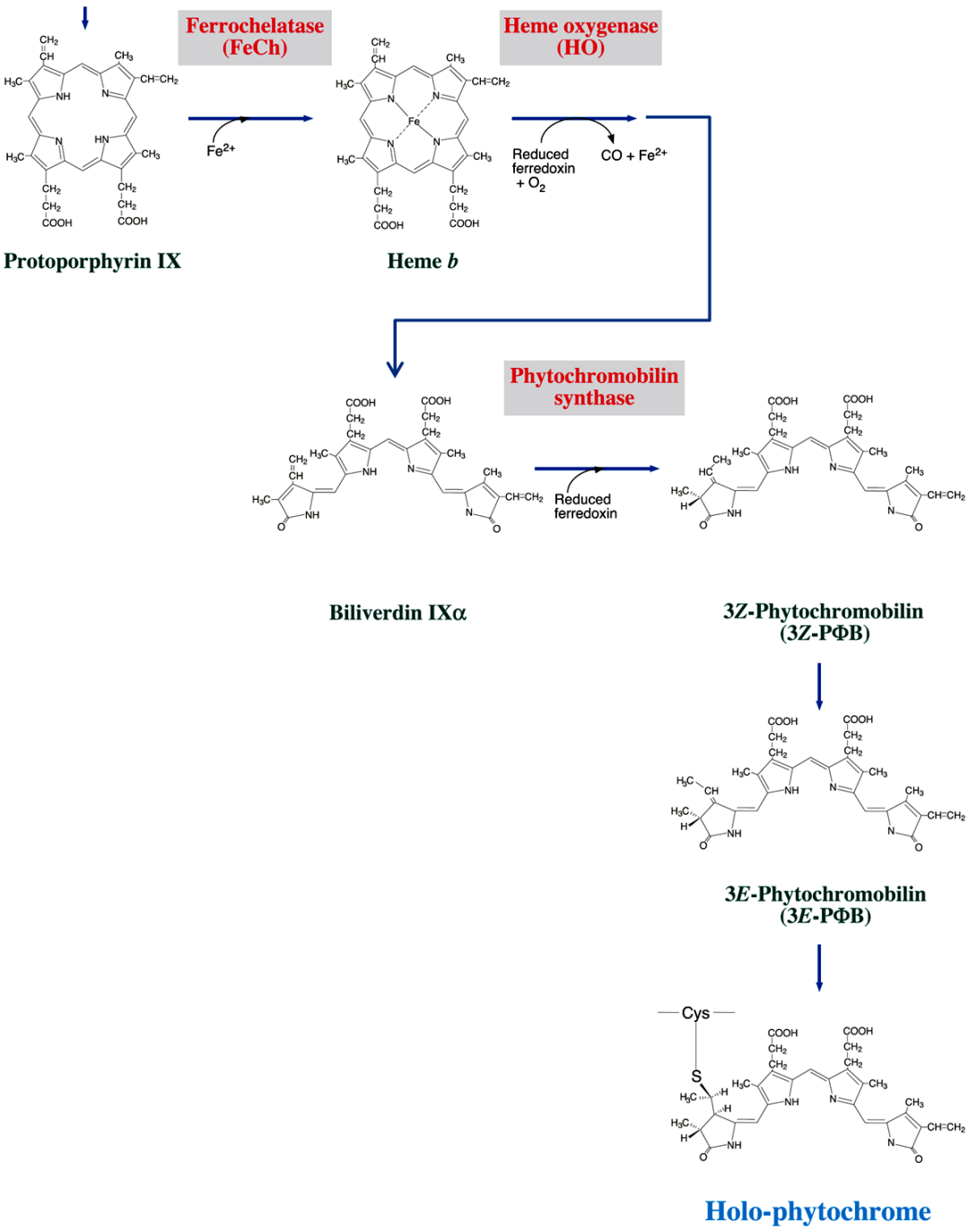

(Tanaka et al., 2011)

Fig.1.4 The heme/bilin branch in higher plants.
The heme *b* (protoheme) is synthesized by the insertion of Fe2+ in the chloroplast. Heme is subsequently oxidized and its ring structure is opened and then transformed into phytochromobilin (PΦB) and exported to the cytosol.

1.4.3 Structure and biochemical chacterization of SOUL-heme binding proteins

A SOUL heme binding protein was first discovered in chicken retina and pineal gland specifically expressed during circadian rhythms and in response to light signaling (Zylka and Reppert, 1999). The near identical protein is the p22 heme binding protein (p22HBP) with 40% identity and high affinity for porphyrins. While, the authors named it SOUL, because they considered the pineal gland as the soul of life. SOUL-HBPs (heme binding proteins) exist in bacteria, plants, and animals. In mouse eyes, SOUL heme binding protein forms from dimers to hexamers in the heme binding state (Sato et al., 2004). The structural determination by NMR revealed that SOUL heme binding protein has a novel hydrophobic cleft flanked by α-helix and the β8-9 loop (Dias et al., 2006).

The Arabidopsis genome have six proteins with a SOUL motif; two of them SOUL4 (At3g10130) and SOUL5 (At5g20140) are predicted to be plastid localized and SOUL1 and 3 were present in the vacuole proteome (Jaquinod et al., 2007). The recombinant SOUL1 and 3 reversibly bind to a range of porphyrins with dissociation constants (Kd) in the nanomolar range. This result demonstrates that their properties are suitable for a role as tetrapyrrole carrier proteins in plant cells (Takahashi et al., 2008). The Arabidopsis SOUL1 is hypersensitive to red light (Khanna et al., 2006). Chloroplast SOUL heme binding proteins were identified earlier as being thylakoid associated (Peltier et al., 2006, 2004), later SOUL4 identified in plastoglobule proteome (Ytterberg et al., 2006; Vidi et al., 2006; Lundquist et al. 2012). In Chlamydomonas, four SOUL heme binding proteins are present (Schmidt et al., 2006; Merchant et al., 2007). At least one is present in the core eyespot phosphoproteome (Wanger et al., 2008). The SOUL heme binding protein may function as tetrapyrrole/heme carriers. A second possibility would be to maintain tetrapyrrole/heme in a protein bound, non-phototoxic form.

1.5 Aim of the thesis

The aims of this thesis are two-fold addressing a fundamental as well as an application-oriented question. In both cases, chloroplast lipid droplets are the target of research. Plastoglobules (PG) are lipid droplets that are present in most types of plastids. Plastoglobulins (PGL; also fibrillins; FBN) are structural proteins covering their surface (Vidi et al., 2006; Ytterberg et al., 2006; Lundquist et al., 2012). The low density of plastoglobules the advantage for rapid purification by floatation centrifugation together with the associated proteins. To take advantage of these properties a strategy was developed in Aim1 to target transplastomic plastoglobulin-vaccine candidate fusion proteins (HIVp24 and HCV core protein) to plastoglobules and also to thylakoid membranes. The transplastomic technology potentially allows to achieve high levels of protein expression in chloroplasts without many of the problems normally occurring in nuclear transgenic plants (Maliga 2004; Bock 2007; Maliga and Bock 2011).

Aim2 of the thesis is the characterization of the PG-associated SOUL protein (AtSOUL4). SOUL proteins were first identified as heme-binding proteins in chicken retina and pineal gland. Here, we test the hypothesis that AtSOUL4 binds heme in the chloroplast and may be involved in the regulation of chloroplast lipid metabolism, chlorophyll catabolism and/or phytochrome-dependent light signal.

2 Results

2.1 Plastoglobules - a new destination for recombinant proteins produced in transplastomic plants

2.1.1 PGL35 (FBN1a) is highly conserved in higher plants

Multiple sequence alignment of the Arabidopsis PGL35 amino acid sequence shows 84% similarity and 72% identity with the protein sequence of its tobacco homolog (PozuetaRomero et al., 1997). The PGL35 amino acid is also highly conserved in other higher plants species (Fig. 2.1).

2.1.2 Chloroplast expression constructs

Tobacco chloroplast transformation DNA constructs pVSB1, pVSB2 and pVSB3 (Figure 2.2A) were engineered based on the pZF7lox plastid vector (Zhou et al., 2008) and pVSB4 was based on the pRB96 plastid vector. The Plastoglobulin35 (PGL35) coding sequence lacking the sequence for the transit peptide and coding N-terminal streptavidin tag and a C-terminal triple TEV protease site was amplified and cloned into pLITMUS28i. Coding sequences for Hepatitis C virus antigen-core protein (kindly provided by Dr. Bruno Martoglio, Novartis) and codon-optimised synthetic HIV p24 (Zhou et al., 2008) transgenes were fused individually to the 3' end of PGL35coding sequence in pLitmus28i. After the initial steps, the coding sequences for the PGL35-HCV core protein, PGL35-HIVp24 and PGL35-GFP were subcloned into the pZF7lox plastid vector by excision and replacement of HIVp24-nef. The expression cassette in pZF7lox is derived from the tobacco plastid P*rrn* promoter and the 5'UTR from the bacteriophage T7 gene 10 (Kuroda and Maliga, 2001). The terminator is the rbcL 3' untranslated region (3'UTR). The PGL35-GFP cassette was subcloned into the pRB96 vector. In pRB96, the coding sequence of PGL35-GFP is under the chloroplast P*atp*I promoter and terminated by the *rps*16 3' untranslated region (3'UTR). Both, pZF7lox plastid vector and pRB96 plastid vector allow homologous recombination with the tobacco plastid genome resulting in insertion between *trnfM* and *trnG* in the large single-copy region of the chloroplast genome.

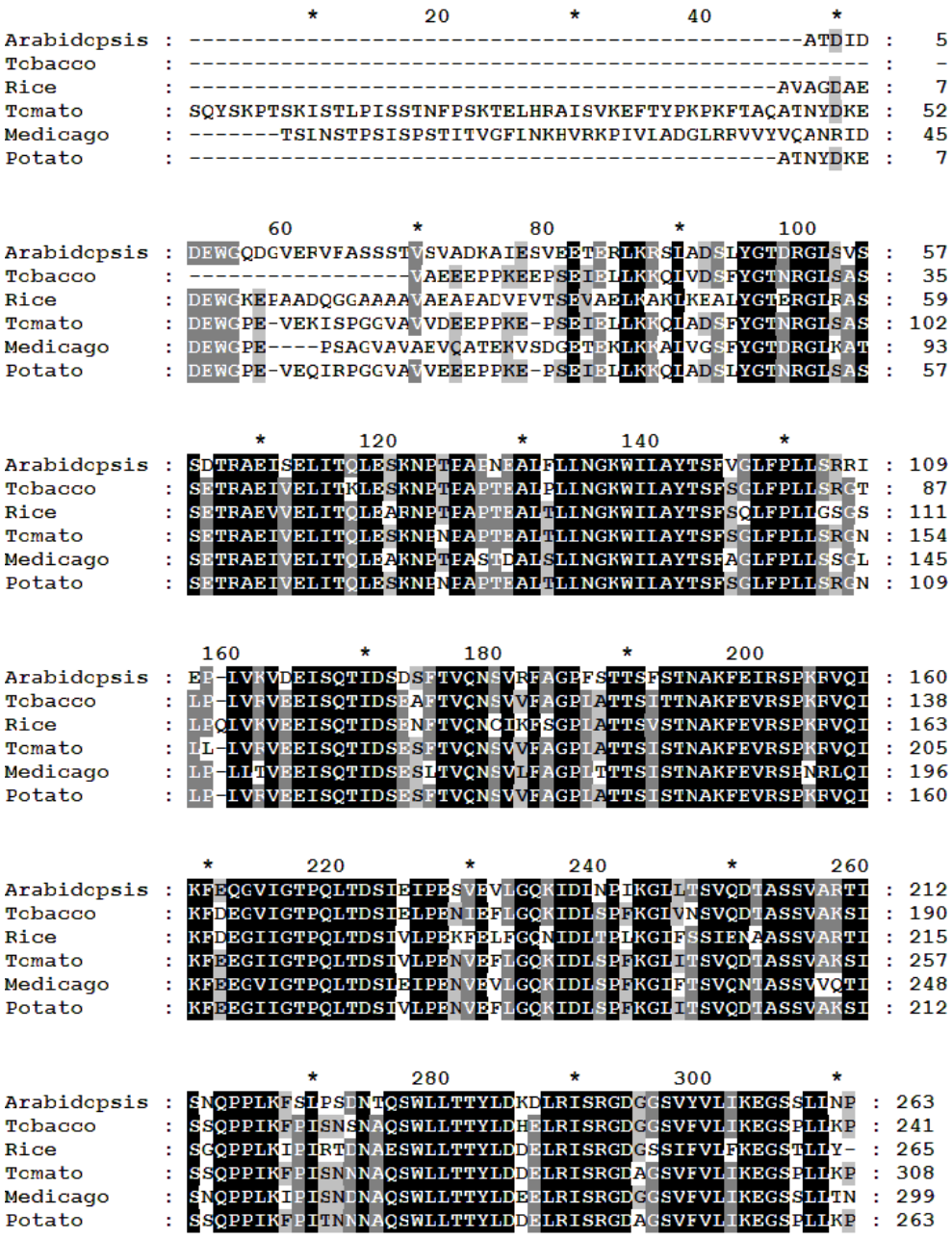

Figure. 2.1 Alignment of amino acid sequences for PGL35 from Arabidopsis, tobacco, rice, tomato and potato. The N-terminal transit peptide amino acids were removed and sequence alignment was performed by CLUSTALW.

An advantage of the pZF7lox plastid vector over is its pRB96 compatibility with the cre-lox system that allows excision of the loxP-flanked selectable marker gene (*aadA*) by site-specific recombination using nuclear encoded CRE recombinase targeted to plastids. (Corneille et al., 2001). This is achieved by crossing homoplasmic transplastomic plants with nuclear transgenic plants expressing the plastid targeted CRE recombinase, using the transplastomic plants as maternal parent and the nuclear transgenic line as the pollen donor.

2.1.3 Introduction of transgenes into the tobacco plastid genome

Chloroplast transformation vector pVSB1, pVSB2, pVSB3 and pVSB4 were introduced into tobacco (*Nicotiana tabacum* cv. Petit Havana) plastids by biolistic transformation (Svab and Maliga, 1993). Primary spectinomycin-resistant tobacco lines were selected on regeneration medium of plants (RMOP) containing 500 mg/L spectinomycin. After 4-8 weeks, the primary spectinomycin-resistant tobacco lines were obtained. The plastid-transformed (transplastomic) lines were all purified to homoplasmy by conducting additional regeneration cycles under increasingly stringent antibiotic selection. The transplastomic lines will subsequently be referred to as Nt-pVSB1 (generated with the HCV core protein construct), Nt-pVSB2 (line containing the p24 expression construct), Nt-pVSB3 (GFP fusion) and Nt-pVSB4 (GFP in pRB96 vector), respectively, and followed by the number of the individual transplastomic lines (e.g., Nt-pVSB1#5A designating transplastomic tobacco line number 1 generated with construct pVSB1 and 5A referred as individual) number 1 generated with construct pVSB1.

2.1.4 RFLP and homoplasmy analysis of transplastomic plants

Several lines isolated from independent transformation events for each construct were characterized in more detail. The correct integration of the transgenes into the plastid genome was confirmed by RFLP analysis of T_0 plants using Southern blotting. Seeds were obtained from selected T_0 plants (Figure 2.2B-E).

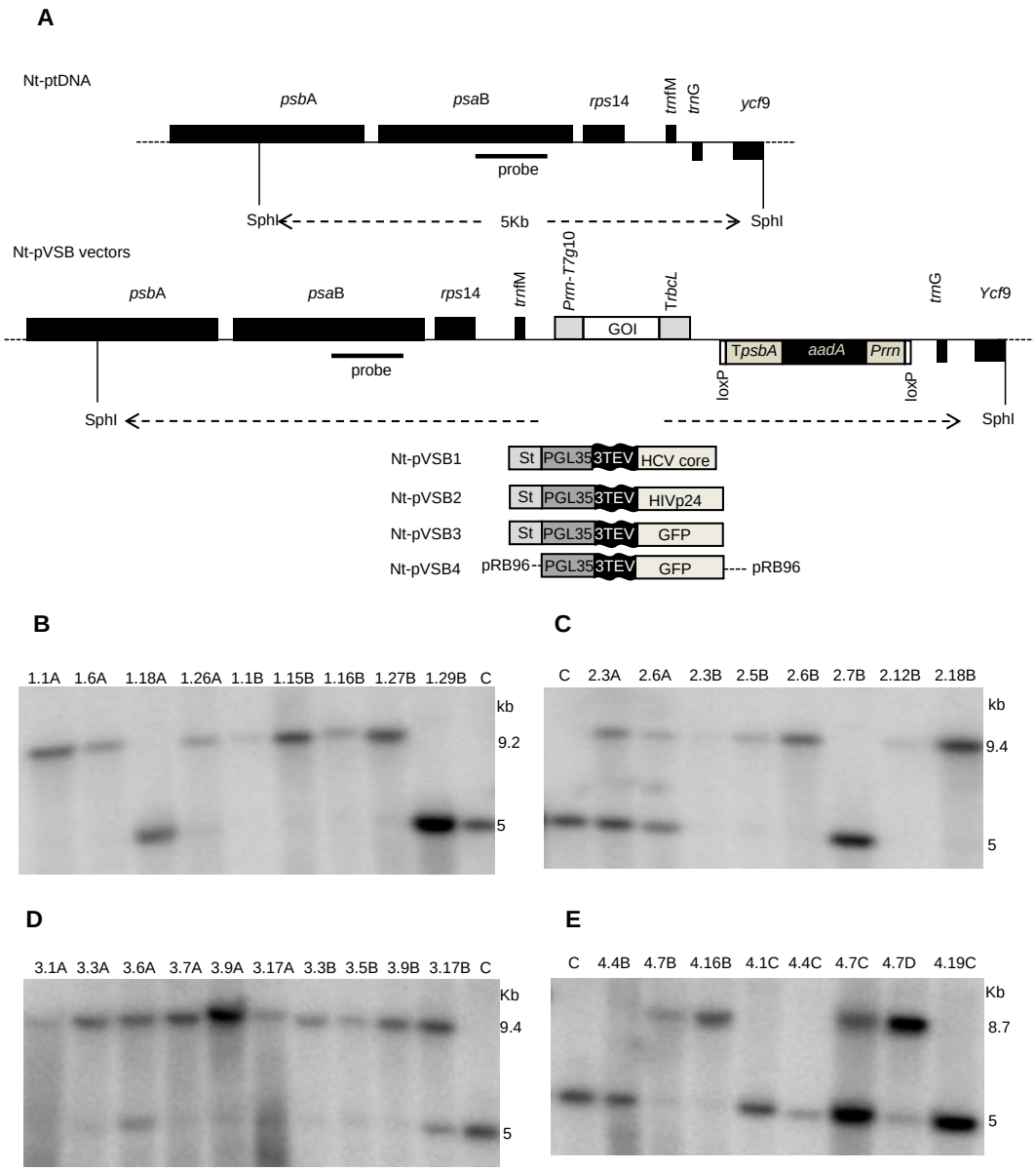

Figure. 2.2 Engineering of plastid transformants with vectors of the pVSB series.
(A) Physical map of the targeting region in the plastid genome and structure of plastid transformation vectors of the pVSB series harboring the "genes of interest" (GOI). The GOIs in this study are the coding regions of the vaccine candidates HCV core protein (pVSB1) and HIVp24 (pVSB2). The transgene expression cassette consists of the Prrn promoter fused to the 5′ untranslated region (5′UTR) from gene 10 of phage T7 (Prrn-T7g10) and the 3′UTR of the plastid rbcL gene (TrbcL). The transgenes are targeted to the intergenic region between *trn*fM and *trn*G. The chimeric selectable marker gene aadA is flanked by loxP sites to facilitate marker excision by the Cre site-specific recombinase. (B-E) RFLP analysis of tobacco plastid T_0 transformants. Total cellular DNA was digested with *Sph*I and hybridized with probe *psaB* (map position shown in Figure 1A). Data are shown for transplastomic lines transformed with plasmids pVSB1-pVSB4 and wild-type lines. The fragment size of the molecular weight marker is indicated on the right. Numbering of independently generated transplastomic lines is indicated above each of the lanes (example: 1.1A: corresponds to construct pVSB1, line 1A).

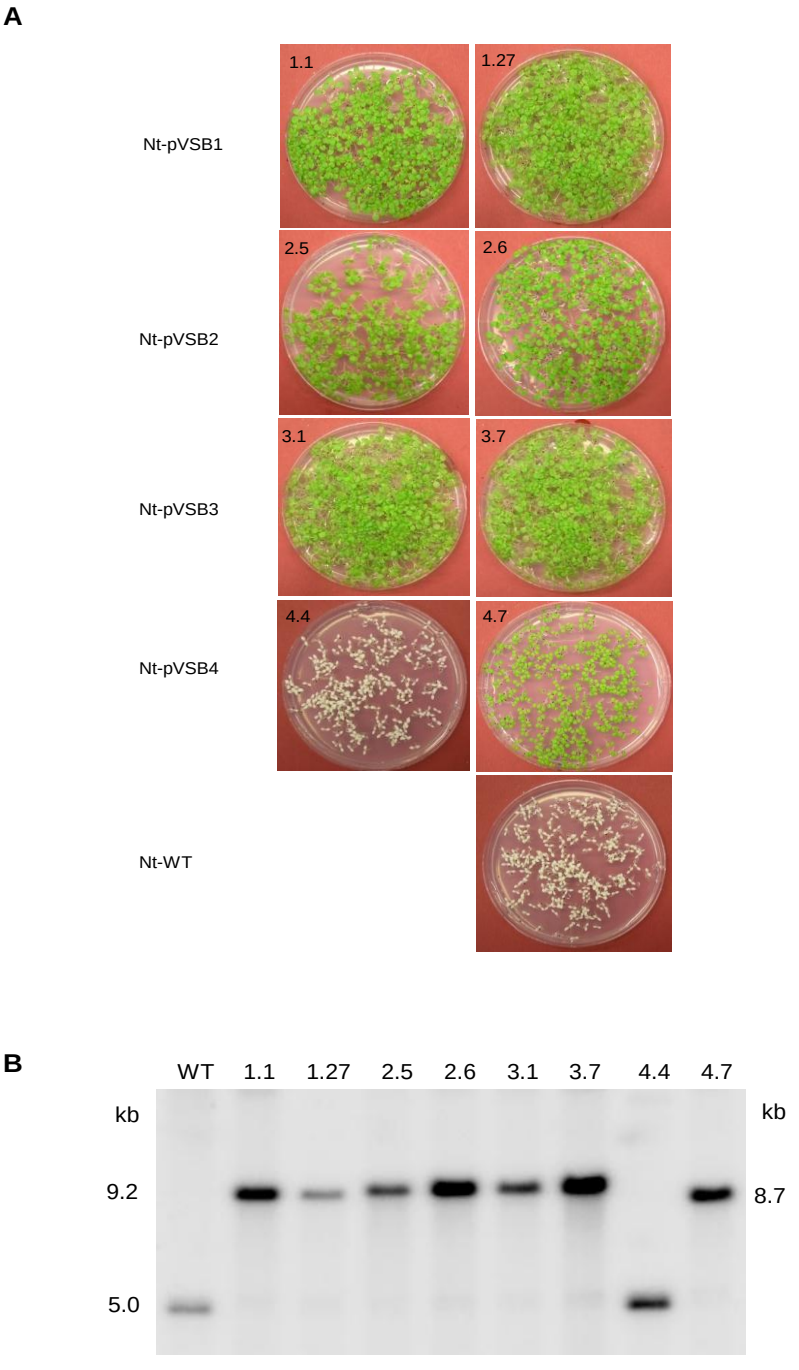

Figure 2.3 Analysis of transplastomic plants.
(A) Seed germination assays on spectinomycin-containing medium to confirm homoplasmy of transplastomic lines. Eight lines representing four different constructs are shown as examples. WT, wild type. (B) DNA gel blot analysis of T_1 transplastomic lines. This blot confirms that stable homoplasmic lines had been isolated for the four expression constructs pVSB1 – 4.

Whereas wild-type seedlings bleach out and die on spectinomycin-containing medium, transplastomic seedlings are resistant and indistinguishable from wild-type seedlings grown in the absence of the antibiotic. The homoplasmic lines were 100% resistant to spectinomycin (Fig. 2.3A). From the resulting T_1 generations, two independently generated transplastomic lines per construct were confirmed by Southern blotting (Fig. 2.3B). The absence of residual copies of the wild-type chloroplast genome from the transplastomic lines revealed that those lines were homoplasmic. In parallel to the RFLP analysis, seed assay for confirm homoplasmy and maternal transgene inheritance were carried out, which provide the most sensitive assays of the homoplasmic state of plastid transformants (Bock, 2001).

2.1.5 Expression and accumulation of the recombinant fusion protein in transplastomic tobacco

Northern-blot analysis of total RNA from the leaves of pVSB1*,* pVSB2, pVSB3 and pVSB4 derived lines and an untransformed control plant was performed using transgene specific probes. Hybridization to a HCV core protein and a HIVP24 probe detected transcripts with the band of 2.6kb (Fig. 2.4A) and 2.9kb (Fig. 2.4B), respectively representing the transplastomic mRNA accumulation in pVSB1 and pVSB2. In the GFP fusion constructs, pVSB3 and pVSB4, the expected 2.9-kb mRNA for the fusion gene was detected only in pVSB3 (Fig. 2.C) but not in pVSB4 (Fig. 2.4D). In pVSB4, the expression cassette derived from the tobacco plastid P*atpI* promoter (Wurbs et al*.,* 2007) is known to be weak compared to the plastid P*rrn* promoter in combination with the 5' UTR of the bacteriophage T7 gene 10 (Kuroda and Maliga, 2001). This could be the reason for the lack of expression in pVSB4.

SDS-PAGE of total protein extracts followed by Western blot analysis using anti-streptavidin and anti-HIVp24 antibodies confirmed expression of the Streptavidin-PGL35-HIVp24 fusion protein in both pVSB2-derived independent transgenic lines (2.5 and 2.6). A major band at 80 kDa was detected in these lines and corresponded to the predicted molecular mass of Streptavidin-PGL35-HIVp24 (Fig. 2.5B). Streptavidin-PGL35-HCV core fusion protein in transgenic line pVSB1 (1.1) was detected by the anti-streptavidin antibody and gave the expected band at around 80 kDa. A lower molecular mass band at 44 kDa was also detected (Fig. 2.5A). The lower molecular mass band may be due to degradation of the fusion protein or the utilization of an alternative translation initiation codon. No recombinant protein was detected in samples extracted from pVSB3 (3.7) and wild type control plants (Fig. 2.5c).

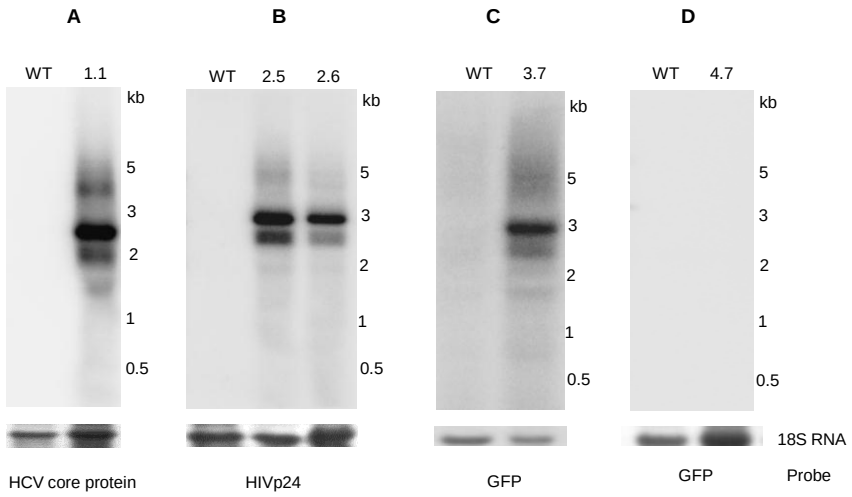

Figure 2.4 Northern blot analysis of pVSB1 – 4 expression in transplastomic tobacco plants.
Total cellular RNA was electrophoretically separated, blotted and hybridized to a radiolabelled HCV core protein probe (A), HIVp24 probe (B), and an GFP probe (C and D). The sizes of major hybridizing bands in all cases corresponded to the expected size. The PGL35-GFP fusion encoded by pVSB4 in line 4.7 was not expressed at a detectable level. Ribosomal 18S RNA is shown as an RNA loading control.

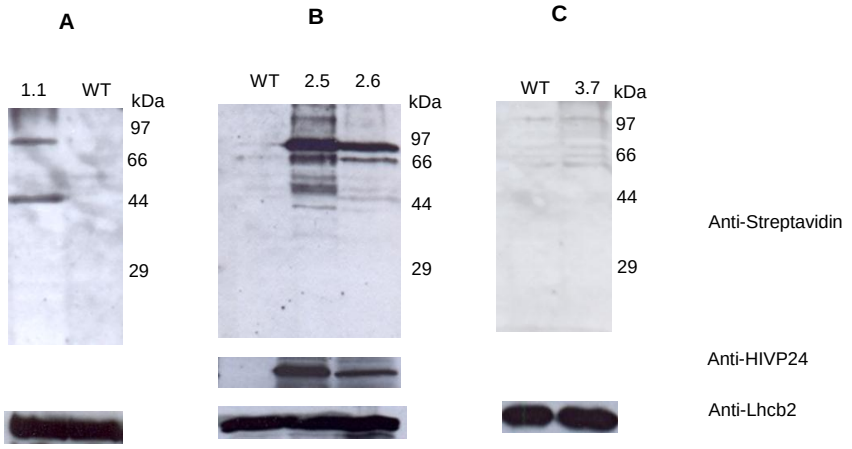

Figure 2.5 Recombinant fusion protein accumulation in transplastomic tobacco plants.
(A-C)Western blot analysis of lines pVSB1 (1.1) pVSB2 (2.5, 2.6) and pVSB3 (3.7) using anti-STREP, anti-HIVP24 and anti-Lhcb2 antibodies. Ten micrograms of total cellular protein were loaded per lane. The Lhcb2 antibody signal (bottom line) was used as a loading control.

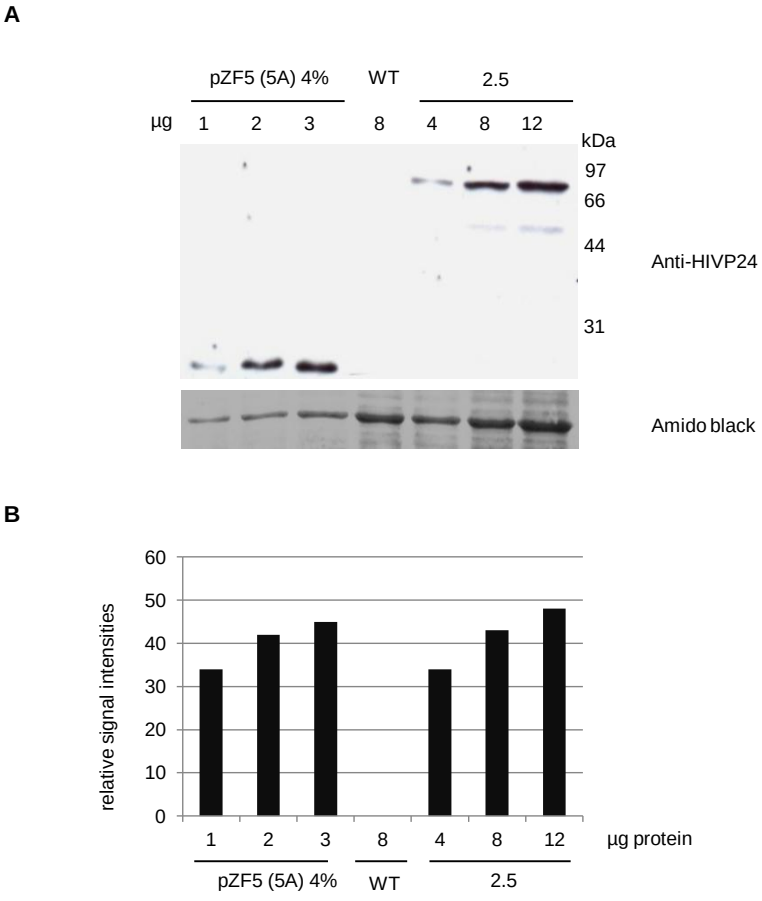

Figure.2.6 Western blot analysis for quantification of fusion protein accumulation in transplastomic pVSB2.5

(A)Total soluble protein extracted from line pVSB2.5 (4, 8 and 12 µg) was used. A dilution series of soluble protein extracted from line pZF5.5A expressing soluble HIVp24 at 4% of total soluble protein (1, 2 and 3 µg) was used as reference for protein quantification and amido black staining of the membrane showing the large subunit of RubisCO (RbcL) was used as a loading control.

(B) Corresponding immunoblot signal intensities were quantified using a Bio-Rad ChemiDoc XRS system

Western blotting using Lhcb2 a (chlorophyll a/b binding protein) antibody was used to control for equal loading. The expression level of Streptavidin-PGL35-HIVp24 fusion protein was quantified by Western blotting using the anti-HIVp24 antibody and a dilution series (4, 8 and 12 µg) of total leaf protein extracted from transplastomic line pVSB2 (2.5). A dilution series of a total extract of tobacco line pZF5.5A (Zhou et al., 2008) expressing soluble HIVp24 to 4% of total soluble protein (1, 2 and 3 µg) was used as reference. The proportion of total recombinant protein in line pVSB2.5 was estimated to be around 1.0% of the total soluble protein (Fig. 2.6). Streptavidin-PGL35-HCV core fusion protein in transgenic line pVSB1 (1.1) was detected using the anti-streptavidin antibody and gave a band of the expected size but of weaker intensity probably indicating lower levels of expression (Fig. 2.5A). For further studies, we only used the pVSB2 (2.5) transplastomic line expressing Streptavidin-PGL35-HIVp24.

2.1.6 Over expression of recombinant fusion proteins leads to enlargement of the plastoglobules

Visually, pVSB1 and pVSB2 transplastomic lines appeared to be wild type. To monitor growth and development at different stages, non-transformed wild type and transplastomic lines pVSB1 (1.1) and pVSB2 (2.5) were raised from seeds in multipurpose compost, without the addition of fertilizer. Initially, plants were grown under defined conditions in a growth room with a 16-h/8-h light/dark cycle for one week and then transferred to a greenhouse. The plants developed normally at the seedling stage and also at the age of 4 and 12 weeks (Fig. 2.7A), having wild-type growth rates. The fertility was normal. Photosynthesis parameters and pigments did not differ significantly from the wild type (Table 1). To investigate chloroplast ultrastructure, we examined chloroplasts in wild-type and transplastomic lines by transmission electron microscopy (Fig. 2.7B). Wild-type chloroplasts had normal size plastoglobules (approx. 50 nm). In contrast, plastoglobules in both transplastomic lines showed a massive expansion up to around 300 nm.

Plant	Total Chlorophyll (mg/g fresh weight±SD)	Fv/Fm
Wild type	1.18±0.02	0.786±0.018
1.1	1.19±0.04	0.776±0.011
2.5	1.17±0.02	0.786±0.019

Table.1 Chlorophyll content and fluorescence in leaves of tobacco wild-type and Streptavidin-PGL35-fusion lines pVSB1 (1.1) and pVSB2 (2.5)

A

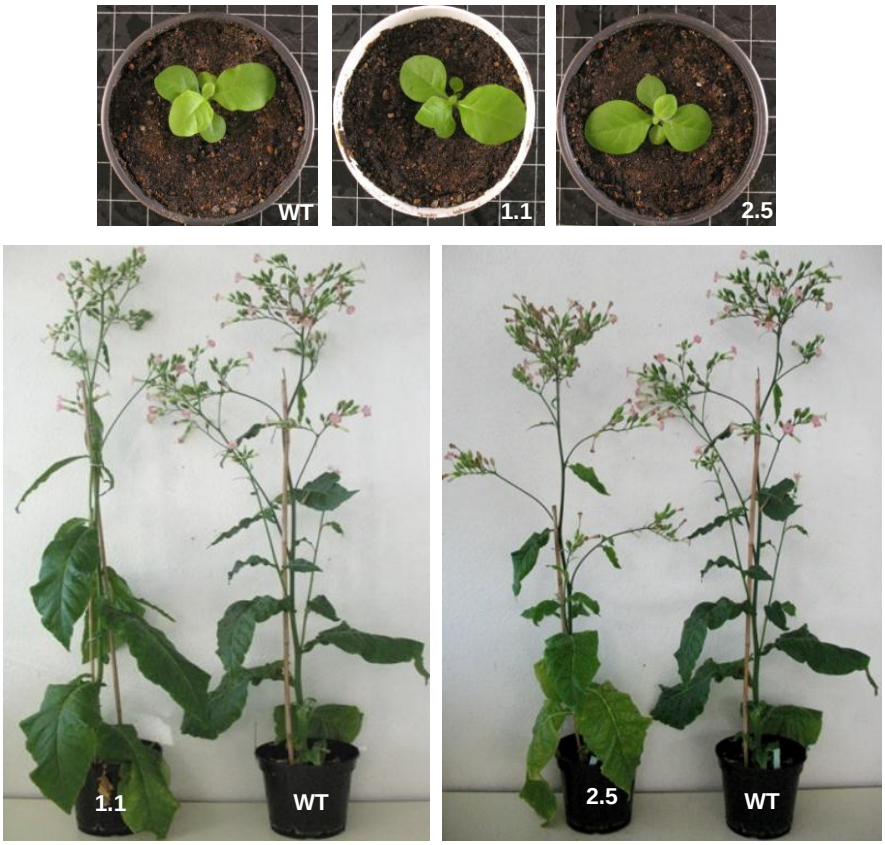

B

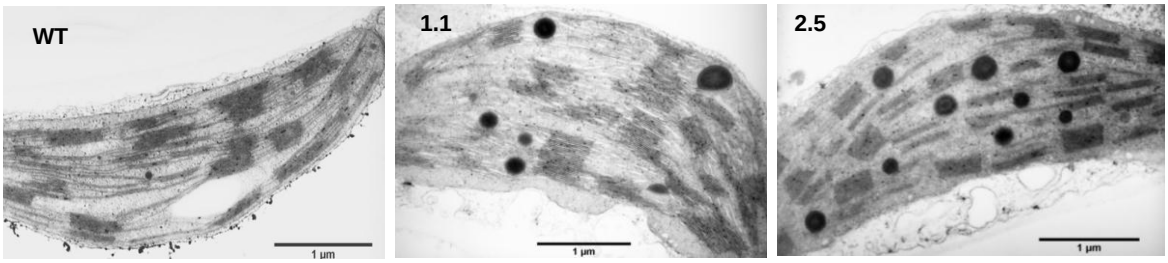

Figure 2.7 Phenotypes and ultrastructure of chloroplast of wild-type and transplastomic lines
(A) Phenotype of homotransplastomic tobacco expressing Streptavidin-PGL35~3TEV- HCV core protein(pVSB1.1) and Streptavidin-PGL35~3TEV-HIVP24 (pVSB2.5) in comparison to wild type (WT) (B) Expansion of plastoglobules in transplastomic lines pVSB1.1 expressing Streptavidin-PGL35~3TEV-HCV core protein and pVSB2.5 expressing Streptavidin-PGL35~3TEV-HIVP24. Samples of intact leaf tissue from wild-type, line 1.1 and line 2.5 were prepared and observed by transmission electron microscopy. (Bars =1.0 µm).

2.1.7 Localization of the Streptavidin-PGL35-HIVp24 fusion protein in transplastomic chloroplasts

Chloroplasts were isolated from homoplasmic line 2.5 expressing Streptavidin-PGL35-HIVp24. Immunofluorescence using *Strep*MAB-Immo Oyster 488 gave an intense punctate fluorescence pattern inside chloroplasts (Fig. 2.8, right panels). This pattern is consistent with plastoglobule localization. *Strep*MAB-Immo Oyster 488 green fluorescence was not observed in wild-type chloroplasts (Fig. 2.8, left panels). Chloroplast position is indicated by differential interference contrast microscopy (DIC).

2.1.8 Targeting of the Streptavidin-PGL35-HIVp24 fusion protein to plastoglobules

To determine whether the recombinant fusion protein properly assembled into plastoglobules, the total chloroplast membrane fractions from WT and pVSB2.5 expressing Streptavidin-PGL35-HIVp24 were subjected to floatation centrifugation on sucrose density gradients (45-5% sucrose) to separate low density plastoglobules from higher density envelope and thylakoid membranes. Starting from the top, the gradient was divided into 25 fractions that were separated by SDS-PAGE followed by immunoblotting with antisera against PGL40 and Lhcb2 as plastoglobule and thylakoid markers, respectively (Fig. 2.9A, B). The results demonstrated the separation of plastoglobules (fractions 1–3) from thylakoid membranes (predominantly in fractions 23–25). Streptavidin-PGL35-HIVp24 detected by anti-HIVp24 antibodies, co-distributed with PGL40 (fractions 1-3, 17-25).

However, relative distribution was not identical. No specific signal was detected with the anti-HIVp24 antibody in the wild-type plastoglobule fractions. To estimate the distribution of the recombinant fusion protein resulting from the gradient floatation, the amount of recombinant protein at 5% sucrose was compared with that at 45% sucrose by immunoblotting. Around 20% of the recombinant fusion protein was present in the low-density plastoglobules (5% sucrose) and around 80% in high density thylakoid membranes (45% sucrose). Five micrograms of isolated plastoglobule protein from wild type (WT) and pVSB2.5 were resolved by SDS-PAGE, transferred to nitrocellulose, and immunoblotted with antisera against Streptavidin, HIVP24, PGL30.4 and PGL40 (Fig. 2.9C). The experiment clearly showed that Streptavidin-PGL35-HIVp24 is present in isolated plastoglobules. Lhcb2

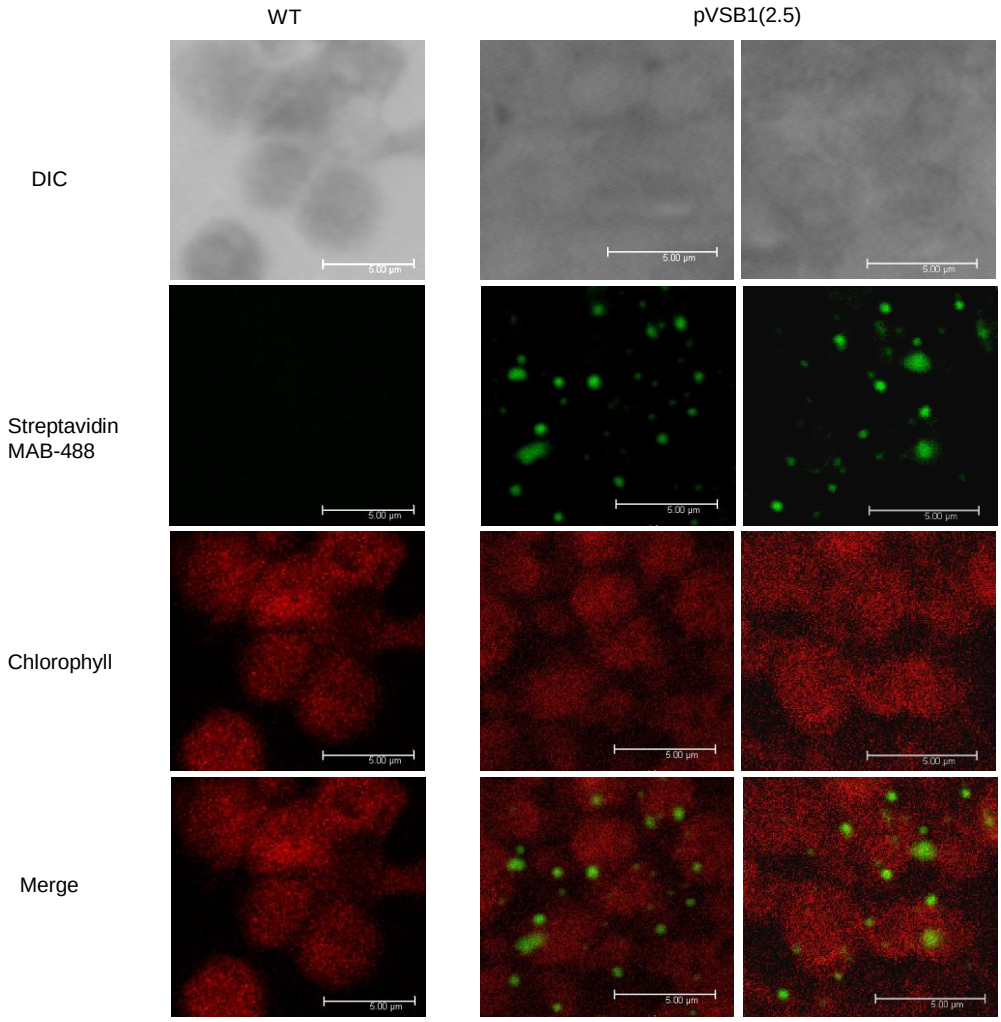

Figure. 2.8 Localization of Streptavidin-PGL35-HIVp24 in transplastomic chloroplasts.
Confocal immunofluorescence microscopic analyses of wild-type and pVSB2 (2.5) chloroplasts. Isolated chloroplasts were decorated with *Strep*MAB-Immo Oyster 488 to detect Streptavidin-PGL35-HIVp24 (green colour signal). Red auto fluorescence (chlorophyll) and the merge of the two signals are also shown. Bars: 5.0 µm.

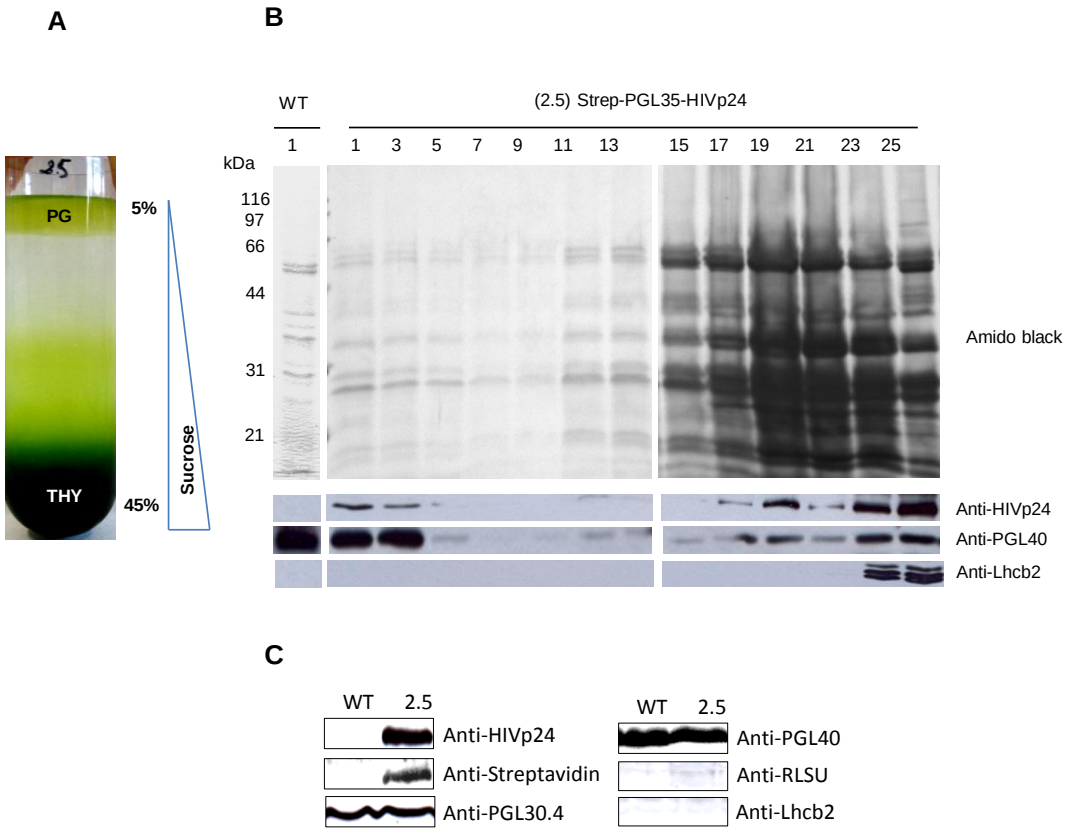

Figure. 2.9 Purification of recombinant plastoglobules by floatation centrifugation.
(A) Total membranes from isolated chloroplasts were separated by floatation on a continuous sucrose gradient. Plastoglobules are visible as a yellowish layer at the top of the gradient. Th, thylakoid membranes; PG, plastoglobules. (B) Western blot analysis of fractions from the density gradient. After ultracentrifugation, 0.5 ml fractions were collected starting from the top of the gradient. Proteins contained in 300 µl of fractions 1-25 were separated by SDS-PAGE, transferred to a nitrocellulose membrane and stained with amidoblack (upper panel). Chloroplast fractions from wild type plants (WT) and pVSB2.5 are shown. Antibodies against HIVp24, PGL40 and CAB were used for immuno blotting, as indicated (lower panels). (C) Plastoglobules were isolated from total chloroplast membranes of wild type (WT) and pVSB2.5. Five micrograms of plastoglobule protein were resolved by SDS-PAGE, transferred to nitrocellulose, and immunoblotted with antisera to the proteins as indicated. HIVP24, Streptavidin (recombinant protein), PGL30.4, PGL40 (plastoglobule), Lhcb2 (thylakoid) and RLSU (stroma).

and RLSU (large subunit of RubisCO) proteins were not detected by the respective antibodies confirming the absence of thylakoids and stroma, respectively, from the plastoglobule fraction.

2.1.9 Purification of HIVp24 using streptavidin-biotin affinity chromatography followed by TEV elution

Only a relatively small fraction of Streptavidin-PGL35-HIVp24 was present in the purified plastoglobule fraction (Fig. 2.10). To optimize the yield during purification, total chloroplasts rather than purified plastoglobules were solubilized with Triton-X-100 (1% v/v) in the homogenization medium. The resulting solubilized fraction was separated from insoluble material by centrifugation at 20,000×g. The Streptavidin-PGL35-HIVp24 fusion protein was present in the supernatant, which was subjected to streptavidin-biotin affinity purification using a 2-iminobiotin column. After washing with ammonium carbonate/sodium chloride buffer (pH 11), HIVp24 was eluted from the column by TEV protease cleavage of the bound Streptavidin-PGL35-HIVp24 fusion protein. After TEV protease elution, the column was again washed with ammonium carbonate/sodium chloride buffer (pH 11) followed by a final elution step using sodium acetate buffer (pH 4.0). Aliquots retained at each of the steps were subjected to SDS-PAGE separation and transferred to nitrocellulose followed by amido black staining. The analysis revealed a single dominant band in the TEV eluate at the predicted molecular weight of HIVp24 (Fig. 8 upper panel). The nature of the band was confirmed by immunoblotting using the anti-HIVp24 antibody clearly indicating the presence of HIVp24 in the TEV protease eluate (Fig. 8, lower panel).

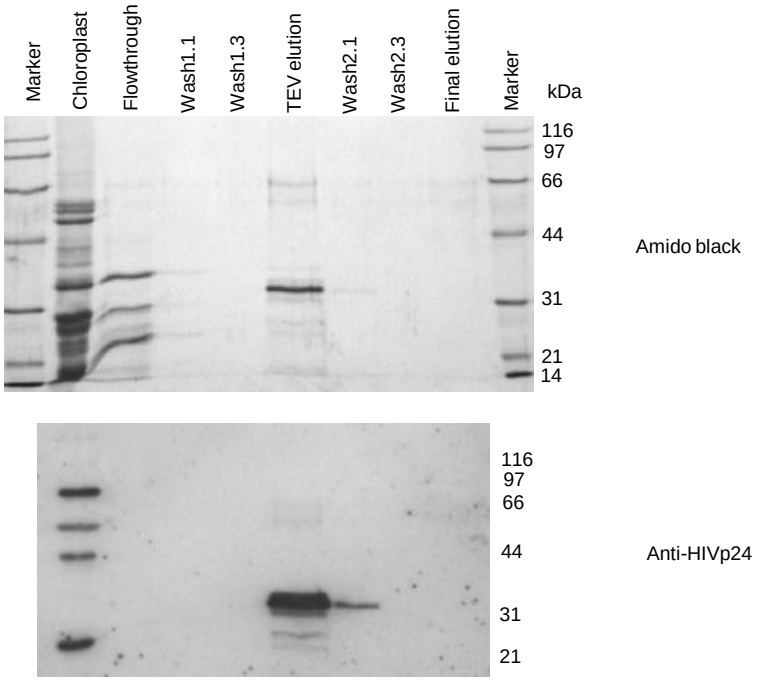

Figure. 2.10 Purification and analysis of recombinant HIVp24 protein from pVSB2 (2.5) chloroplasts. Upper panel: Amidoblack-stained nitrocellulose membrane of HIVp24 purified from pVSB2 (2.5) chloroplasts using a 2-iminobiotin column for avidin affinity chromatography and TEV elution. Note the major band in TEV eluate (TEV-HIVp24 elution; lane 6). Lower panel: Western-blot analysis of the same nitrocellulose membrane using sheep anti-HIVp24 as the primary antibody.

2.2 Characterization of plastidial At-SOUL heme binding proteins

2.2.1 Homologs and putative topology of At-SOUL heme binding proteins

A SOUL/HBP homolog, SOUL4, has been identified in Arabidopsis plastoglobules. To identify further homologs, we used the animal p22HBP/SOUL (human and murine) amino acid sequences to conduct a BLAST search of the Arabidopsis genome data bases. A total of five expressed homologues (AtSOUL1-5), At1g17100, At1g78460, At2g37970, At3g10130 and At5g20140 were identified based on the Arabidopsis Information Resource, http://www.arabidopsis.org/). A 6th family member exists but is a non-expressed pseudogene. A multiple sequence alignment of AtSOUL heme binding protein amino acid sequences is shown in Fig. 2.12A. The murine p22HBP/SOUL structure (Dias et al., 2006) consists of a nine-stranded twisted β-barrel flanked by two α-helices flanking a conserved novel hydrophobic cleft for heme (Fig. 2.11). When compared with p22HBP/SOUL (human and murine) Arabidopsis SOUL heme binding proteins give similar primary structural predictions including a novel hydrophobic cleft between αA helix and the β8-β9 loop (Takahashi et al., 2008). In addition AtSOUL4 and AtSOUL5 acquired predicted chloroplast transit peptides at the N-terminus. While AtSOUL4 was identified in proteomic studies of plastoglobules, AtSOUL5 was found in the thylakoids. AtSOUL1 and AtSOUL3 are predicted to be localized in the cytosol but were found in the vacuole proteome. Phylogenetic analysis of Arabidopsis SOUL heme binding proteins (Fig. 2.12B) showed two pairs of closely related AtSOUL heme binding proteins (AtSOUL2 and -3; AtSOUL4 and -5), the fifth homolog being on a separate branch.

2.2.2 Localization of AtSOUL4 heme binding protein

AtSOUL4 is a nuclear-encoded protein imported into chloroplast

AtSOUL4 is a nuclear-encoded plastid protein that, after import and processing, is targeted to plastoglobules inside the plastid. The AtSOUL4 preprotein was synthesized in a coupled transcription/translation system in the presence of [^{35}S]methionine and imported into chloroplasts isolated from 3 week old Arabidopsis seedlings. After chloroplast reisolation, the

plastid proteins were separated by SDS-PAGE and analyzed using a PhophorImager. Two major radioactively labeled proteins were detected: one with an apparent molecular mass (MM) of 36 kDa corresponding in mass to the *in vitro*-synthesized product of the AtSOUL4 gene and the second with an apparent MM of 30 kDa (Fig. 2.13A upper panel). After treatment of chloroplasts with thermolysin, most of the 35 kDa polypeptide had been digested, whereas the 30 kDa protein was largely protected against proteolytic attack. This shows that AtSOUL4 preprotein is imported into the chloroplast. To confirm the localisation of AtSOUL4 in chloroplast, we engineered a construct encoding a CFP fusion under the control of the cauliflower mosaic virus (CaMV) 35S promoter. The AtSOUL4-CFP and empty vectors were transformed into *Nicotina benthamiana* leaves by agroinfiltration and analysed by confocal laser scanning microscopy. The AtSOUL4-CFP fluorescence was present in chloroplast punctate structures (Fig. 2.13.B upper pannel), but was detected neither in the thylakoid nor the envelope membranes. No fluorescence was detected in empty vector agroinfilterated leaves (Fig. 2.13.B lower pannel).

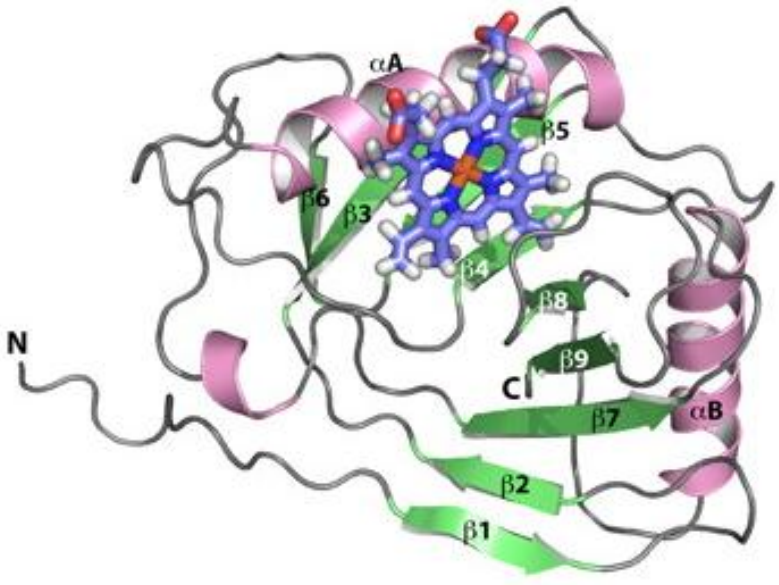

Figure 2.11 Ribbon model of the p22HBP/SOUL crystal structure.

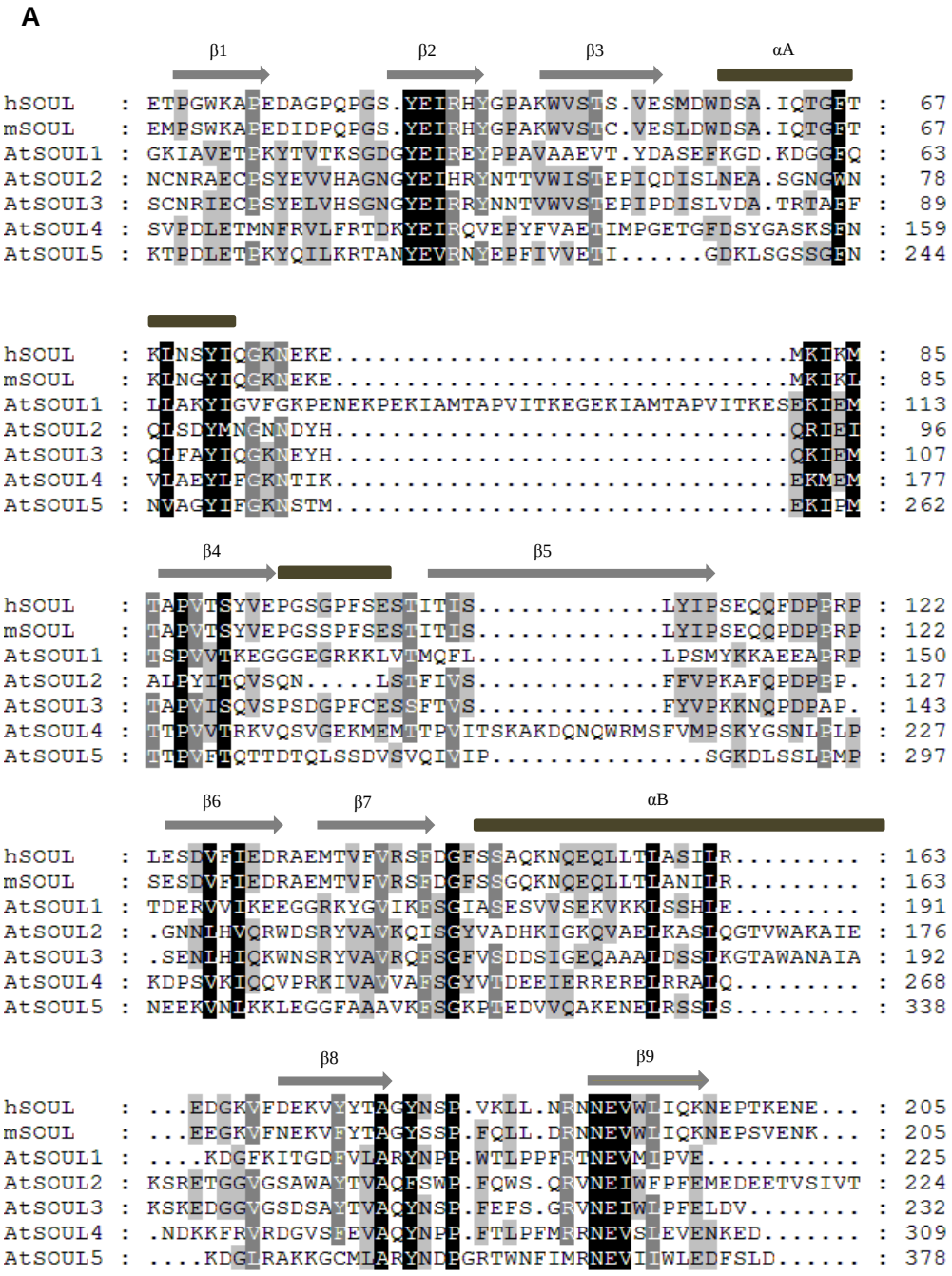

Figure 2.12 The Arabidopsis SOUL heme binding protein family and primary structures (see caption on page 45)

B

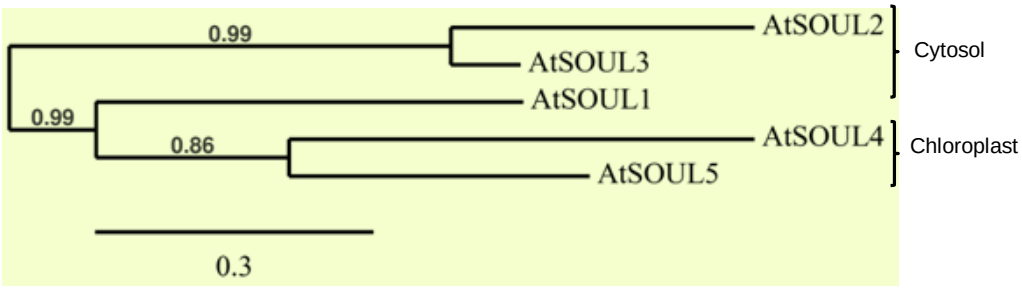

Figure 2.12 Primary structure and phylogenetic analysis of SOUL heme binding proteins (continued). (A) Alignment of amino acid sequences for Arabidopsis SOUL1, SOUL 2, SOUL3, SOUL4 and SOUL5, and human as well as mouse SOUL. The predicted N-terminal transit peptide sequences were removed from SOUL4 and SOUL5. Sequence alignment was performed using CLUSTALW software. The following features are highlighted: 9-stranded β-barrel flanked by two long α-helices. (B) Phylogenetic analysis of SOUL in Arabidopsis. The neighbour-joining phylogenetic tree was constructed using TreeDyn 198.3 after CLUSTALW alignment of the amino acid sequences of SOUL heme binding proteins in Arabidopsis.

Colocalisation of AtSOUL4-CFP and AtPGL35-YFP

To determine whether AtSOUL4 heme binding protein colocalised with the plastoglobule marker AtPGL35, the two proteins were co-expressed as CFP and YFP fusion proteins in *Nicotina benthamiana* leaves by agroinfilteration. In this transient expression experiment, AtSOUL4-CFP AtPGL35-YFP as well as AtPGL35-YFP fluorescence was present in globular structures inside chloroplasts (Fig. 2.13C). Both the merge of the independent fluorescence images and the pixel intensity analysis showed an overlap of the fluorescence, indicating co-localization of AtSOUL4 and AtPGL35 in plastoglobules. The higher magnification of single chloroplasts together with the fluorescence images clearly shows AtSOUL4-CFP presence in the plastoglobule (Fig. 2.13D).

Heterologous expression of AtSOUL4 heme binding protein

The AtSOUL4 gene was amplified from Arabidopsis cDNA using gene specific primers. The coding sequence of AtSOUL4 was cloned in pET21d vector resulting in a C-terminal His_6-tag. The full-length preprotein was expressed in *E. coli* BL21 (DE3) (Novagen) and purified under denaturing conditions by Ni-NTA chromatography using an ACTA prime system (Fig. 2.14A). The purified protein was used to raise antibodies in rabbits. Antibodies were affinity-purified using recombinant AtSOUL4 coupled to Affi-Gel 10 (Fig. 2.14B). AtSOUL4 was detected intotal protein extracts prepared from Arabidopsis using the purified AtSOUL4 antibody (Fig. 2.14C).

The ORF of the AtSOUL4 cDNA predicts 309 amino acids including a chloroplast transit peptide of 72 amino acids at the N-terminus. For further studies, a pET21d construct lacking the transit peptide was engineered. This lead to the production of soluble, mature AtSOUL4 in *E. coli* BL21(DE3) cells. The AtSOUL4 heme binding proteins without transit peptide was expressed at high levels upon IPTG induction (Fig. 2.15A, lane I compare with UI) and around 30% of recombinant AtSOUL4 heme binding protein was soluble (Fig. 2.15A, lane S compare with P) which was confirmed by immunoblotting (Fig. 2.15B). From the soluble fraction of the bacterial extract AtSOUL4 heme binding protein was purified to near homogeneity by Ni-NTA affinity chromatography (Fig. 2.15C).

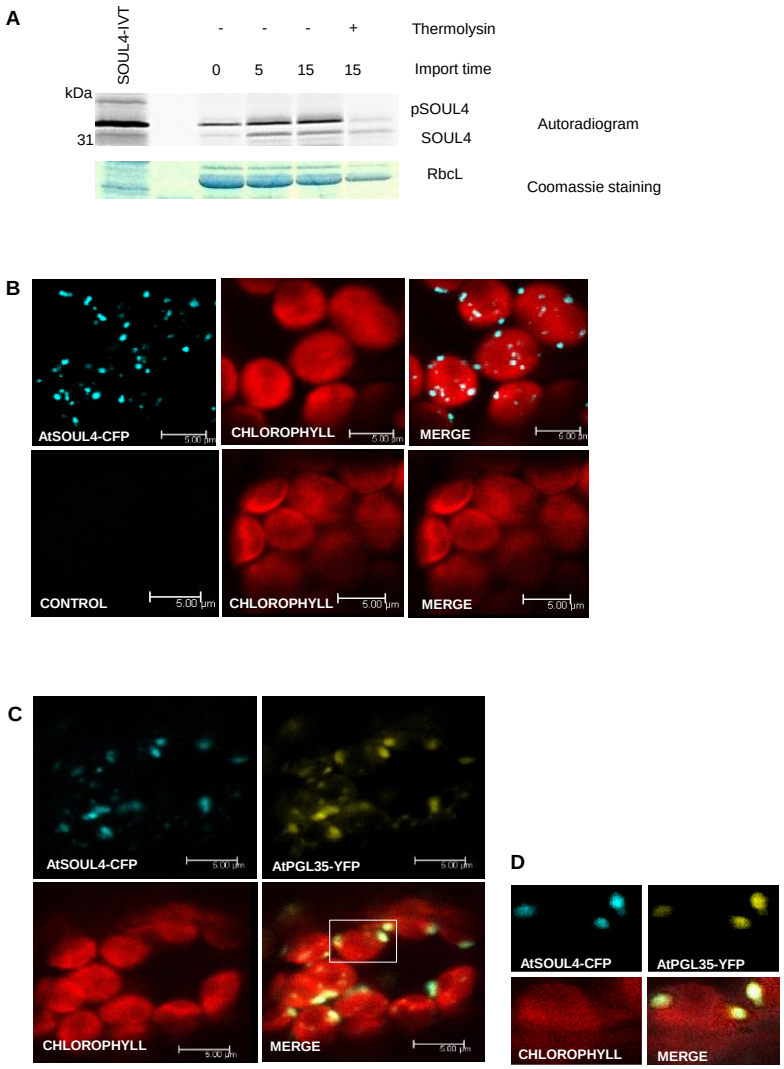

Figure 2.13 Localisation AtSOUL4 heme binding protein
(A) Imported of AtSOUL4 preprotein into isolated chloroplasts. *In vitro* synthesized [^{35}S]AtSOUL was incubated with isolated Arabidopsis chloroplasts in a time course experiment. After reisolation and thermolysin treatement the samples were analyzed by SDS-PAGE (lower panel) followed by autoradiography (upper panel). Preprotein (35-kDa Fragment) and after thermolysin treatment (31-kD Fragment) mature protein are indicated. (B) Transient expression in *Nicotina benthamiana* leaves by agroinfilteration of AtSOUL4-CFP and empty vector (CONTROL). Fluorescent proteins were visualized by confocal laser scanning microscopy 48h after agroinfilteration. Chlorophyll, CFP and merge indicate chlorophyll autofluorescence, CFP fluorescence, and the superposition of both fluorescent signals, respectively. Bar length: 5 µm. (C) Colocalisation analyses of AtSOUL4-CFP and AtPGL35-YFP. The AtSOUL4-CFP and AtPGL35-YFP were transiently co-expressed in leaves of *Nicotiana benthamiana* and localization was examined by fluorescence microscopy. All images were taken at the same magnification. Chlorophyll: chlorophyll autofluorescence, merge: superposition of YFP and CFP signals (Yellowish green colour). The scale bar represents 5µm. (D) Higher magnification of the boxed region from colocalisation of AtSOUL4-CFP and AtPGL35 (merge).

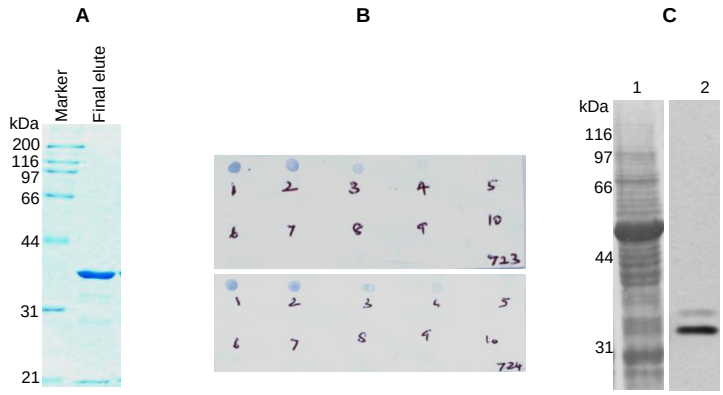

Figure 2.14 At SOUL4 protein purification, antibody production and detection intotal leaf extract.
(A) Full length insoluble AtSOUL4 expressed in *E.coli* was purified by denaturing nickel affinity chromatography on a ACTA prime system. Purified AtSOUL4 protein was analyzed by SDS-PAGE and Coomassie Blue staining. (B) Polyclonal antibodies raised aganist AtSOUL4 were affinity-purified and the presence of IgG was confirmed by spotting on nitrocellulose and Amido black detection in fractions 1 to 3 of the purification procedure. (C) Detection of AtSOUL4 intotal protein extract prepared from wild type Arabidopsis leaves. 30 µg of protein was resolved by SDS-PAGE, transferred to nitrocellulose membrane and stained with amidoblack (lane 1). AtSOUL4 was detected by immunoblotting using a specific affinity purified antibody (lane 2).

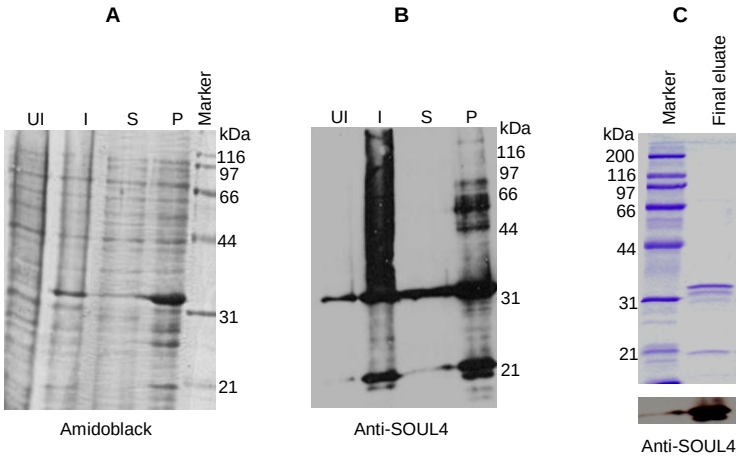

Figure 2.15 Expression of mature AtSOUL4 with a hexahistidinyl-tag
(A) Mature AtSOUL4 was expressed in *E.coli* BL21(DE3) cells. Uninduced (UI), induced (I), soluble (S) and insoluble pellet (P) fractions were separated by SDS-PAGE, transferred to nitrocellulose membrane and stained with Amido black (B) Immunoblot using the anti-SOUL4 antibody shows overexpression of the AtSOUL4 protein (C) AtSOUL4 expressed in *E.coli* was purified by nickel affinity chromotography (ACTAprime) and purified soluble AtSOUL4 protein was seperated by SDS-PAGE and detecte with anti-SOUL4 antibody by Western blotting.

At SOUL4 heme binding protein present in plastoglobule fractions

To determine whether the AtSOUL4 heme binding protein is present in plastoglobules, the total membranes of isolated chloroplasts were separated from stromal proteins by centrifugation at 100,000×*g*. To separate plastoglobules from chloroplast membranes, the membrane pellet was resuspended in a 45% sucrose solution and overlaid with a continuous 45% to 5% sucrose gradient and centrifuged overnight at 100,000×*g*. This resulted in the separation of membrane fractions corresponding to broad and partially overlapping peaks of marker proteins by immunoblotting analysis (Fig. 2.16). Antibodies against the Lhcb2 protein gave strong signals in fractions 23-27, indicating the presence of thylakoid membranes in the high density sucrose fractions. AtTOC75, a protein of the outer envelope membrane, was detected in fractions 19–23. The lower density fractions 1–9 contained no detectable envelope membranes. The results demonstrated the separation of plastoglobules (fractions 1–5) from thylakoid membranes (predominantly in fractions 21–27). AtSOUL4 heme binding protein was detected by anti-AtSOUL4 antibodies and co-distributed with AtPGL40 (fractions 1-5, 19-27). However, their relative distribution was not identical.

2.2.3 Heme binding to AtSOUL4 *in vitro* and *in vivo*

To determine, whether AtSOUL4 binds to heme, a pull-down assay was performed. Soluble recombinant AtSOUL4 was passed over hemin-agarose as well as agarose alone as a negative control. Input, flow through, last wash, and eluted fractions were analyzed by immunoblotting. AtSOUL4 bound to hemin-agarose and was detected in the eluate fraction (Fig.2.17A, left panel, lane E), while it was not found in the agarose negative control (Fig.2.17A, right panel, lane E). To exclude non-specific binding to the hemin agarose, a heme competition assay was carried out. 100 µM AtSOUL4 was incubated with 10 mM hemin. After the incubation, the reaction mixture was passed over the hemin-agarose and subsequently washed and eluted. The fractions were analysed by SDS-PAGE followed by immunoblot analysis. This experiment demonstrated that AtSOUL4 did not bind to hemin-agarose after incubation with 10mM hemin (Fig. 2.17 B lane W1). These data indicate that AtSOUL4 binds to heme *in vitro.*

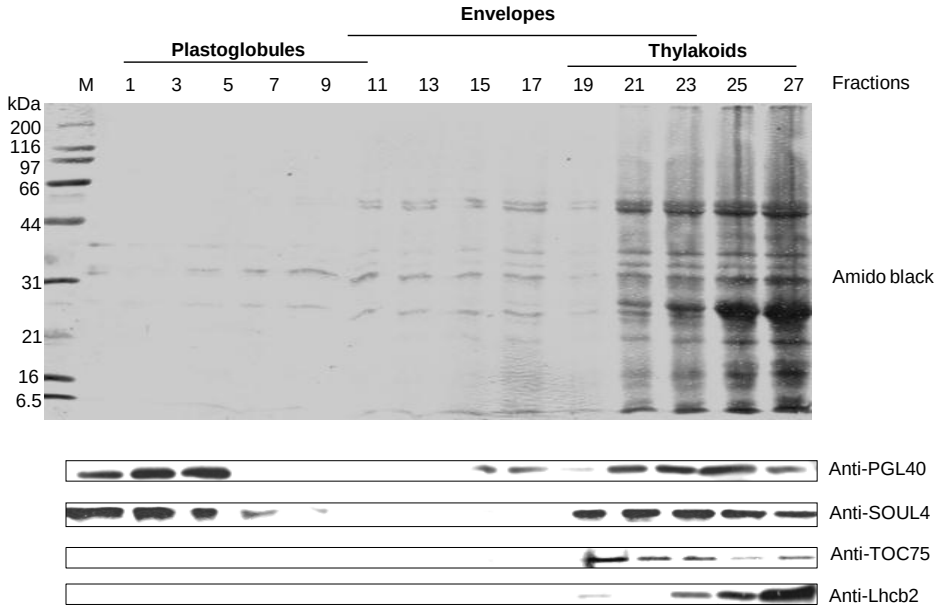

Figure 2.16 Western blot detection of AtSOUL4 in chloroplast membrane fractions. After sucrose gradient floatation of total chloroplast membranes, fractions were collected starting from the top of the gradient. Equal volumes of fractions 1-27 were separated by SDS-PAGE, transferred to a nitrocellulose membrane and stained with Amido black (upper panel). Antibodies against AtSOUL4, AtPGL40 (plastoglobulin), AtTOC75 (outer envelope membrane protein) and Lhcb2 (thylakoid) were used for immunoblotting, as indicated (lower panels).

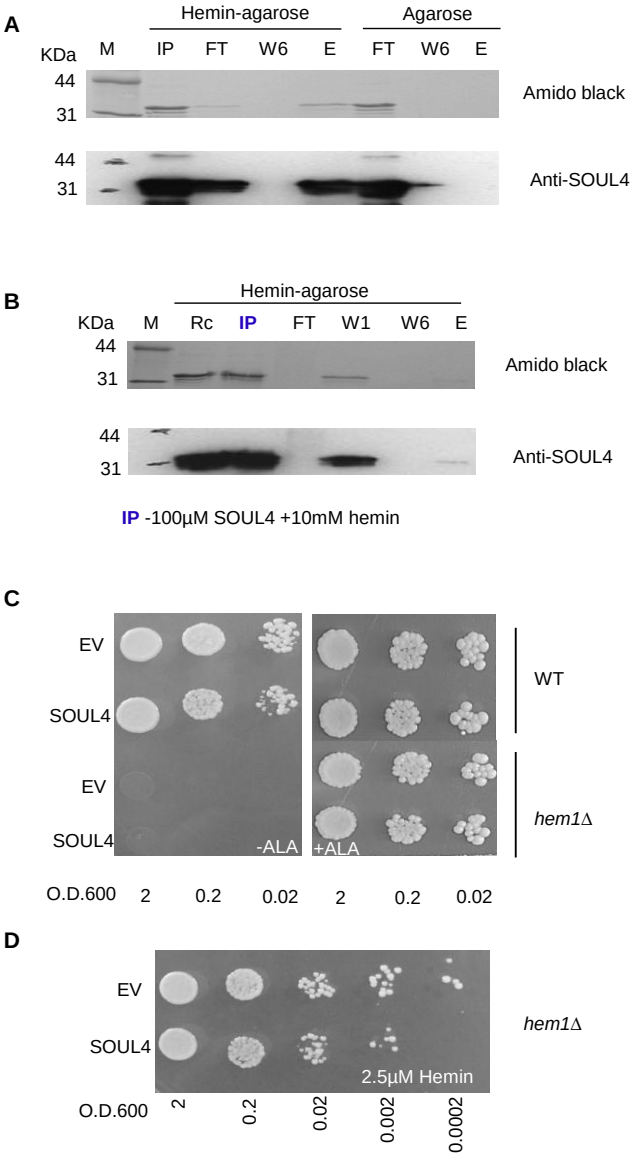

2.17 AtSOUL4 binds heme *in vitro* and *in vivo*

(A) Binding of AtSOUL4 to hemin-agarose or agarose alone, as negative control. The input (IP), flow-through (FT), wash (W1, W6) and eluted (E) fractions were analyzed by SDS-PAGE, transferred to a nitrocellulose membrane and stained with Amido black (upper panel). Antibodies against AtSOUL4 were used for immuno blotting, as indicated (lower panels). (B) AtSOUL4 binding to hemin-agarose in the presence of 10mM added soluble hemin. The input (IP), flow-through (FT), wash (W1, W6) and eluted (E) fractions were analyzed by SDS-PAGE, transferred to a nitrocellulose membrane and stained with Amido black (upper panel). Antibodies against AtSOUL4 were used for immuno blotting, as indicated (lower panels). (C) Expression of AtSOUL4 in wild type and *hem1Δ* yeast. Growth on synthetic (SG) medium with or without ALA supplementation is shown; WT, wild-type; EV, empty vector; SOUL4, over expression of AtSOUL4. (D) Expression of AtSOUL4 in *hem1Δ* yeast. Growth on half-strength synthetic GAL (SG) medium with 2.5µM Hemin supplementation is shown; EV, empty vector; SOUL4, over expression of AtSOUL4.

To test for *in vivo* heme binding (Protchenko et al., 2008), the effect of overexpression of AtSOUL4 in the wild type and *hem1*Δ strain yeast was analyzed. Recombinant AtSOUL4 expression did not alter the growth of wild type yeast (Fig. 2.17C, left panel). We further tested the effects of At-SOUL4 heme binding protein overexpression on the *hem1*Δ strain, which shows growth dependence on heme uptake systems and relies on heme or chemical precursors such as ALA. The empty vector and overexpression of AtSOUL4 in the *hem1*Δstrain had no effect on growth when the medium contained ALA (Fig. 2.17C, right panel). The heme deficiency of a *hem1*Δ strain can also be rescued by exogenous hemin. It was therefore tested whether overexpression of AtSOUL4 affected growth in the presence of hemin. Overexpression of AtSOUL4 inhibited growth in the presence of hemin, indicating that these suggesting that At-SOUL4 compete for heme-binding with the endogenous hemin utilizing systems. The empty vector showed no effect (Fig.2.17D). In summary, these data suggest that the AtSOUL4 specifically binds to heme *in vivo.*

2.2.4 *In vitro* phosphorylation of AtSOUL4

The serine–threonine protein kinase family member, casein kinase II (CKII), is highly conserved in all eukaryotes. One of the five Arabidopsis casein kinase II (CKII) alpha-subunits (At2g23070) is localized in the chloroplast stroma (Salinas et al., 2006) (http://ppdb.tc.cornell.edu/dbsearch/gene.aspx?id=8788&detail=all). The C-terminal region of AtSOUL4 has a conserved CKII target consensus sequence (S/T-D/E-X-E/D) in higher plants (Fig. 2.18A) and may therefore be a target of this kinase. To demonstrate that AtSOUL4 is an *in vitro* substrate of CKII, we incubated recombinant AtSOUL4 heme binding protein with (Fig. 2.18B, lane 3) or without (Fig. 2.18, lane 2) the recombinant maize CKII alpha-subunit in a phosphorylation assay. To test whether AtSOUL4 is a potential substrate of the stromal CKII, the *in vitro* phosphorylation assay using recombinant AtSOUL4 was carried out with (Fig. 2.18B, lane 3) or without (Fig. 2.18B, lane 2) Arabidopsis stromal fraction. All the samples were incubated in the presence of [γ^{33}P] ATP. The experiment was analyzed by SDS-PAGE followed by PhosphorImaging. The results demonstrate that AtSOUL4 acts as an *in vitro* substrate for CKII and most likely also of CKII contained in the chloroplast stroma.

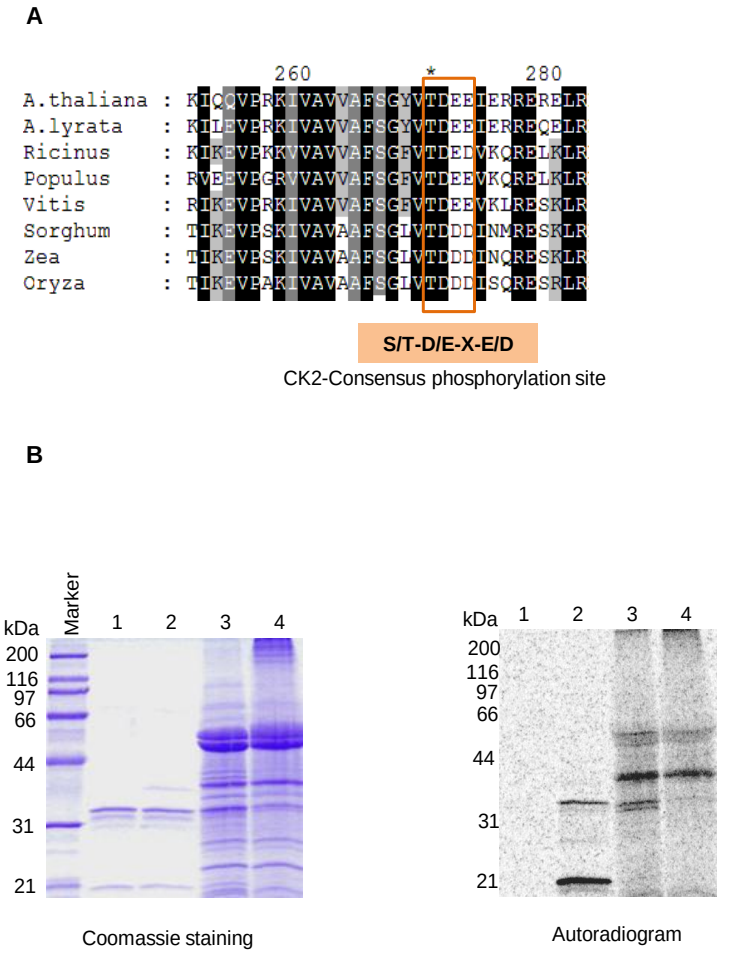

Figure 2.18 Phosphorylation of recombinant AtSOUL4 heme binding protein by CK2 and stromal fractions

(A) Alignment of the putative AtSOUL4 with CKII phosphorylation site. SOUL4 from *A. thaliana* NP_187624.1, *A. lyarata* XP_002882654.1, *Ricinus communis* XP_002528755.1, *Populus trichocarpa* XP_002323500.1, *Vitis vinifera* XP_002282544.1, *Sorghum bicolor* XP_002452205.1, *Zea mays* NP_001147650.1, *Oryza sativa* NP_001047029.1 aligned by ClustalW. The C-terminal conserved CKII motif is highlighted and boxed. (B) 3 µg of purified recombinant AtSOUL4 were incubated without (lane 1) or with (lane 2) recombinant *Zea mays* CKII alpha and [γ^{33}P] ATP as the phosphate donor. In addition, recombinant AtSOUL4 was incubated with (lane 3) or without (lane 4) isolated *Arabidopsis* stromal fraction. The samples were separated by SDS-PAGE followed by Coomassie blue staining (left panel) and PhosphorImager analysis (right panel).

2.2.5 Reverse genetic study of plastid SOUL heme binding proteins

T-DNA insertion mutants of *AtSOUL4*

We isolated two independent mutant alleles of *AtSOUL4*. These "knock-outs" containing T-DNA insertions in the 5' untranslated region (*SALK_00393848.05X*) and the 2nd intron (*SALK_01815531.15X*), respectively, were obtained from the Arabidopsis Biological Resource Center (ABRC) and were designated as *soul4-1* and *soul4-2* (Figure 2.19A). Lines homozygous for the T-DNA insertion were identified by PCR (Fig. 2.19B and C). When grown on soil under normal conditions, the homozygous lines of *soul4-1* and *soul4-2* grew normally and did not exhibit a visible phenotype (Fig. 2.19D). Immunoblot analysis shows that AtSOUL4 was detected in total leaf extracts of the wild type and *soul4-1,* but not of *soul4-2.* This indicates that the T-DNA insertion in the 5'-untranslated region of *AtSOUL4* is not a knock out (*soul4-1)* (Fig. 2.19E).

T-DNA insertion mutants of *AtSOUL5*

To complete our investigation of Arabidopsis chloroplast SOUL homologs, a reverse genetic study was initiated for the *AtSOUL5* gene. We searched the Arabidopsis databases for T-DNA insertion lines of *AtSOUL5* and identified only one line (*SAIL_215_CO2*) that was obtained from the Arabidopsis Biological Resource Center (ABRC) and designated *soul5-1*. The T-DNA insertion is located in the 3rd intron (Figure 2.20A). Plants homozygous for the T-DNA insertion were identified by PCR (Fig. 2.20B). The RT-PCR was done and confirmed that *soul5-1* is knock out for *AtSOUL5*. When grown on soil under standard conditions, plants homozygous of *soul5-1* developed normally and did not exhibit a visible phenotype (Fig. 2.20C).

2.2.6 AtSOUL4 is present both as a monomer and in very large complexes

To determine whether AtSOUL4 forms complexes, Blue native gel electrophoresis (BN-PAGE) (Schägger et al., 1994) was carried out. Wild-type as well as mutant chloroplasts were solubilized with 1% digitonin and separated by BN-PAGE followed by immunoblot analysis with the affinity purified AtSOUL4 antibody. The majority of AtSOUL4 migrated as a

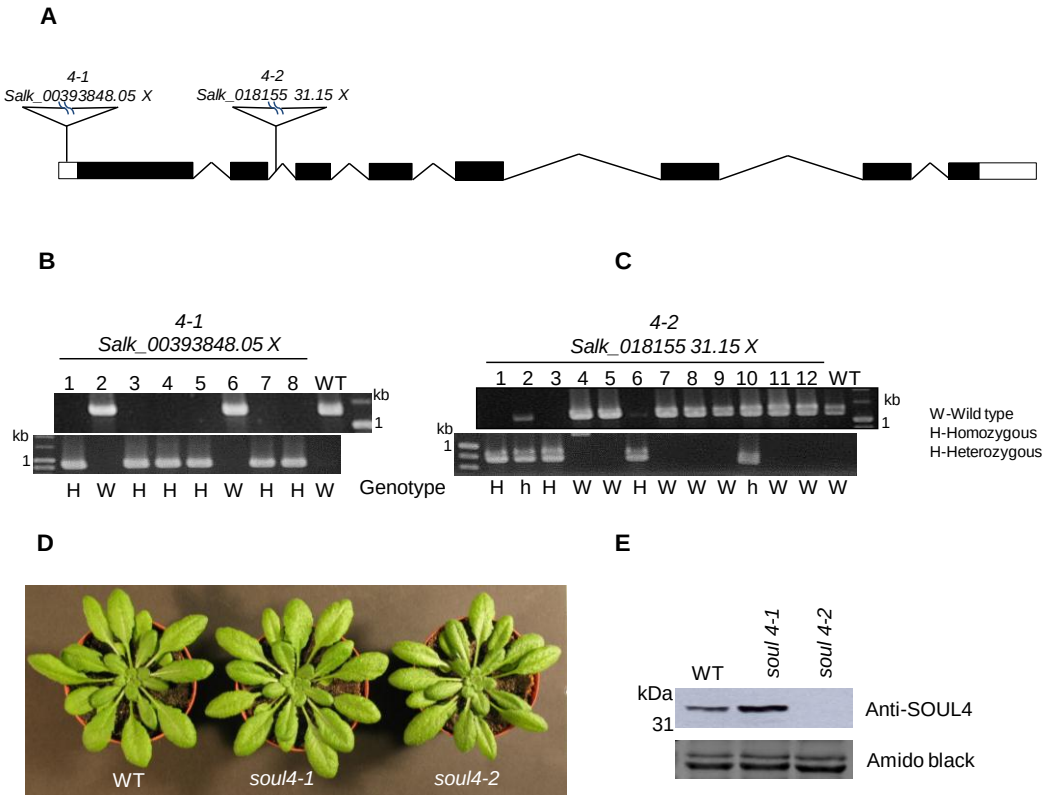

Figure 2.19 Characterization of T-DNA insertion mutants of *AtSOUL4*
(A) Scheme showing the position of the T-DNA insertion in the *AtSOUL4 gene*. Introns are represented by black boxes and exons by black lines; 5'- and 3'-untranslated regions are shown as empty boxes. (B-C) PCR analysis of genomic DNA from heterozygous and homozygous lines of *soul4-1* and *soul4-2*. The absence of the wild-type background identifies homozyguous mutant lines, a wild-type control (WT) is included. Lane M shows molecular size markers (bp). The genotypes are indicated beneath the gel images. (D) Four weeks old wild type (Col-0), *soul4-1* and *soul4-2* plants grown on soil. (E) Western blot analyses of total protein extracts for WT and two *soul4* mutant lines (*soul4-1 and soul4-2*) were separated by SDS-PAGE, transferred to a nitrocellulose membrane and stained with Amido black for a loading control (lower panel). Antibodies against AtSOUL4 were used for immunoblotting, as indicated (upper panel).

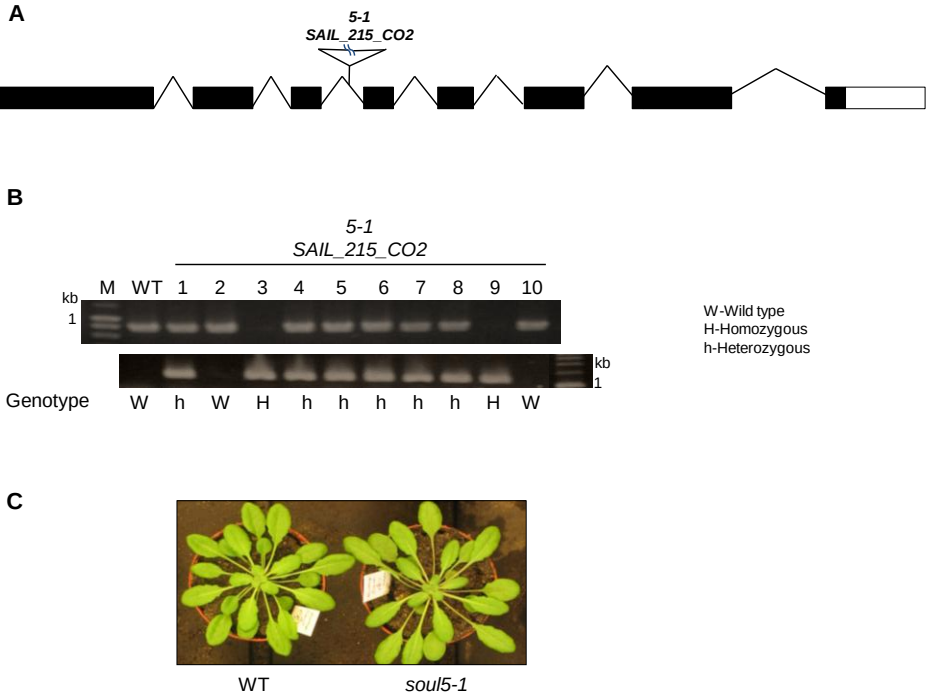

Figure 2.20 Characterization of a T-DNA insertion mutant in the *AtSOUL5* gene
(A) Scheme showing the position of the T-DNA insertion in *AtSOUL5.* Introns are represented by black boxes and exons by black lines; 5'- and 3'-untranslated regions are shown as empty boxes. (B) PCR analysis of genomic DNA from heterozygous and homozygous lines of *soul5-1*. The absence of the wild-type background identifies homozyguous lines; a wild-type control (WT) is included. Lane M shows molecular size markers (bp). The genotypes are indicated beneath the gel images. (D) Four weeks old wild type (Col-0) and *soul5-1* plants grown on soil.

monomer visible as a band below the 66 kDa marker (Figure 2.21A). In addition, AtSOUL4 was present in large molecular mass complexes of 600kDa and 440kDa. None of the bands were observed in the *AtSOUL4* mutant *soul4-2* that was used as a negative control. These experiments demonstrate that AtSOUL4 exists both as monomer and in very large protein complexes (Fig. 2.21A).

For future investigations of AtSOUL4 protein complexes, we engineered a TAP (tandem affinity purification) tag expression construct (Rigaut et al., 1999). This tag is composed of two IgG binding domains of *Staphylococcus aureus* Protein A (ProtA), and a calmodulin binding peptide (CBP) separated by a TEV (Tobacco Etch Virus) protease cleavage site (Fig. 2.21B, upper panel). The coding region of AtSOUL4 was fused to the coding sequence of a C-terminal TAPi tag (CTAPi) and cloned into a binary vector (pEARLYGATE205) containing the cauliflower mosaic virus 35S promoter and a phosphinotricin (BASTA)-resistance gene for selection of the transformants. Wild type (Col0) was transformed with this construct by floral dipping (Clough and Bent, 1998). Immunoblot analysis was performed on total chloroplast proteins extracted from pooled T_1 AtSOUL4-CTAPi transgenic lines. The results show the expected size of the fusion protein at 55kDa present in the AtSOUL4 -CTAPi transgenic lines using the AtSOUL4 mutant *soul4-2* as a negative control (Fig. 2.21B, lower panel). We screened six independent T_1 lines by segregation analysis to obtain single copy plants segregating 1:3 on selection media. This resulted in one single copy line (lines 5). Single copy T_2 phosphinothricin-resistant plants (lines 5) were grown on soil under short day conditions to check the expression in different individuals (5.1...5.14). The strong signal observed in all fourteen individuals suggests a high level of fusion protein expression (Fig. 2.21C). These lines will be useful for purification of the AtSOUL4 -TAP tag complex in future studies.

In an approach to both localization and immunopurification of complexes using anti-YFP antibodes, we engineered Arabidopsis plants expressing AtSOUL4-YFP. The coding region of AtSOUL4 was fused to the coding sequence C-terminal of YFP and cloned into a binary vector (pEARLYGATE201) containing the cauliflower mosaic virus 35S promoter and a phosphinothricin (BASTA)-resistance gene for selection of the transformants (Fig. 2.22A, upper panel). Wild type (Col0) was transformed with these two constructs by floral dip (Clough and Bent, 1998). Fluorescence analysis was carried out in transgenic AtSOUL4-YFP T_1 plant leaves by confocal laser scanning microscopy. The YFP fluorescence was present in chloroplast in typical globular structures. These were absent from wild type used as a negative control (Fig. 2.22A lower panel).

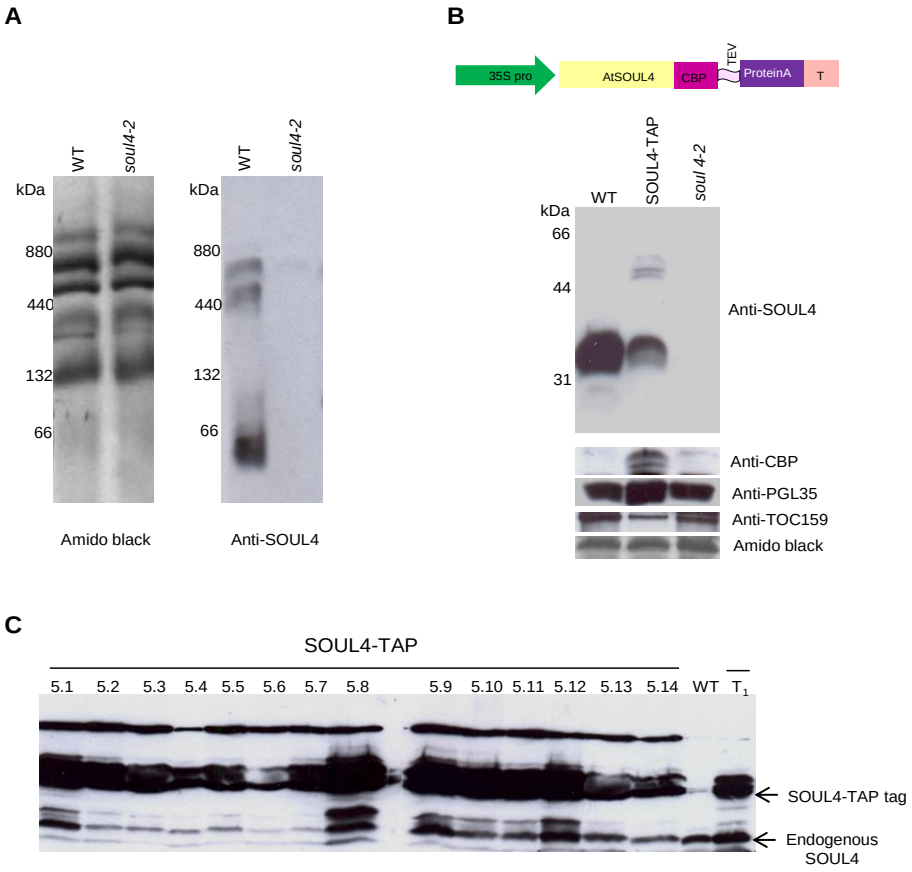

Figure 2.21 Identification of AtSOUL4 complexes and engineering of AtSOUL4-CTAP-tag lines
(A) Chloroplast proteins (50µg) from wild type (WT) and *soul4-2* were solubilized with 1% digitonin (w/v) and separated by Blue native gel electrophoresis (4 to 12% gel), transferred to a nitrocellulose membrane and stained with Amido black (left panel). Antibodies against AtSOUL4, were used for immunoblotting, as indicated (right panels). Ferritin (880 and 440 kDa) and BSA (132 and 66 kD) were used as molecular mass marker proteins. (B) Schematic drawing of AtSOUL4 CTAP-tag expression cassettes (upper panel). Total chloroplast proteins (20µg) were separated by SDS-PAGE, transferred to a nitrocellulose membrane and stained with Amido black. Antibodies against AtSOUL4, AtPGL35, AtTOC159 and CBP (TAP-tag) were used for immunoblotting, as indicated. (C) Immunoblot analysis of stably transformed AtSOUL4-CTAP-tag T_2 generation plants (line 5) and wild type (WT).

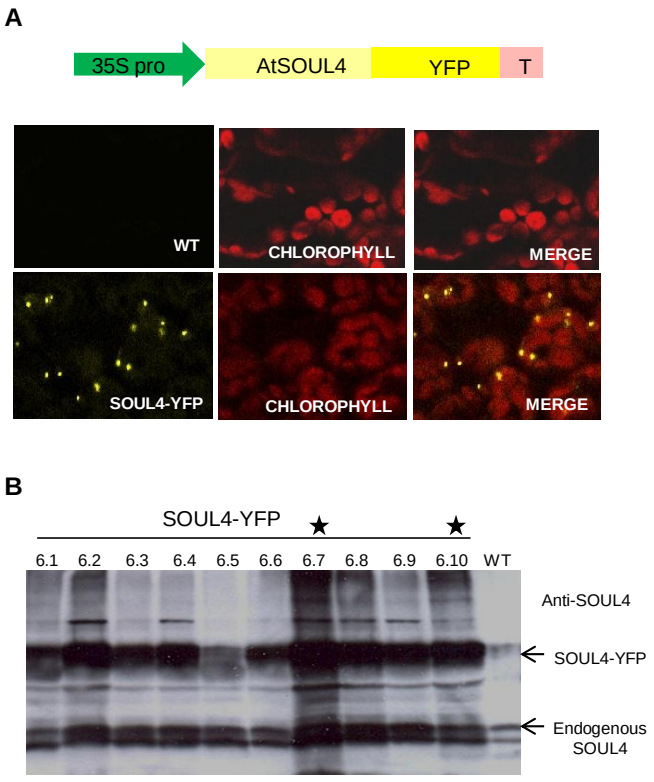

Figure 2.22 Confocal and Western blotting Analysis of AtSOUL4-YFP transgenic plants
(A) Schematic drawing of AtSOUL4-YFP expression cassettes (upper panel). Detection of YFP fluorescence in stably transformed AtSOUL4-YFP T_1 generation plants (line6) and wild type (WT) by confocal laser-scanning microscopy. Yellow fluorescence, red fluorescence of the chlorophyll and the overlay of the two fluorescences are shown for the wild type (WT) and a transgenic AtSOUL4-YFP line. (B) Western blot detection of AtSOUL4-YFP protein accumulation in stably transformed AtSOUL4-YFP T_2 generation plants line 6. Total soluble proteins from ten individual plants from line 6 were separated by SDS-PAGE, blotted and probed with anti-AtSOUL4 antibody.

We screened five independent T_1 lines by segregation analysis to obtain single copy plants (segregation 1:3 on BASTA selection media). One independent single copy line was obtained (lines 6). Single copy T_2 phosphinothricin resistant plants (lines 6) were grown on soil under short day conditions to check the expression in different individuals (6.1...6.10). The strong signal observed in all ten individuals suggested a high level of fusion protein expression (Fig. 2.22B). This line will be another useful tool for future localization and purification studies of the AtSOUL4-YFP complexes.

2.2.7 Lipidomics analysis of *soul4* mutant and wild type

Earlier reports have shown that the plastoglobule proteins, tocopherol cyclase (VTE1) and NAD(P)H dehydrogenase C1 (NDC1) are involved in the prenylquinone metabolism. To check whether AtSOUL4 may also play a role in the prenylquinone metabolism, we performed untargeted as well as targeted lipidomics analyses. In these studies, we used both WT and *soul4-2* mutant. Total lipid extracts of plants grown under normal conditions, as well as after wounding and highlight (1200µmol m–2 s–1) for 2 days were prepared. The samples were analyzed by HPLC–quadrupole time-of-flight mass spectrometer (UHPLC-QTOFMS). We didn't observe any distinct clustering by principal component analysis of untargeted lipidomics data (data not shown). In a targeted approach, we quantified five different prenyllipids: plastochromanol-8 (PC-8), plastoquinone-9 (PQ-9), tocopherol-α (Toco-α), tocopherol-γ (Toco-γ) and vitamin K (Vit-K) by using UHPLC-QTOFMS. The results suggest that, there is no significant difference between WT and *soul4-2* under the three different conditions (Fig. 2.23).

2.2.8 Involvement of the plastidic AtSOUL proteins in photomorphogenesis?

Isolation of *soul4-2/soul5-1* T-DNA mutants

To test for possible redundancy of the *AtSOUL4* and *AtSOUL5* genes, double mutants were generated by crossing homozygous *soul4-2 and soul5-1* T-DNA mutant lines. The double heterozygous F_1 progeny was selected on MS medium containing kanamycin and phosphinothricin (ppt) and allowed to self-pollinate to isolate homozygous double mutants. In the F_2 generation, a 15: 1 ratio of double homozygous to heterozygous or wild type plants is expected for *soul4-2/soul5-1*. We screened a total of 40 different F_2 plants by PCR and plant

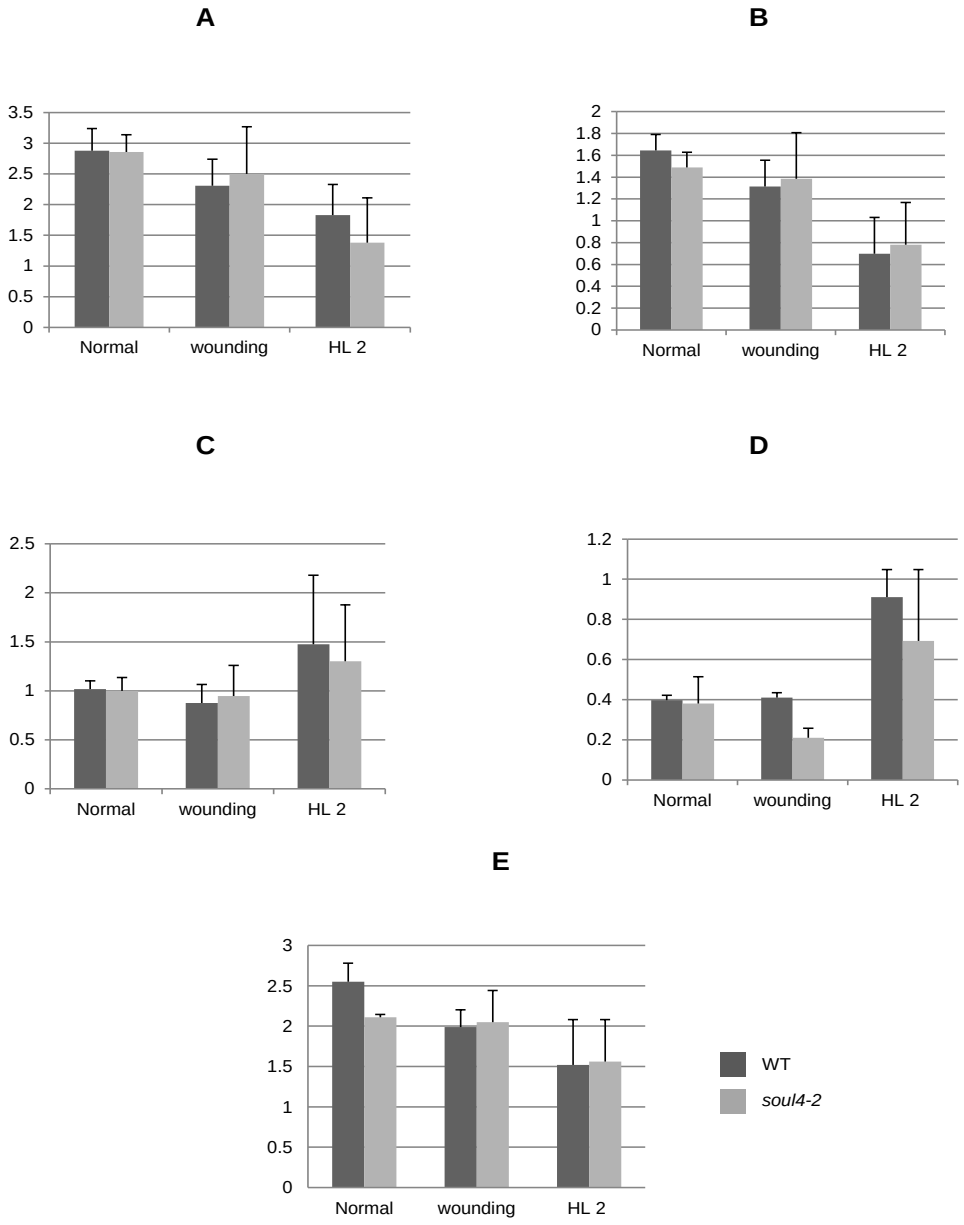

Figure 2.23 Mass spectrometric identification of prenylquinones in WT and *soul4-2* mutant after HL exposure and wounding
(A) Plastochromanol-8 (748.615) (B) Plastoquinone-9 (749.61) (C) α-tocopherol (429.37) (D) γ-tocopherol (415.35) (E). Vitamin-K (450.35) quantified by using ultra HPLC–quadrupole time-of-flight mass spectrometer. Datas are from 3 biological replicates (± SD).

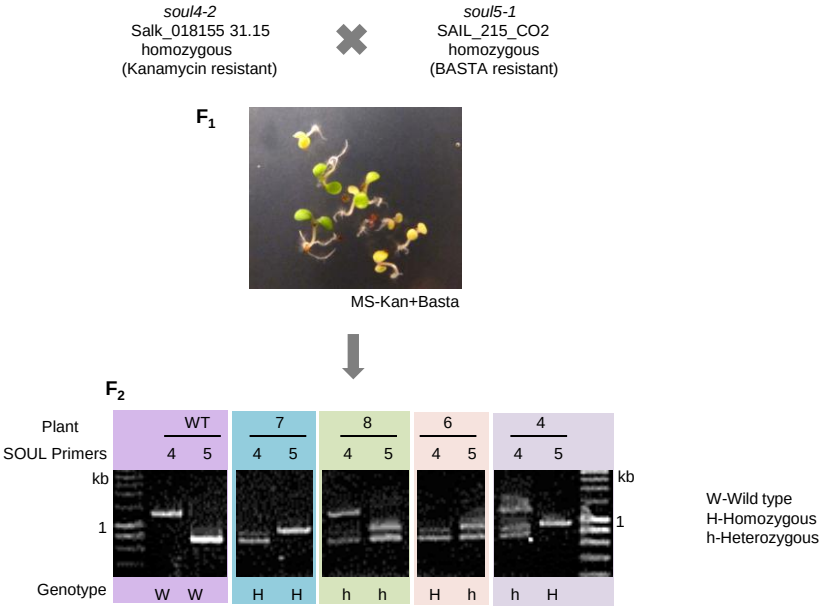

	S4/S4	S4/WT	WT/S4	WT/WT
S5/S5	S5/S5 S4/S4	S5/S5 S4/WT	S5/S5 WT/S4	S5/S5 WT/WT
S5/WT	S5/WT S4/S4	S5/WT S4/WT	S5/WT WT/S4	S5/WT WT/WT
WT/S5	WT/S5 S4/S4	WT/S5 S4/WT	WT/S5 WT/S4	WT/S5 WT/WT
WT/WT	WT/WT S4/S4	WT/WT S4/WT	WT/WT WT/S4	WT/WT WT/WT

Figure 2.24 Isolation of a *soul4-2/soul5-1*double mutant.
The plastid AtSOUL4 mutant *soul4-2* (kanamycin resistant) *and soul5-1* (phosphinothricin resistant) were crossed. A F_1 generation was selected on MS agar medium containing kanamycin and phosphinothricin. In the F_2 generation, PCR analysis of genomic DNA isolated from different plants with heterozygous (h) and homozygous (H) of *soul4-2, soul5-1* and double knockout *soul4-2/soul5-1* was carried out. The absence of wild-type PCR products confirmed the homozygous mutant background; a wild-type control (WT) is included. All possible combinations of the double knockout *soul4-2/soul5-1* genotypes are shown in a Punnett square (lower panel).

homozygous for both T-DNA insertions was identified (Fig. 2.24 middle panel).

The *soul4-2/soul5-1* double knock-out displays a photomorphogenic phenotype

In plastids, heme is the substrate for the synthesis of phytochromobilin, which is the chromophore in phytochrome (Terry et al., 2002). To check whether the double mutant may show a phytochrome-related phenotype, we performed initial characterization of the double mutant. Prior to the experiment, the genotype were confirmed by PCR (Fig. 2.25C). When the double mutant was grown on half strength MS agar medium for two weeks under standard light conditions (120µmol m–2 s–1) it developed long petioles when compared to the wildtype or the single mutants. To further analyze this phenotypic character plate grown plants were transferred to dim light (50 µmol m–2 s–1) for one week. The result confirms that the double mutant (*soul4-2/soul5-1)* has a long petiole, suggesting a photomorphogenic phenotype, when compares to the single mutant or the wild type (Fig. 2.25A). Interestingly, four weeks old soil grown double mutant (*soul4-2/soul5-1)* plants showed a phenotype, when compare to either the single mutant or the wild type as the double mutant (*soul4-2/soul5-1)* petioles were rotated (Fig. 2.25B). Immunoblot analysis using the Anti-SOUL4 antibody gave an intense band in the *soul5-1* back ground, when compare to the wild type (Fig. 2.25D) whereas as expected the single mutant (*soul4-2)* and the double mutant (*soul4-2/soul5-1)* didn't give any signal. This result suggests cross talk between *AtSOUL4* and *AtSOUL5* gene expression. We further checked the expression of *AtSOUL4* and *AtSOUL5* in wildtype, *soul4-2, soul5-1* and *soul4-2/soul5-1* backgrounds.

Tetrapyrrole and chlorophyll pigment levels are unaffected in plastidic SOUL mutants and overexpressing lines

In higher plants chlorophyll and heme tetrapyrrole pathways have a essential role in cellular and chloroplast function (Tanaka and Tanaka, 2007; Mochizuki et al., 2010). The plastidic *AtSOUL* double mutant (*soul4-2/soul5-1)* showed a photomorphogenic phenotype, when compare with the single mutant or the wild type (Fig. 2.26A, B). To check whether the photomorphogenic phenotype is due to the defective of heme we measured chlorophyll *a* and *b*, Mg-protoporphyrin IX, Mg-protoporphyrin IX monomethylester and heme from wild type, *soul4-2, soul5-1*, *soul4-2/soul5-1* and AtSOUL4-YFP overexpressing lines (SOUL4-YFP6.7 and SOUL4-YFP6.10). The result shows that there are no significant differences between WT, *AtSOUL* mutants and overexpressing plants (Fig. 2.26A-D)

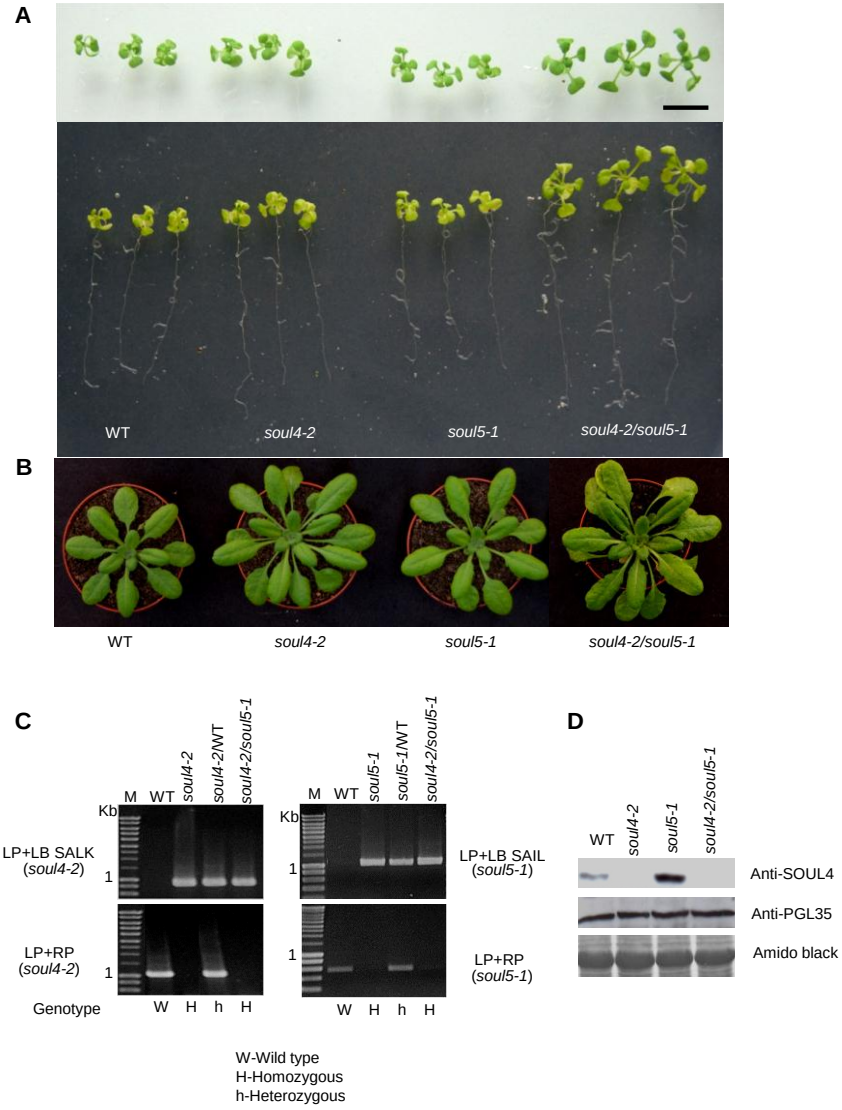

Figure 2.25 Characterisation of the *soul4-2/soul5-1* double mutant
(A) Wild type (Col-0), *soul4-2, soul5-1* and double knockout *soul4-2/soul5-1* seedlings were grown on ½ MS agar medium for two weeks and then transferred to dim light (50µM) for one week. Scale; 1cm. (B) Wild type (Col-0), *soul4-2, soul5-1* and double knockout *soul4-2/soul5-1* plants grown on soil for four weeks. (C) PCR analysis of genomic DNA from heterozygous and homozygous of *soul4-2, soul5-1* and double knockout *soul4-2/soul5-1*. The absence of the wild-type PCR product indicates the homozygous nature of an allele; a wild-type control (WT) is included. Lane M shows molecular size markers (bp). (D) Western blot analyses of total protein extracts from wild type, *soul4-2, soul5-1* and double knockout *soul4-2/soul5-1* plants were separated by SDS-PAGE, transferred to a nitrocellulose membrane and stained with Amido black (bottom panel). Antibodies against AtSOUL4 and AtPGL35 were used for immuno blotting, as indicated (upper panels).

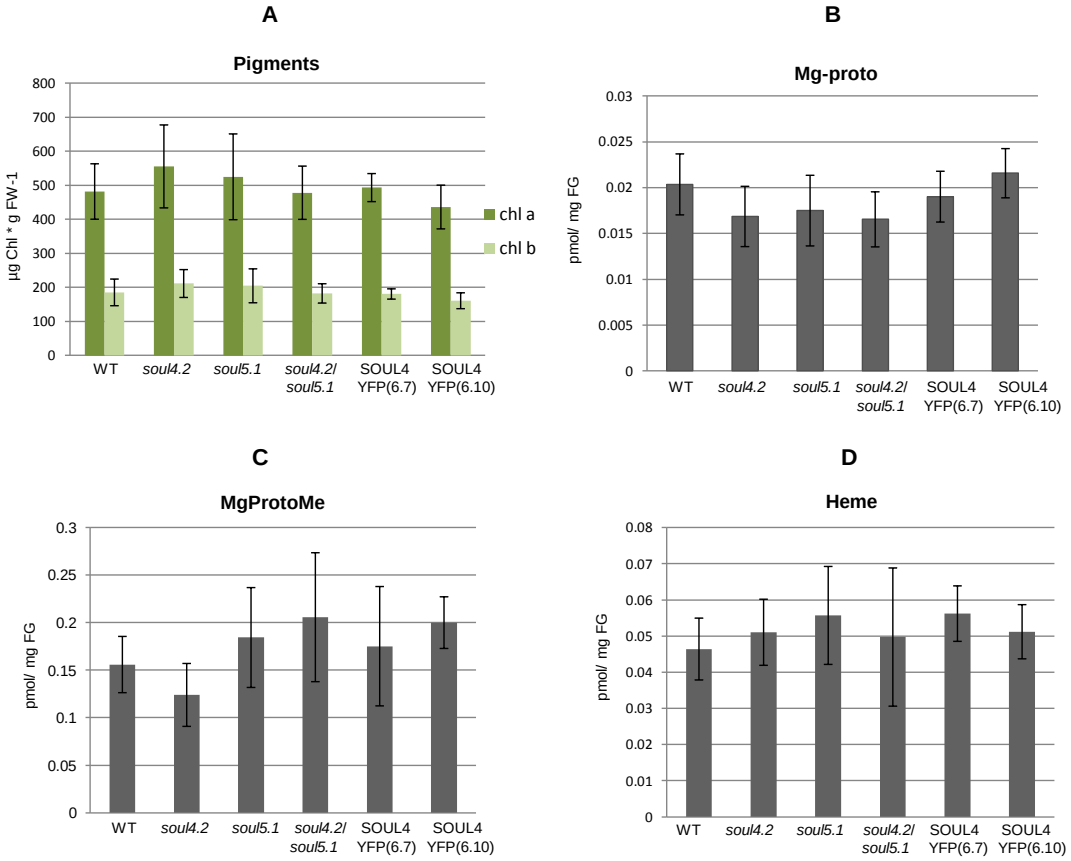

Figure 2.26 Comparison of tetrapyrroles and chlorophyll pigment levels
Chlorophyll a, b (A), Mg-protoporphyrin IX (B), Mg-protoporphyrin IX monomethylester (C) and Non covalently bound Heme (C) contents measured from wild type, *soul4-2, soul5-1*, *soul4-2/soul5-1* and AtSOUL4-YFP overexpressing lines (SOUL4-YFP6.7 and SOUL4-YFP6.10). The samples were extracted from three week old arabidopsis seedlings grown on soil under short day condition. Data are averages from four biological replicates (± SD).

2.2.9 *soul5-1* mutant is hypersensitive to red and far red light

It was previously shown that *soul1* is hypersensitive to red light (Khanna et al., 2006). The plastidic *AtSOUL* double mutant (*soul4-2/soul5-1)* shows a typical photomorphogenic phenotype, when compared with single mutants and wild type (Fig. 2.25A, B). To evaluate the photomorphogenic behaviour of these mutants, we tested the wild type, *soul4-2, soul5-1*, and *soul4-2/soul5-1* seedlings grown in the dark or white light, red and far-red light conditions, respectively. Interestingly, the *soul5-1* mutant showed short hypocotyls in Red and Far Red light, when compare to *phy*A, *phy*B seedlings grown under the same conditions (Fig. 2.27A-C).

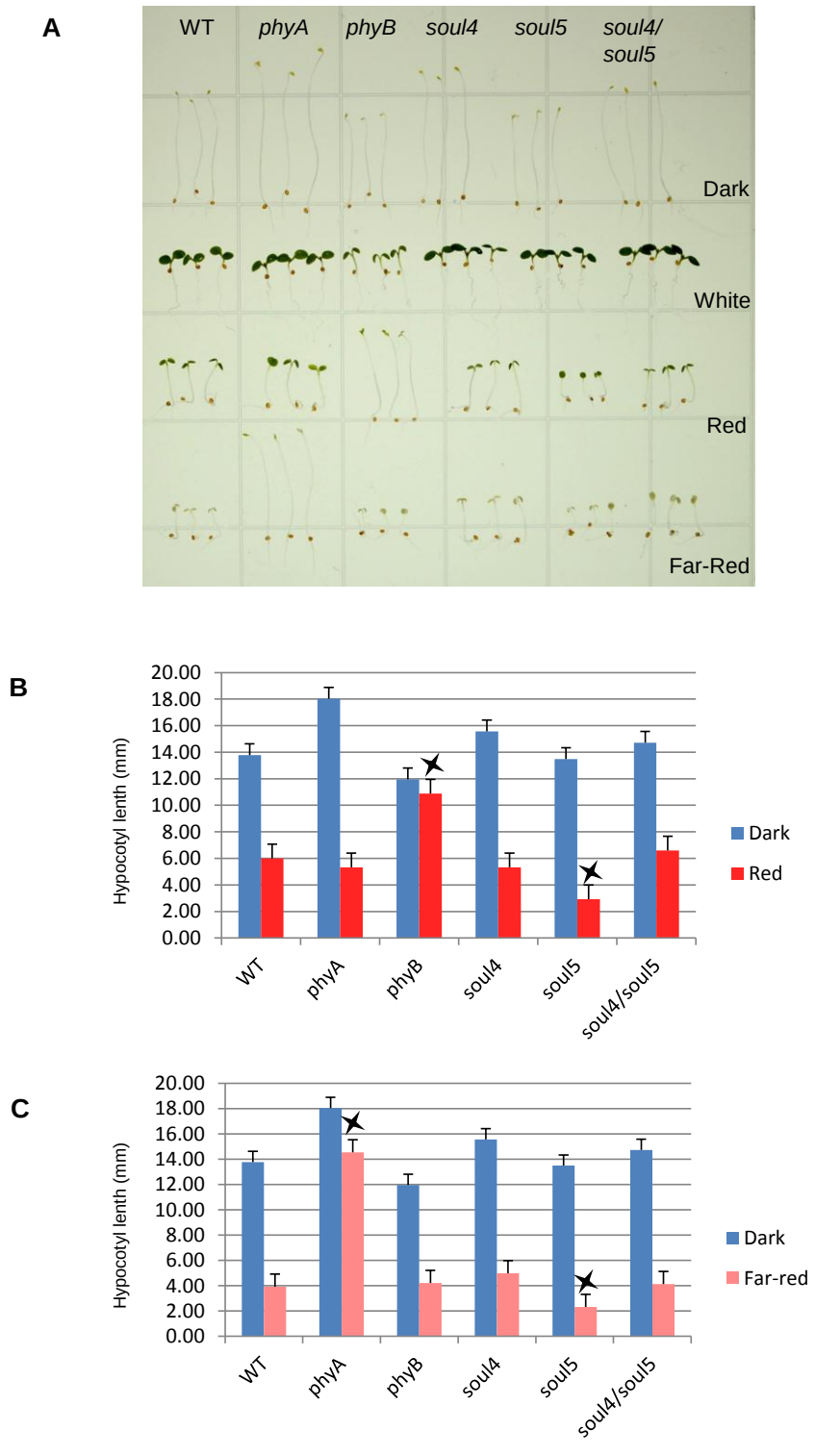

Figure 2.27 *Atsoul5* mutant is hypersensitive to Red and Far Red light
(A) Phenotype of wild type, *soul4, soul5* and double knockout *soul4/soul5* seedlings, grown under dark, white light, red and far-red light. The *phyA* and *phyB* mutants were used as reference for the evaluation of the kind and strength of photomorphogenic phenotypes. (B) Hypocotyl lengths of seedlings grown in red light. (C) Hypocotyl lengths of seedlings grown in far-red light. Values are mean ± standard error of twenty seedlings. Significant difference was set at $P \leq 0.05$ (✶) relative to WT *Arabidopsis*.

3 Discussion

3.1 A PGL35 fusion protein targets to plastoglobules and thylakoids in transplastomic tobacco chloroplasts.

3.1.1 Transplastomic tobacco is a suitable system to target recombinant proteins to plastoglobules and thylakoid membranes.

In this work, the expression and the purification of human immunodeficiency virus (HIV) antigen p24 and Hepatitis C virus (HCV) antigen HCV core protein using a plastoglobule-based system was tested. HIVp24 is expected to be a key component of any AIDS vaccine (Obregon et al., 2006) and HCV core protein is a target for vaccine development against Hepatitis C infection (Elmowalid et al., 2007). An advantage of plastids is the absence of protein glycosylation pathways, which makes them suitable for expression of HCV core protein (Moradpour et al., 2007). Expression of the truncated C-terminus of the 16 kDa core polypeptide from Hepatitis C virus has been reported and an accumulation up to approximately 0.1% total plant protein in transplastomic tobacco was observed (Madesis et al., 2010). The expression of HIVp24 by nuclear transformation reached yields only 0.35% of total soluble protein (Zhang et al., 2002). Up to ~0.8% of total soluble protein were reported by TMV-derived viral transfection (Perez-Filgueira et al., 2004). The HIVp24–immunoglobulin A (IgA) fusion molecule expression strategy resulted in fusion protein accumulation up to 1.4% of total soluble protein (Obregon et al., 2006).

An earlier report showed that transplastomic tobacco plants expressing HIVp24 protein accumulated the protein only in the youngest leaves to relatively high levels of approximately ~2.5% total soluble protein; (McCabe et al., 2008). The HIVp24 and a fusion of HIVp24 with the HIV negative regulatory protein Nef (p24-Nef) accumulated to 4% and 40%, respectively, of the total soluble protein. The 40% accumulation level of HIVp24-Nef induced a slightly pale-green phenotype (Zhou et al., 2008). Importantly, the immunogenicity of the chloroplast-produced HIVp24 following oral or subcutaneous administration in experimental animals could also be demonstrated (Gonzalez-Rabade et al., 2011). In this work, we examined the expression and targeting of the plastoglobule protein PGL35 mature form

fused to either human immunodeficiency virus (HIV) antigen p24 or Hepatitis C virus (HCV) antigen HCV core protein in transplastomic tobacco plants. Arabidopsis PGL35 shares 84% similarity and 72% identity with the protein sequence of its closest tobacco homolog (PozuetaRomero et al., 1997). Moreover, the PGL35 amino acid is highly conserved in other higher plant species (Fig. 2.1) and is therefore likely to be suitable for work in many different species.

3.1.2 Overexpression of PGL35 leads to enlargement of the plastoglobules

The Streptavidin-PGL35-HIVp24 protein, containing a codon optimised HIVp24 sequence, accumulated to moderate levels (around 1%) when compared to other fusion constructs (Tregoning et al., 2003; Glenz et al., 2006). The streptavidin-PGL35-HCV core fusion protein accumulated at lower levels, possibly due to the lack of codon optimization in the HCV coding sequence. The first codon immediately downstream from the AUG start codon have already been identified as an important regulator of translation efficiency in chloroplasts (Kuroda and Maliga, 2001). A recent study showed codon optimization of the TGFb3 coding sequence leading to a 75-fold increase in recombinant protein accumulation relative to the native human coding sequence (Gisby et al., 2011).

By visual examination, the transplastomic plants expressing the HIVp24 or the HCV core fusion protein had a wildtype phenotype. Moreover, the photosynthetic parameters were normal. At the ultra-structural level, however, transplastomic plastoglobules were enlarged 5-6 fold in diameter when compared to the wild type. The mechanisms and significance of variations of plastoglobule size and number are not completely understood. The enlargement of plastoglobules has been described in chloroplasts under abiotic stress, such as drought (Eymery and Rey, 1999) and nitrogen starvation (Bondada and Syvertsen, 2003). In the case of nitrogen starvation this observation was attributed to chlorophyll degradation and concomitant accumulation of phytyl esters in plastoglobules (Gaude et al., 2007). The up-regulation of several plastoglobulin genes also correlated with stress and potentially also correlate with the increase in plastoglobule size (Gillet et al., 1998).

3.1.3 Recombinant protein targeting to plastoglobules depends on hydrophobicity and isoelectric point

The immunofluorescence experiment showed that the recombinant PGL35-HIVp24 fusion protein localized to plastoglobule-like structures inside the chloroplast. In contrast, by membrane fractionation only around 1/5 of the recombinant HIVp24 fusion protein localized to the plastoglobules and much of it was present in the much denser thylakoid fractions. PGL40, a known plastoglobule marker, showed a similar distribution pattern but appeared to be more highly enriched in the plastoglobule fractions (Fig. 2.9B). One possibility therefore is that many plastoglobules remained attached to the thylakoid membranes and stayed at the bottom of the gradient. Alternatively, some of the PGL40 as well as PGL35-HIVp24 may directly associate with the thylakoid membranes and thereby reduce the proportion associated with plastoglobules. These data could be reconciled with the observed dot-like immunofluorescence if the thylakoid PGL35-HIVp24 localizes to zones where the plastoglobules are attached.

A study employing comparative quantitative proteomics of sub-plastid localization of the fibrillin (plastoglobulin) family members showed that their distribution between plastoglobule and thylakoids correlated with their hydrophobicity and isoelectric points (Lundquist et al., 2012). In that study, a 34-fold enrichment of PGL35 in plastoglobules over thylakoids was observed. Any fusion partner of PGL35 would change its hydrophobicity and isoelectric point and thereby likely affect its distribution between the thylakoid membranes and the plastoglobules. Indeed, our own calculations demonstrate that the fusion of PGL35 to HIVp24 should shift its distribution towards the thylakoids (Fig. 3.1). Although plastoglobulins associate with lipid bodies and membranes (Lundquist et al., 2012), their overall amino acid composition is not hydrophobic and it is apparent from hydropathy plots that, unlike oleosin they lack a strongly hydrophobic structural element. Therefore, association of PGLs with plastoglobules probably involve interactions with the polar head group of membrane lipids at the plastoglobule surface (Kim et al., 2001).

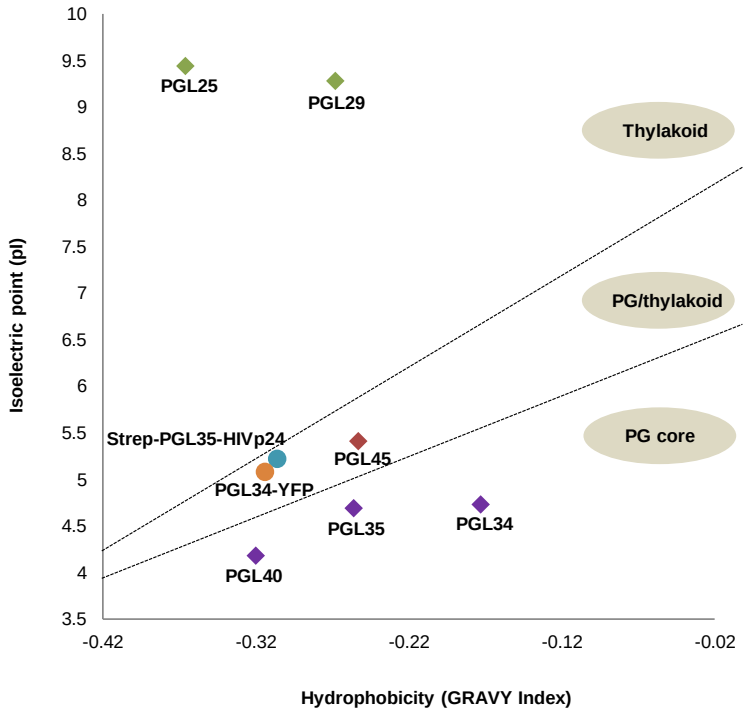

Figure 3.1 Plastoglobulin (fibrillin) and Streptavidin-PGL35-HIVP24 fusion protein distribution between thylakoids and plastoglobules correlates with isoelectric point and hydrophobicity. The graph was adapted from Lundquist et al. 2012 (Lundquist et al., 2012).

A previous study from this laboratory showed that a PGL34 fusion protein containing a chloroplast targeting sequence (transit peptide) was properly targeted to plastoglobules in nuclear transgenic Arabidopsis plants (Vidi et al., 2007). The targeting of a plastome-encoded PGL35-fusion proteinto plastoglobules (as well as thylakoids) demonstrates that the transit peptide of PGL35 is not required for proper assembly. Moreover, it also suggests that plastoglobulin assembly into plastoglobules and/or thylakoids occurs post-import and after folding inside the chloroplast. Based on the findings that hydrophobicity as well as the isoelectric point determines the distribution between plastoglobules and the thylakoids suggests that the net charge and hydrophobic properties at the surface of a folded plastoglobulin may hold the key to understanding the partitioning between the two compartments.

3.1.4 Recombinant HIVp24 purified from the fusion proteinto near homogeneity

Our construct has an N-terminal streptavidin tag with high affinity for 2-iminobiotin (Humbert et al., 2005) and includes three TEV protease sites between PGL35 and HIVp24. We took advantage of these features to purify HIVp24 from a total chloroplast detergent solubilize using simple 2-iminobiotin column affinity chromatography followed by TEV proteolytic cleavage to release HIVp24. We used total chloroplasts rather than purified plastoglobules for the purification procedure, because 60-80% of the PGL35-HIVp24 remained in the thylakoid fraction. Apart from the probable bona fide thylakoid localization of a part of the PGL35-HIVp24 protein, plastoglobule separation from the thylakoid membranes could still be improved to take better advantage of the plastoglobule low density properties in any future purification protocol resembling the one in the oleosin system (Vanrooijen and Moloney, 1995; Boothe et al., 2010).

3.1.5 Future prospective for improvement of the plastoglobule targeting system

In conclusion, the PGL35 fusion protein was targeted to plastoglobules as well as to the thylakoid membrane of the transplastomic plants. Although, the PGL35 fusion protein allowed a simple enrichment of recombinant protein by a floatation method the yields were limited by its thylakoid association. We anticipate that selecting more hydrophobic and lower isoelectric point fusion partners together with improved purification methods of plastoglobules using phase separation techniques will improve this promising methodology.

3.2 Unraveling the functions of plastidial SOUL heme binding protein

3.2.1 AtSOUL4 heme binding protein is located in plastoglobules

There are five SOUL/p22HBP homologs In *Arabidopsis thaliana* (Takahashi et al., 2008). *Chlamydomonas reinhardtii* has one homolog that was found in the eyespot phosphoproteome (Wagner et al., 2006, 2008). AtSOUL1-3 and AtSOUL5 present in the vacuole and thylakoids, respectively, were identified by proteomics approaches (Jaquinod et al., 2007a, b; Peltier et al., 2006, 2004). AtSOUL4 was found in plastoglobule in three independent proteomics studies (Vidi et al., 2006; Ytterberg et al., 2006; Lundquist et al., 2012). Based on quantitative comparative proteomics AtSOUL4 was enriched to around 1.8% of the total plastoglobule proteome (Lundquist et al., 2012). This thesis demonstrates that AtSOUL4 is present in globular structures together with PGL35 in a colocalisation experiment. This result independently confirms the plastoglobule localisation of AtSOUL4 (Fig. 2.13C). Furthermore, AtSOUL4 heme binding protein co-distributed with AtPGL40 in the sucrose gradient fractionation experiment of total Arabidopsis chloroplast membrane (Fig 2.16). While as expected the relative distribution of the two proteins was not identical (Lundquist et al., 2012) they were both present together in the lightest fractions containing plastoglobules providing a third line of evidence for plastoglobule localization of AtSOUL4.

3.2.2 Heme binds to recombinant AtSOUL4

In plants, plastids are the major site of tetrapyrrole synthesis. This includes chlorophyll, heme, siroheme and phytochromobilin. In the heme branch, ferrochelatase catalyzes the insertion of $Fe2^{+}$ into protoporphyrin IX to produce protoheme (heme *b*). Recent structural studies of p22HBP/SOUL revealed a novel hydrophobic cleft flanked by α-helix and the β8-β9 loop is essential for heme binding ability (Dias et al., 2006). In *A. thaliana,* all five homologous have this novel hydrophobic cleft for tetrapyrrole binding. AtSOUL1 and AtSOUL2 are well known examples of tetrapyrrole carrier proteins and have well characterized biochemical properties (Takahashi et al., 2008). Recombinant, mature AtSOUL4 was expressed in *E.coli* and purified as soluble native protein. It robustly bound to heme in an *in vitro* heme binding assay (2.17A, B). Heme-binding activity was demonstrated

by efficient reduction of binding in the presence of excess free hemin. In an *in vivo* heme binding assay in the yeast system involving the growth of the *hem1*Δ mutant in the presence of hemin was reduced in the presence of AtSOUL4 expression. (2.17C, D).

3.2.3 AtSOUL4 heme binding protein is phosphorylated by CKII and stromal protein extract

Chloroplastic stromal alpha-subunit casein kinase II characterization has been done previously in mustard (Ogrzewalla et al., 2002; Baginsky et al., 1999) as well as Arabidopsis (Salinas et al., 2006). Chloroplastic CKII might have many different prospective phosphorylation substrates (Baginsky and Gruissem, 2009). *C. reinhardtii* SOUL3 was present in the eyespot phosphoproteome (Wagner et al., 2008). Based on this evidence, we analysed AtSOUL4 in Arabidopsis and other species for the presence of phosphorylation motifs. Indeed, AtSOUL4 has a conserved CKII target consensus sequence (S/T-D/E-X-E/D) in higher plants. Recombinant AtSOUL4 was readily phosphorylated *in vitro* by recombinant maize CKII alpha-subunit. The recombinant AtSOUL4 was also *in vitro* phosphorylated by isolated stromal extracts. This isolated extract is known to contain stromal CKII but also contains other types of kinases. It is therefore possible that stromal kinases other than CKII are able to phosphorylate AtSOUL4 *in vitro*. It appears likely that phosphorylation is regulatory mechanism at AtSOUL4 but in view of the absence of a well characterized function its purpose remains unclear.

3.2.4 AtSOUL4 is present in lipid droplets but is not involved in lipid metabolism

Plastoglobules are rich in non-polar lipids (triacylglycerols, phytol esters, prenylquinones, plastoquinone and tocopherols). Plastoglobules are normally associated with thylakoid membranes, suggesting an exchange of lipids between the two compartments. Three separate proteome studies show that two dozens of proteins are present in plastoglobules (Vidi et al., 2006; Ytterberg et al., 2006; linquest et al., 2012). The proteins can be divided into three categories: PAPs/fibrillins, chloroplast metabolic enzymes, and unclassified proteins. A number of known chloroplast metabolic enzymes and previously unclassified proteins are known to function in plastoglobule lipid metabolism, eg. the tocopherol cyclase VTE1 (Vidi et al., 2006), NDC1 (Piller et al., 2011), PES1 and 2 (Lippold et al., 2012) are

involved in prenylquinone metabolism. These results suggested that AtSOUL4 may also be implicated in lipid metabolism. Therefore both targeted prenylquinone profiling and non-targeted lipidomics analysis of WT and *soul*4-2 mutant after wounding and high light stress were carried out. No significant differences in *soul4-2* (prenyl)lipid profiles were detected in comparison to the wild type. While it cannot be excluded that minor lipid components may have escaped detection in our system, the results suggest that AtSOUL4 is not implicated in major (prenyl) lipid pathways.

3.2.5 Putative model for potential function of plastidial AtSOUL4 heme binding protein

The SOUL heme binding protein was identified as a component of chicken retina and pineal gland light signaling pathways (Zylka and Reppert, 1999). In *C. reinhardtii*, the SOUL3 heme-binding proteins is likely to be a component of a light-signalling pathway in the eyespot. AtSOUL1 is highly expressed in Arabidopsis and the *soul1* mutant is hypersensitive to red light. This isoform may act as a heme carrier and/or maintaining heme in a bound form and thereby be indirectly involved in light signalling. AtSOUL4 has been identified in tetrapyrrole protein complexes (personal communication from Prof. Bernhard Grimm, Humboldt University Berlin, Germany). Our native gel result showed that AtSOUL4 is present as a monomer (30kDa) as well as in large protein complexes (600kDa and 440kDa). In the future, it will be interesting to isolate AtSOUL4 -TAP tagged protein complexes to the interaction partners (Fig. 2.21). The double mutant (*soul4-2/soul5-1)* plant shows photomorphogenic phenotype (Fig. 2.25A, B). However this not likely due to changes of the heme or other tetrapyrrole levels (Fig. 2.26). Interestingly *AtSOUL*4 and *AtSOUL*5 exhibited molecular cross talk at the transcript level. The *soul5-1* mutant is hypersensitive to Red and Far Red light (Fig. 2.27). At least two hypothetical models for the potential function of plastidic AtSOUL4 heme binding protein could currently be considered:

Model1 (Function in a heme and phytochromobilin dependent pathway)

In this model, we propose that stress leads to higher rates of tetrapyrroles production that could be toxic to the plant cell and especially so in the heme branch of the tetrapyrrole pathway. Plastidic AtSOUL may act as the carrier to balance and buffer the state of free heme in plastid. Moreover, heme is the precursor of the phytochromobilin synthesis. We speculate that, any fluctuation of heme level may affect the phytochromobilin level. Phytochromobilin must be transported from the plastid to cytosol and bind to

apophytochrome and then form a holophytochrome to participate in light signaling pathways. AtSOUL5 may bind excess heme at the thylakoid and transport it to plastoglobules. The stromal CKII kinase may be activated by stress or specific light conditions and phosphorylate and activate AtSOUL4. Finally, the activated AtSOUL4 exports the excess heme from plastoglobule towards the chloroplast envelope (Fig. 3.2).

Model2 (Senescent dependent pathway)

In the chlorophyll catabolic pathway, Mg^{2+} is removed from the porphyrin ring by 'metal chelating substance' (MCS) and phytol is generated by breakdown of chlorophyll by the pheophytin phytol hydrolase (PPH) (Hortensteiner and Krautler, 2011). Potentially the remaining tetrapyrrole head group could be trapped by the thylakoid SOUL5 heme-binding protein and delivered in plastoglobules. The PG-localized SOUL4 heme-binding protein may carry the tetrapyrrole and deliver it to the stroma for further degradation (Fig. 3.2). This process may be regulated by phosphorylation by CKII.

In conclusion, a solid initial characterization of the AtSOUL4 heme-binding protein has been carried. As a drawback for this research, AtSOUL4 was not represented on any microarrays. Therefore no expression data are available or co-expression networks are available that may hint at functions that escaped us during this thesis work. In the future, additional experiments need to be carried out to determine the precise functions of the AtSOUL proteins and to at least partly validate the proposed Model 1 or Model 2.

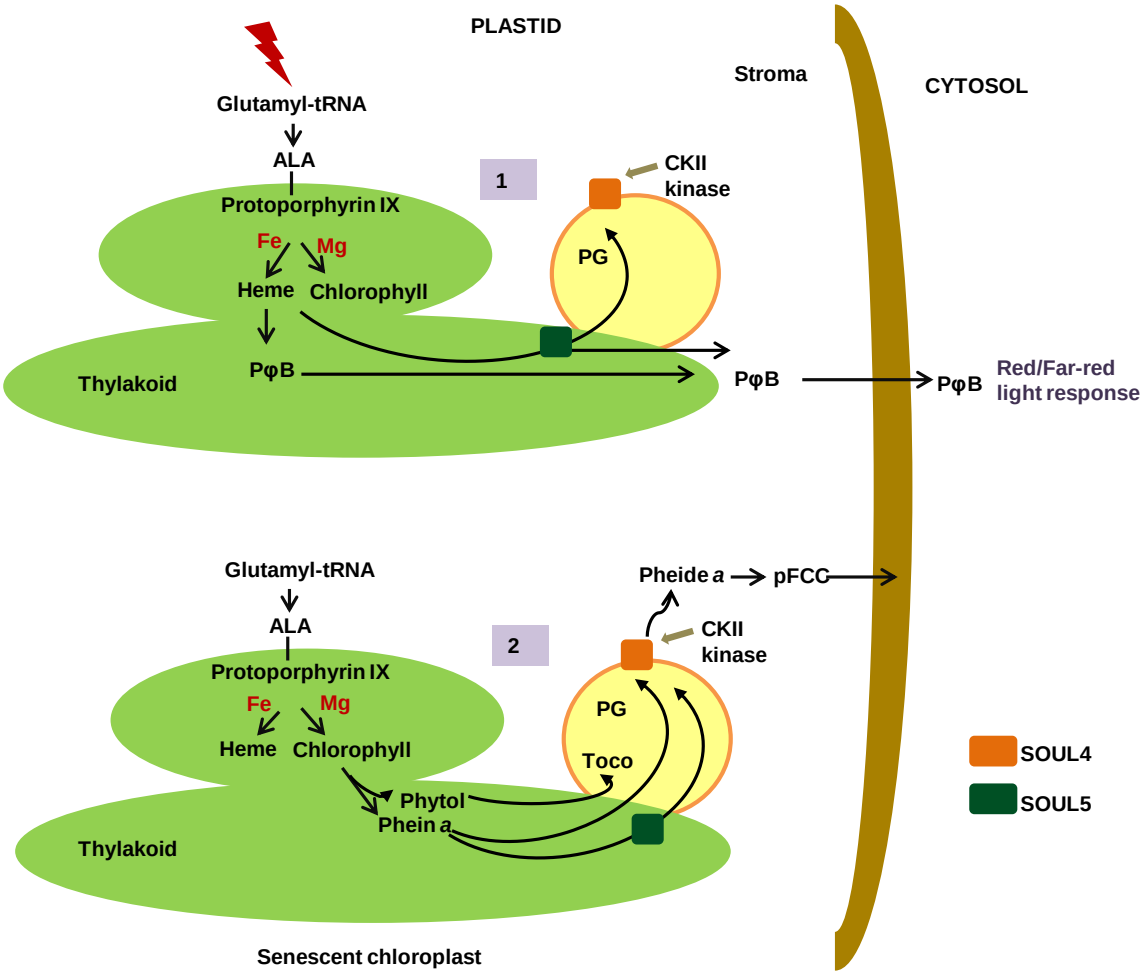

Figure 3.2 Schematic model illustrate the potential function of plastidial AtSOUL4 heme binding protein. Model 1 represents the heme and phytochromobilin dependent pathway. Model 2 represents the senescent dependent pathway

4 Materials and Methods

4.1 Materials

4.1.1 Biological material

Arabidopsis

Wild type (wt) Arabidopsis plant always refers to *Arabidopsis thaliana* (L.) Heynh. var. Columbia 2. T-DNA insertion lines from the SALK and SAIL collection were obtained from the Nottingham Arabidopsis Stock Centre (NASC, http://arabidopsis.info).

Tobacco

Wild type tobacco (*Nicotiana tabacum* cv. Petit Havana) was kindly provided by Prof. Ralph Bock.

Nicotiana benthamiana

Wild type *N. benthamiana* was grown on soil under long day conditions.

Micro-organisms

Escherichia coli DH5-α were from Invirogen and E. coli BL21 (DE3) cells were from Novagen. *Agrobacterium tumefaciens*, strain C58 was kindly originally provided by Dr. Roger Kuhn (Institute of Plant Sciences, ETH Zurich, Switzerland). The yeast strains DY1457 and MH002 ∆hem1::LEU2 were a kind gift by Prof. Jerry Kaplan (Department of Pathology, University of Utah Health Sciences Center, U.S.A).

4.1.2 Oligonucleotides

Oligonucleotides were synthesized at Microsynth GmbH.

Name	Sequence (5 ’-3’)
PGL 35-F	GATTTCAAAATCCCCATGGCGGACATCGACGACG
PGL 35-R	CTTGTTCTAGATCATATGGCCTTGCAGATAGACCAGT TCGGGCCCCTGCCCGTAGAACAGCTCCCCCTGCTTG TACATCATTTCAGGGTTTAAGAGAGAGC
Strep-F	GATATACCCATGGCTAGCATGACTGG
Strep-R	CGCGCCATGGGCTGAACGGCGTCGAGC
HCV-F	CCGTGCCATATGAGCACGAATCC
HCV-R	GGAAGATCTAGAAAGAGCAACCAGG
HCV-BclI	CCTAGGTTGATCATCTAGAAAGAGCAACCGG
PGL35-BclI	CCACGAATGATCACCCATGGCGGACATCG
P24-BclI	CCTAGGTTGATCATCTAGAGGAATTCTACTCTAGC
GFP-BclI	CCTAGGTTCATCATCTAGATGTACAGCTCGTCC
P24-F	CGCCCTTCATATGGCTAGCGGATCC
P24-R	CGCCCTTTCTAGAGGAATTCTACTCTAGC
e.GFP F	CCCTTTCATGGTGAGCAAGGGCGAGGAGC
e.GFP R	CCATCTAGATGTACAGCTCGTCCATGC
SOUL4ORF-F	CGA AGAGCC ATG GTG ATG ATC AGC TCC
SOUL4ORF-R	GGGC CAT GGCTTC TTT GTT TTC AAC TTC G
SOUL 4- LP1	TCG ACCCTTGTA AAGTTG TGC
SOUL 4- RP1	CTTGGGAAACACATATTTCGC
SOUL 4- LP2	TTTGAGGGCATGACAAAAGAC
SOUL 4- RP2	ATGCCCAATTACTTACTCCGG
SOUL 5- LP1	CTTTGG AGTTTCCCAAGTCTGGCG
SOUL 5- RP1	GGTCTTGTTGATGTTTTTAAGCAG
SOUL4 ATTB1 F	GGGGACAAGTTTGTACAAAAAAGCAGGCTATGGTCA TGATCAGCTCC
SOUL4 ATTB1 R	GGGGACCACTTTGTACAAGAAAGCTGGGTGGGCTTC TTTGTTTTCAACTTCG
SOUL4 F	CCTTGCTCCCATGGCTCAAGCTTCCTCTG
SOUL4 SphI F	CCTTGCTCGCATGCCTCAAGCTTCCTCTG
SOUL4 SphI R	CCTTGCTCGCATGCCTTCTTTGTTTTCAACTTCG
pptR F	GCCCAGAACGACGCCCGGCCGAC
pptR R	CGGTGACGGGCAGGACCGGACGG
KanR F	GTTCTGGCTGGACAGGCCACGGGAC
KanR R	GTCTCAGGGCGAGTCTTCTTGAGC
LBpROK2 SALK	TGGACTCTTGTTCCAAACTG
LBCSA110 SAIL	GCCTTTTCAGAAATGGATAAATAGCC

Above the oligonucleotides used in this work

4.1.3 cDNA clones

The cDNA clones were obtained from the Riken Bio Resource Centre (http://www.brc.riken.jp/lab/epd/Eng/catalog/pDNA.shtml)

4.1.4 Chemicals

Unless stated otherwise, the chemicals were purchased from Fluka Chemie GmbH. (35S)L-methionine was purchased from Hartmann Analytic GmbH, Braunschweig, Germany.

4.1.5 Antibodies

Antibodies specific to AtTOC159 or AtTOC75 have been described (Bauer et al., 2000; Hiltbrunner et al., 2001). Sera against AtPGL40, AtPGL35, and AtPGL30.4 were available in the laboratory. Antibody specific to AtPGL35 have been described (Vidi et al., 2006). Antibodies specific to HIVp24 (sheep anti-p24 antibody; Aalto Bio Reagents, Dublin, Ireland), Lchb2 (Genscript), RLSU (Agrisera), Streptavidin (Abcam), His-tag and *Strep*MAB-Immo Oyster 488 (iba) were purchased from different companies. Sera against AtSOUL4 were affinity purified using recombinant AtSOUL coupled to Affi-Gel10 (Bio-Rad Laboratories).

4.1.6 Plasmids

pENTR221, pEG100, pEG101, pEG102, pEG100 and pYES2 were obtained from Invitrogen, USA. The pET21d was purchased from Novagen, USA. pLITMUS28i was obtained from NEB. Plastid transformation vectors pRB96 and pZFU7-loxp were kindly provided by Prof. Ralph Bock, Max Planck Institute of Molecular Plant Physiology, Germany.

4.2 Methods

4.2.1 Physiological methods

4.2.1.1 Growing *Arabidopsis thaliana* on Murashige and Skoog (MS) medium

Seeds were incubated 10 minutes in 70% with 0.05% v/v Triton X-100 with ethanol, 20 minutes in absolute ethanol and finally rinse with sterile ddH_2O. Sterile seeds were spread on 1% (w/v) phyto-Agar (Duchefa) containing 0.5x MS medium (MS; Duchefa) supplemented with 0.1% (w/v) sucrose and appropriate antibiotic (kanamycin and/or phosphinotricin). Germination was synchronized by exposing the seeds 2 days at 4°C in the dark. Plants were grown under short-day conditions (8 hours light [120µmol $m^{-2}.s^{-1}$], 22°C; 16 hours dark, 17°C).

4.2.1.2 Growing Arabidopsis on soil

Seeds were soaked overnight in tap water and grown on 1/3 perlite (bottom) and 2/3 soil (top) under long-day conditions (16 h light [120 µmol m-2 s-1], 21 °C; 8 h dark, 17 °C). Germination was induced by vernalisation at 4 °C for 2 days.

4.2.1.3 *In-viro* propagation of tobacco

Aseptically grown tobacco (*Nicotiana tabacum* cv. Petit Havana) plants were raised on agar-solidified MS medium (Murashige and Skoog., 1962) containing sucrose (30 g/L). Regenerated shoots of transplastomic lines were rooted and propagated on the same media. Rooted homoplasmic plants were transferred to soil and grown to maturity under standard greenhouse conditions.

4.2.2 Cloning methods

4.2.2.1- PCR, restriction digest and ligation reaction

Standard protocols were used for cloning (Sambrook, 2001). DNA fragments for cloning were PCR amplified using pfu-polymerase (Promega), according to the supplier's recommendation. Suitable restriction sites were introduced into PCR primers. Pre-existing plasmid constructs were used as templates for PCR. PCR fragments and vectors were digested with the respective restriction enzymes (New England Biolabs, Inc., Beverly MA, USA) and purified from agarose gels using the QIAquick kit (Quiagen). Vectors were dephosphorylated using Phosphatase Antarctica (New England Biolabs, Inc., Beverly MA, USA). T4 DNA ligase (New England Biolabs) was used according manufacturer's recommendation to ligate vectors and inserts.

4.2.2.2- Transformation of thermo-competent *E. coli* cells

Ligation reactions were subsequently transformed by heat shock into competent *E.coli* DH5-α or BL21 cells (Sambrook, 2001). Competent *E.coli* cells were prepared as described (Inoue et al*.,* 1990). Selection was done on LB medium (25 g/l LB Broth Miller [Becton Dickinson Diagnostic Systems], 1% (w/v) Agar Bacteriological grade [ICN Biomedicals])

supplemented with appropriate antibiotics. Clones were selected by PCR and restriction digestion.

4.2.2.3- Plasmid isolation and purification

The small-scale plasmid isolation, the GenElute Plasmid MiniPrep Kit (Sigma) was used according to the supplier's instructions.

.

4.2.2.4- DNA sequencing

DNA sequences were checked by sequencing (Microsynth GmbH, Balgach, Switzerland).

4.2.2.5- Transformation of Yeast

Yeast transformation was performed as described in the Yeast protocols handbook (Clontech Laboratories Inc.).

4.2.2.6- Transformation of electro-competent *Agrobacterium tumefaciens*

A. tumefaciens, strain C58, was grown in YEB medium (0.5% (w/v) Bacto-Trypton, 0.5% (w/v) Bacto-Pepton, 0.1% (w/v) yeast extract (from Difco), 2mM MgCl2), supplemented with appropriate antibiotics, until an optical density of 0.6, at 526 nm, was reached. Cells were pelleted (4000 g, 10 min, 4°C) and washed with 10% glycerol. 50ng of plasmid DNA was used for electroporation in a MicroPulser (Biorad laboratories) according to the manufacturer's instructions. Transformants were selected on YEB medium, 1% (w/v) Agar supplemented with appropriate antibiotics.

4.2.3 DNA constructs

4.2.3.1 Plasmid constructs for chloroplast transformation

The plastid transformation vectors constructed in this study are based on the pZF7lox plastid vector (Zhou et al., 2008). The pZF7lox plastid transformation vectors are derived from plasmids pZSJH1 (Birch-Machin et al., 2004) and pRB95 (Ruf et al., 2001). The plastoglobulin35 (PGL35)-ORF without the coding sequence for the transit peptide gene was

amplified from pCL61-PGL35 with PGL35-F forward primer introducing a NcoI restriction site at the 5'-end and with PGL35-R reverse primer introducing the coding sequence for three TEV protease sites as well as NdeI and XbaI restriction sites at the 3' end. Finally, the amplified product was ligated into the NcoI and XbaI sites of the pLITMUS28i vector, resulting in pLITMUS28i-PGL35. Coding sequences for Hepatitis C virus antigen-core protein from pSV-sport HCV CE1E2 plasmid (kindly provided by Dr. Bruno Martoglio, Novartis Pharma AG, Basel, Switzerland) was amplified using HCV-F forward primer introducing NdeI restriction site at the 5' end and with 3'-end HCV-R reverse primer introducing a XbaI restriction site. The codon-optimized synthetic HIVp24 (Zhou et al., 2008) from pCR4TOPO-p24 was amplified using the HIVp24-F forward primer introducing a NdeI restriction site at the 5'-end and with HIVp24-R reverse primer introducing a XbaI restriction at the 3'-end. The GFP coding sequence amplified from pCL60 (Bauer et al., 2000)

The HCV core protein, HIVp24 and GFP amplification products were digested with the NdeI and XbaI and ligated into the corresponding site of pLITMUS28i-PGL35. The PGL35-HCV core protein, PGL35-HIVp24 and PGL35-GFP fusion genes were amplified from the pLITMUS28i-PGL35 constructs using the PGL35-BclI forward primer introducing a 5' BclI restriction site and HCV-BclI, HIV-BclI and GFP- BclI reverse primers, respectively, introducing a 3' BclI restriction site. The amplified product was cloned into pZF7lox plastid transformation vector using the BamHI restriction site compatible with BclI as well as cloned into pRB96 transformation vector. Finally, the streptavidin tag coding sequence from the pET11b-SAV plasmid was amplified using the Strep-F forward primer and Strep-R reverse primer introducing an NcoI restriction site. The amplified product was ligated to the 5'-end of the PGL35-HCV, PGL35-HIVp24 and PGL35-GFP coding sequences in the pZF7lox plastid transformation vector. This resulted in the constructs pVSB1 (*Streptavidin-PGL35:3TEV-HCV core protein)*, pVSB2 (*Streptavidin-PGL35:3TEV-HIVp24)*, pVSB3 (*Streptavidin-PGL35:3TEV-GFP)* and pVSB4 (PGL35:3TEV-*GFP).* All steps of the cloning were confirmed by restriction digestion and sequencing.

4.2.3.2 Plasmid constructs for SOUL4 heme binding protein

pET21d constructs

*AtSOUL*4 was amplified from C-DNA (pda 08804) using primers SOUL-ORF F and SOUL-ORF R including NcoI site. The PCR product was then ligated into the NcoI site of pET21d.

*AtSOUL*4 without transit peptide sequence was amplified with SOUL inter F and SOUL-ORF R primers including NcoI site. The construct was verified by sequencing.

pEarleyGate constructs

The Gateway recombination cloning technology (Invitrogen, USA) is based on the site specific recombination of bacteriophage lambda (Landy, 1989). *AtSOUL*4 full reading sequence was amplified with SOUL4-AttB1 and SOUL4-AttB12 primers and cloned into pENTR221 vector by BP Clonase. Finally *AtSOUL*4 recombine with destination vector pEarleyGate101, pEarleyGate102 and pEarleyGate205 by LR reactions. The constructs were verified by sequencing

pYES2 construct

*AtSOUL*4 was amplified with SOUL-F and SOUL-R primer including *Sph*I site. The PCR product was then ligated into the *Sph*I site of pYES2. The construct was verified by sequencing.

4.2.4 Chloroplast isolation and in vitro import reactions

4.2.4.1 Coupled in vitro transcription/translation

Construct pET21d-SOUL4 contain a T7promoter upstream of the start codon allowing in vitro protein synthesis using the TNT® T7 Quick Coupled Transcription/Translation System (Promega Corporation, Madison WI, USA) as recommended by the supplier.

2.2.4.2 Isolation of Arabidopsis chloroplasts

Arabidopsis plants were grown on Murashige and Skoog medium as described. Intact chloroplasts were isolated according to (Fitzpatrick and Keegstra, 2001).

2.2.4.3 In vitro protein import into Arabidopsis chloroplasts

Chloroplasts corresponding to 25 µg chlorophyll were used for import assays. The import experiment of the SOUL4 into intact isolated chloroplast has been described previously (Agne et al., 2009).

4.2.5 Generation of affinity-purified antibodies

4.2.5.1 Bacterial expression and purification of recombinant protein

The pET21d constructs (with/without transit peptide) were transformed into *E.coli* BL21 (DE3) cells. Bacteria were grown until 0.6 OD_{600} was achieved and expression was induced during 4 hours with 0.5 mM IPTG at 37°C with moderate shacking. The recombinant SOUL4 proteins with transit peptide was insoluble. The insoluble SOUL4 protein pellet was denatured with 8M urea and subsequently purified on a pre-packed HisTrap HP chromatography column on a AKTA PrimePlus (GE Healthcare). The soluble, mature AtSOUL4 without transit peptide was purified under nondenaturing conditions using pre-packed HisTrap HP chromatography column on the AKTA PrimePlus system. The column was washed and eluted on a gradient from 0 to 100% of French Press Buffer (50 mM Tris/HCl pH 8, 300 mM NaCl) containing 500 mM imidazole and 1 mM β-mercaptoethanol. Fractions containing the protein were dialyzed overnight against dialysis buffer (PBS buffer with 10% (v/v) glycerol).

4.2.5.2 Purification of anti-AtSOUL4 antibody

Recombinant AtSOUL4 protein was used to produce rabbit polyclonal antibodies (Eurogentec). Antibodies were affinity purified using recombinant AtSOUL4 coupled to Affi-Gel10 (Bio-Rad Laboratories). Recombinant AtSOUL4 protein was coupled to Affi-gel10 (Bio-Rad Laboratories) according to the supplier's instructions. Serum from the immunized rabbit was incubated with the Affi-Gel slurry for 2 h on a rolling shaker. Affi-Gel beads were washed extensively with PBS (140 mM NaCl, 2.7mM KCl, 10 mM Na2HPO4, 1.8 mM KH2PO4 pH 7.4). Bound antibodies were eluted with 0.2M glycine (pH 2.2). Tris/HCl pH 9.0 was added to affinity-purified antibodies to adjust the pH to 7.

4.2.6 Transient transformation of *N. benthiamiana* leaves by agroinfiltration

Agroinfiltration of *N. benthiamiana* was performed as published by (Wroblewski et al., 2005) agrobacterium cultures were grown in LB medium. Transgene expression was observed after 3 or 4 days using a Leica SP5 confocal microscope**.**

Confocal laser scanning microscopy

After 48 h incubation at 22 °C in the dark, transiently transformed leaves were analysed by confocal laser scanning microscopy (LEICA TCS 4D microscope, LEICA Microsystems) was used to detect fluorescence. For double fluorescent experiments, CFP and YFP were detected sequentially using 458 and 514 nm laser lines, as well as 460-510 nm and 520-588 nm detection windows, from a LEICA SP2 AOBS microscope. Chlorophyll autofluorescence was monitored using either 594 nm or TRITC (568 nm) excitation wavelengths.

4.2.7 Stable transformation of *A. thaliana* and tobacco chloroplast

4.2.7.1 Transformation of *Arabidopsis thaliana*

A. thaliana plants were transformed using the floral dip method as described (Clough and Bent, 1998). Transformants were selected on MS medium containing phosphinothricin.

4.2.7.2 Transformation of tobacco chloroplasts

Plastid transformation was carried out using the biolistic protocol (Svab et al.,1990). Young leaves from aseptically grown tobacco plants were bombarded with plasmid DNA coated 0.6 µm gold particles using the PDS-1000/He biolistic gun with the Hepta Adaptor (Bio-Rad, Munich, Germany). Primary spectinomycin-resistant lines were selected on a MS-based regeneration medium containing 500 mg/L spectinomycin. Spontaneous spectinomycin-resistant mutants were eliminated by double resistance tests on regeneration medium containing both spectinomycin and streptomycin 500 mg/L each (Bock, 2001). For each transgene construct, several independent transplastomic lines were generated and subjected to two to three additional rounds of regeneration on spectinomycin-containing medium to obtain homoplasmic lines. T_0 plants were then transferred to soil and allowed to self-pollinate and set seeds. To determine homoplasmy, T_1 seeds were surface sterilized and grown on MS-based regeneration medium containing 500 mg/L spectinomycin.

4.2.8 PCR analysis of plants

2.2.8.1 DNA extraction

DNA was prepared from leaf material using the simple DNA preparation method. Leaf tissue was ground in 0.2 M Tris/HCl pH 9, 0.4 M LiCl, 25 mM EDTA, 1% w/v SDS. The

homogenate was cleared by centrifugation (5 min, 16'000x g, 4 °C), supplemented with an equal volume of isopropanol and centrifuged again (45 min, 16'000x g, RT). The supernatant was discarded and the DNA pellet was washed with 80% v/v ethanol. Finally, the DNA was dried and resuspended in 50 µl TE (10 mM Tris/HCl pH 8, 1 mM EDTA).

2.2.8.2 PCR analysis

PCR reactions contained 2 µl DNA solution, 1 U GoTaq DNA polymerase (Promaga), as well as 0.2 mM dNTPs (Eurobio) in a total volume of 25 µl. The primer sets SOUL4- LP1, SOUL 4-RP1 with LBpROK2 SALK and SOUL4- LP2, SOUL4-RP2 with LBpROK2 SALK were used for genotyping for *soul4-1* and *soul4-2.* The SOUL5-LP1, SOUL5-RP1 and LBCSA110 SAIL primers used for genotyping for *soul5-1.*

4.2.9 Southern and northern blot analyses

Total plant DNA was extracted from leaves using the cetyltrimethylammonium bromide (Doyle and Doyle, 1990). Five micrograms of total DNA were digested with *Sph*I, separated on a 1% (w／v) agarose gel and transferred to a Hybond XL membrane (GE Healthcare). A 550 bp PCR product was generated by amplification of a portion of the *psaB* coding region (Wurbs et al., 2007) and was used as RFLP probe to verify plastid transformation and assess the homoplasmic state of the transformants. Probes were labelled with α[^{32}P] dCTP by random priming using the Multiprime DNA labelling system (GE Healthcare). Total cellular RNA was extracted using the peqGOLD TriFast reagent (Peqlab GmbH, Erlangen, Germany) following the manufacturer's protocol. Electrophoretically separated RNA was transferred onto Hybond XL (GE Healthcare) membranes by capillary blotting using standard protocols. Membranes were stained with Methylene blue to check the RNA quality and loading. Gene specific probes for the HCV core protein and HIVp24 were amplified by PCR and labelled with α[^{32}P] dCTP by random priming using the Multiprime DNA labelling system (GE Healthcare).

4.2.10 Western blot analysis

Leaves of transformed and untransformed plants grown in a greenhouse were ground in liquid nitrogen. Leaves (100 µg) were homogenized in 250 µL of Rensink buffer (100 mM NaCl, 50 mM Tris-HCl, pH 7.5, 0.5% (v/v) Triton X-100, and 10 mM β-mercaptoethanol) supplemented with protease inhibitor mixture (Sigma P9599) and centrifuged at 20,000g for

5 min. Protein was quantified using the Bradford method. Proteins were concentrated by chloroform-methanol precipitation, separated by SDS-PAGE, and blotted onto nitrocellulose membrane. Membranes were stained with amidoblack to check protein quality and control loading. Blots were probed with anti-HIVp24 (sheep anti-p24 antibody; Aalto Bio Reagents, Dublin, Ireland), anti-Lhbc2 (Genscript), anti-RLSU (Agrisera), anti-Streptavidin (abcam), anti-PGL40, anti-PGL30.4 and anti-SOUL4 sera (Eurogentec). Detection was performed using the chemiluminescence ECL Western blotting system (GE Healthcare). Quantification of HIVp24 was performed by comparing dilution series of protein extracted from tobacco line pZF5.5A (Zhou et al. 2008). For each protein, adequate amounts were loaded on an SDS–PAGE gel, electrophoretically separated and then analysed by Western blotting. For quantification, chemiluminescent immunoblot signals were analysed using a Bio-Rad ChemiDoc XRS system.

4.2.11 Phosphorylation Assays

Three micrograms of recombinant SOUL4 protein was incubated with or without 37.5 units of recombinant maize (Zea mays) CK2 a-subunit (Biaffin) and with or without stromal fractions in the presence of 25 mM Tris-HCl, pH 8.0, 5 mM MgCl2, 1 mM dithiothreitol (DTT), 50 mM ATP, and 1µCi of [γ-33P] ATP for 30 min at 25^0C. Reactions were stopped by diluting in ice-cold buffer and CHCl3-methanol precipitation. The samples were separated by SDS PAGE and examined by autoradiography.

4.2.12 Heme binding assay

4.2.12.1 *In-vitro* heme binding assay

The *in vitro* heme binding assay was carried out as described (Vanhee et al., 2010). 100µM recombinant SOUL4 protein was incubated with hemin-agarose (Sigma-Aldrich) or agarose beads for one hr on a rotating wheel. The flow through was collected and the beads washed with PBS buffer and eluted with SDS-PAGE-loading buffer. For the heme competition assay, 100µM of recombinant SOUL4 protein was pre-incubate with 10mM hemin for 1 hr before incubation with the hemin-agarose. The flow through was collected and the beads washed with PBS buffer and eluted with SDS-PAGE-loading buffer. The input, flow-through, last wash, and elution were analyzed by SDS-PAGE and Western blot.

4.2.12.2 *In vivo* heme binding assay

The *in vivo* heme binding assay in the yeast system was carried out as described previously (Protchenko et al., 2008).

4.2.13 Blue native PAGE

4-16% native polyacrylamide gradient gels, as well as the electrophoresis buffers, were purchased from Invirogen. Chloroplasts (50µg chlorophyll) were solubilized in 50µl of 1x solubilization buffer containing 1% digitonin and incubated for 20 min on ice. Samples were centrifuged at 100,000*g* for 10 min at 4^0C. The supernatant was mixed with 5% G-250 (Invitrogen). Electrophoresis was performed at 30 V for 14 hrs in a cold chamber (4°C) overnight. Immunoblotting was performed as described in (Kikuchi et al., 2006).

4.2.14 Prenyllipid analysis

Four week-old Arabidopsis rosettes leaves were ground in a mortar with liquid nitrogen. 100 mg of leaf material were processed with 500 µL ethanol and centrifuged at 14,000 × g for 3 min. Finally 400 µL of supernatant were transferred to an appropriate glass vial for UHPLC-QTOFMS analysis. The untargeted and targeted analyses have been described previously (Piller et al., 2011).

4.2.15 Arabidopsis Crossing

The flower buds were opened between petals and sepals using a forceps. Immature anthers were carefully removed and emasculated with donor anthers, using a NikonSMZ 1000 binocular and marked. Siliques were harvested after 15-25 days. F_1 progeny was selected by double antibiotic then furtherly screened 50 F_2 plants with PCR to select the double knock of homozygous double knock out.

4.2.16 Porphyrin Analysis

Porphyrins were extracted and analysed has been described previously (Papenbrock et al., 1999).

4.2.17 Heme Extraction

The non-covalently bound heme was extracted by acidic acetone containing 5% HCl, transferred to diethyl ether, concentrated, and washed on a DEAE-Sepharose column. The heme content measured has been described previously (Castelfranco and Jones, 1975)

4.2.18 Photomorphogenic experiments

Seeds were surface sterilized and plated on ½ MS medium. The Red and far-red light experiment was performed as described previously (Lorrain et al., 2008). Hypocotyl length was measured using ImageJ software.

4.2.19 Gradient floatation centrifugation of chloroplast membranes

Leaves from transplastomic and wild-type plants grown on soil for 8 weeks were harvested and immersed in tap water in the dark at 4°C for 30 min. Leaf material was homogenized in HB buffer (450 mM sorbitol, 20 mM Tricine/KOH pH 8.4, 10 mM EDTA, 10 mM $NaHCO_3$, 1 mM $MnCl_2$) with a blender and filtered through cheesecloth and Miracloth. Chloroplasts were sedimented (2 min 700×g), washed with HB buffer. The chloroplasts were resuspended in TE buffer (50 mM Tricine/HCl pH 7.5, 2 mM EDTA) containing 0.6 M sucrose and supplemented with 0.5% (v/v) protease inhibitor cocktail (Sigma P9599) for 10 min. The chloroplasts were lysed by freezing at -20 °C for 1 hr, thawed on ice, diluted 3 times with TE buffer and homogenised with a Potter homogeniser. Total membranes, corresponding to 10 mg of chlorophyll, were sedimented at 100,000×g and resuspended in 2 ml 45% sucrose in TE buffer. Membranes were overlaid with a linear sucrose gradient created using 15 ml 5% sucrose and 15 ml of 45% sucrose in TE buffer and centrifuged for 17 h at 100,000×g and 4°C (SW41Ti rotor, Beckman). 0.5 ml fractions were collected starting from the top of the gradient and used for western blotting.

4.2.20 Fluorometry and chlorophyll measurement

Maximum quantum efficiency of photosystem II (Fv/Fm) was measured with the Mini-PAM Portable Chlorophyll fluorometer fitted with a 2030-B leaf clip holder (Walz GmbH, Germany). Detached leaves from 6 week-old plants were dark-adapted 15 min prior to measurements. Leaf chlorophyll was quantified in 80% (v/v) acetone extracts by measuring

the A663 and A645 and using the Arnon equations for total chlorophyll content (Arnon 1949).

4.2.21 Electron microscopy

Pieces of leaf tissue from 42-day-old light-grown control and transplastomic plants were fixed with 5% glutaraldehyde and 4% formaldehyde in 100 mM phosphate buffer pH 6.8 overnight at 4°C, rinsed several times in phosphate buffer, and post-fixed for 2 h with 1% osmium tetroxide in 100 mM phosphate buffer pH 6.8 at 20°C. After two washing steps in buffer and distilled water, the pieces were dehydrated in ethanol and embedded in Spurr's low-viscosity resin. Ultrathin sections of 50–70 nm were cut with a diamond knife and mounted on uncoated copper grids. The sections were post-stained with uranyl acetate and Reynold's lead citrate. Observations were made with a Philips CM 100 transmission electron microscope (Philips Electron Optics BV, Eindhoven, the Netherlands). For light microscopy, semithin sections with a thickness of 750 nm were cut with a diamond knife, mounted onto glass slides, and stained with toluidine blue.

4.2.22 Immunofluorescence

Chloroplast isolation was performed as previously described (Smith et al., 2002). Chloroplasts were isolated from transplastomic and wild type plants. Isolated chloroplasts were fixed by 2% paraformaldehyde dissolved in TAN buffer. Fixed chloroplasts were treated by 20 µg/ml proteinase-K in TE buffer containing 0.5% Triton X-100 at 37°C for 10 min. Chloroplasts was washed twice with PBS. After blocking with 3% skim milk in PBS for 30 min, the samples were incubated for 16 h at 4°C with the anti-streptavidin antibody with *Strep*MAB-Immo Oyster 488 diluted 1:200. Chloroplasts were then washed twice with 3% skim milk in PBS and then once with PBS buffer (Kabeya et al., 2010). Fluorescence was detected using the FITC (488 nm) laser line from a LEICA TSC SP5 microscope (LEICA Microsystems).

4.2.23 Purification of HIVp24

Leaves from transplastomic plants were harvested and immersed in tap water in the dark at 4°C for 30 min. Leaf material was homogenized in HB buffer (450 mM sorbitol, 20 mM Tricine/KOH pH 8.4, 10 mM EDTA, 10 mM $NaHCO_3$, 1 mM $MnCl_2$) with a blender and filtered through cheesecloth and Miracloth. Chloroplasts were sedimented (2 min 700×g),

washed with HB buffer. The chloroplasts were resuspended in TE buffer (50 mM Tricine/HCl pH 7.5, 2 mM EDTA) with 0.6 M sucrose supplemented with 0.5% (v/v) protease inhibitor cocktail (Sigma P9599) and incubated for 10 min. The chloroplasts were lysed by freezing at -20~ for 1 hr, thawed on ice, diluted 3 times with TE buffer and homogenised with a Potter homogeniser. Total membranes, corresponding to 200 µg of chlorophyll, were solubilized with 0.5% (v/v) Triton X-100 in Rensink buffer (100 mM NaCl, 50 mM Tris-HCl, pH 7.5, 10mM β-mercaptoethanol) supplied with protease inhibitor mixture (Sigma P9599) at 4°C for 10 min. The insoluble membranes were sedimented at 20,000×g and the soluble supernatant was subjected to dialysis in Rensink buffer. The 2-iminobiotin column (Sigma) was washed several times with 50 mM ammonium carbonate at pH 11, containing 0.5 M NaCl. 200 µg of total soluble protein was loaded onto the pre-washed column. After binding, the resin was washed with the same pH 11 buffer until the absorbance of effluent at 280 nm reached base line values. Subsequently, the column was eluted overnight at 4°C using 100 units of Tobacco Etch Virus Protease (TEV; Invitrogen) in 1 ml of cleavage buffer with 50 mM Tris-HCl, pH 8.0, 0.5 mM EDTA and 1 mM DTT. Then, the column was washed with buffer containing 50 mM ammonium carbonate at pH 11 and 0.5 M NaCl three times. The final elution was carried out using 50 mM sodium acetate pH 4.0 to release streptavidin and was detected by absorbance measurements at 280nm. Finally, all the fractions were subjected to SDS-PAGE and western blot analysis.

REFERENCES

Adhikari, N.D., Orler, R., Chory, J., Froehlich, J.E., and Larkin, R.M. (2009). Porphyrins Promote the Association of GENOMES UNCOUPLED 4 and a Mg-chelatase Subunit with Chloroplast Membranes. J. Biol. Chem. **284,** 24783-24796.

Agne, B., Infanger, S., Wang, F., Hofstetter, V., Rahim, G., Martin, M., Lee, D.W., Hwang, I., Schnell, D., and Kessler, F. (2009). A Toc159 Import Receptor Mutant, Defective in Hydrolysis of GTP, Supports Preprotein Import into Chloroplasts. J. Biol. Chem. **284,** 8661-8670.

Armstrong, G.A., Runge, S., Frick, G., Sperling, U., and Apel, K. (1995). Identification of NADPH-protochlorophyllide oxidoreductase-a and oxidoreductase-b - a branched pathway for light-dependent chlorophyll biosynthesis in Arabidopsis thaliana. Plant Physiol. **108,** 1505-1517.

Austin, J.R., Frost, E., Vidi, P.A., Kessler, F., and Staehelin, L.A. (2006). Plastoglobules are lipoprotein subcompartments of the chloroplast that are permanently coupled to thylakoid membranes and contain biosynthetic enzymes. Plant Cell **18,** 1693-1703.

Baginsky, S., and Gruissem, W. (2009). The Chloroplast Kinase Network: New Insights from Large-Scale Phosphoproteome Profiling. Mol. Plant. **2,** 1141-1153.

Baginsky, S., Tiller, K., Pfannschmidt, T., and Link, G. (1999). PTK, the chloroplast RNA polymerase-associated protein kinase from mustard (Sinapis alba), mediates redox control of plastid in vitro transcription. Plant Mol.Biol. **39,** 1013-1023.

Bally, J., Paget, E., Droux, M., Job, C., Job, D., and Dubald, M. (2008). Both the stroma and thylakoid lumen of tobacco chloroplasts are competent for the formation of disulphide bonds in recombinant proteins. Plant Biotechnol. J. **6,** 46-61.

Bauer, J., Chen, K.H., Hiltbunner, A., Wehrli, E., Eugster, M., Schnell, D., and Kessler, F. (2000). The major protein import receptor of plastids is essential for chloroplast biogenesis. Nature **403,** 203-207.

Birch-Machin, I., Newell, C.A., Hibberd, J.M., and Gray, J.C. (2004). Accumulation of rotavirus VP6 protein in chloroplasts of transplastomic tobacco is limited by protein stability. Plant Biotechnol. J. **2,** 261-270.

Bock, R. (2001). Transgenic plastids in basic research and plant biotechnology. Journal of Molecular Biology **312,** 425-438.

Bock, R. (2007). Plastid biotechnology: prospects for herbicide and insect resistance, metabolic engineering and molecular farming. Current Opinion in Biotechnology **18,** 100-106.

Bock, R., and Warzecha, H. (2010). Solar-powered factories for new vaccines and antibiotics. Trends in Biotechnology **28,** 246-252.

Bondada, B.R., and Syvertsen, J.P. (2003). Leaf chlorophyll, net gas exchange and chloroplast ultrastructure in citrus leaves of different nitrogen status. Tree Physiology **23,** 553-559.

Boothe, J., Nykiforuk, C., Shen, Y., Zaplachinski, S., Szarka, S., Kuhlman, P., Murray, E., Morck, D., and Moloney, M.M. (2010). Seed-based expression systems for plant molecular farming. Plant Biotechnol. J. **8,** 588-606.

Brehelin, C., and Kessler, F. (2008). The Plastoglobule: A Bag Full of Lipid Biochemistry Tricks. Photochem. Photobiol. **84,** 1388-1394.

Brehelin, C., Kessler, F., and van Wijk, K.J. (2007). Plastoglobuies: versatile lipoprotein particles in plastids. Trends Plant Sci. **12,** 260-266.

Briggs, W.R., and Christie, J.M. (2002). Phototropins 1 and 2: versatile plant blue-light receptors. Trends Plant Sci. **7,** 204-210.

Castelfranco, P.A., and Jones, O.T.G. (1975). Protoheme turnover and chlorophyll synthesis in greening barley tissue. Plant Physiol. **55,** 485-490.

Chamovitz, D.A., Wei, N., Osterlund, M.T., vonArnim, A.G., Staub, J.M., Matsui, M., and Deng, X.W. (1996). The COP9 complex, a novel multisubunit nuclear regulator involved in light control of a plant developmental switch. Cell **86,** 115-121.

Chen, H.C., Klein, A., Xiang, M.H., Backhaus, R.A., and Kuntz, M. (1998). Drought- and wound-induced expression in leaves of a gene encoding a chromoplast carotenoid-associated protein. Plant J. **14,** 317-326.

Chen, J.J., Yang, J.M., Petryshyn, R., Kosower, N., and London, I.M. (1989). Disulfide bond formation in the regulation of eIF-2-alpha-kinase by heme. J. Biol. Chem. **264,** 9559-9564.

Chory, J. (1992). A genetic model for light-regulated seedling development in arabidopsis. Development **115,** 337-354.

Chory, J. (1993). Out of darkness - mutants reveal pathways controlling light-regulated development in plants. Trends Genet. **9,** 167-172.

Chory, J., Peto, C., Feinbaum, R., Pratt, L., and Ausubel, F. (1989). Arabidopsis thaliana mutant that develops as a light-grown plant in the absence of light. Cell **58,** 991-999.

Clough, S.J., and Bent, A.F. (1998). Floral dip: a simplified method for Agrobacterium-mediated transformation of Arabidopsis thaliana. Plant J. **16,** 735-743.

Conley, A.J., Joensuu, J.J., Jevnikar, A.M., Menassa, R., and Brandle, J.E. (2009). Optimization of Elastin-Like Polypeptide Fusions for Expression and Purification of Recombinant Proteins in Plants. Biotechnology and Bioengineering **103,** 562-573.

Cornah, J.E., Terry, M.J., and Smith, A.G. (2003). Green or red: what stops the traffic in the tetrapyrrole pathway? Trends Plant Sci. **8,** 224-230.

Corneille, S., Lutz, K., Svab, Z., and Maliga, P. (2001). Efficient elimination of selectable marker genes from the plastid genome by the CRE-lox site-specific recombination system. Plant J. **27,** 171-178.

Daniell, H., Singh, N.D., Mason, H., and Streatfield, S.J. (2009). Plant-made vaccine antigens and biopharmaceuticals. Trends Plant Sci. **14,** 669-679.

Davis, S.J., Kurepa, J., and Vierstra, R.D. (1999). The Arabidopsis thaliana HY1 locus, required for phytochrome-chromophore biosynthesis, encodes a protein related to heme oxygenases. Proc. Natl. Acad. Sci. U. S. A. **96,** 6541-6546.

Davis, S.J., Bhoo, S.H., Durski, A.M., Walker, J.M., and Vierstra, R.D. (2001). The heme-oxygenase family required for phytochrome chromophore biosynthesis is necessary for proper photomorphogenesis in higher plants. Plant Physiol. **126,** 656-669.

De Cosa, B., Moar, W., Lee, S.B., Miller, M., and Daniell, H. (2001). Overexpression of the Bt cry2Aa2 operon in chloroplasts leads to formation of insecticidal crystals. Nat. Biotechnol. **19,** 71-74.

De Marchis, F., Pompa, A., Mannucci, R., Morosinotto, T., and Bellucci, M. (2011). A plant secretory signal peptide targets plastome-encoded recombinant proteins to the thylakoid membrane. Plant Mol.Biol. **76,** 427-441.

de Virgilio, M., De Marchis, F., Bellucci, M., Mainieri, D., Rossi, M., Benvenuto, E., Arcioni, S., and Vitale, A. (2008). The human immunodeficiency virus antigen Nef forms protein bodies in leaves of transgenic tobacco when fused to zeolin. J. Exp. Bot. **59,** 2815-2829.

Deng, X.W., and Quail, P.H. (1992). Genetic and phenotypic characterization of cop-1 mutants of arabidopsis thaliana. Plant J. **2,** 83-95.

Deng, X.W., Caspar, T., and Quail, P.H. (1991). COP1 - A regulatory locus involved in light-controlled development and gene-expression in arabidopsis. Genes Dev. **5,** 1172-1182.

Deruere, J., Bouvier, F., Steppuhn, J., Klein, A., Camara, B., and Kuntz, M. (1994). Structure and expression of 2 plant genes encoding chromoplast-specific proteins - occurrence of partially spliced transcripts (VOL 199, PG 1144, 1994). Biochem. Biophys. Res. Commun. **201,** 486-486.

Dias, J.S., Macedo, A.L., Ferreira, G.C., Peterson, F.C., Volkman, B.F., and Goodfellow, B.J. (2006). The first structure from the SOUL/HBP family of heme-binding proteins, murine P22HBP. J. Biol. Chem. **281,** 31553-31561.

Do, T.Q., Hsu, A.Y., Jonassen, T., Lee, P.T., and Clarke, C.F. (2001). A defect in coenzyme Q biosynthesis is responsible for the respiratory deficiency in Saccharomyces cerevisiae abc1 mutants. J. Biol. Chem. **276,** 18161-18168.

Doyle, J.J., and Doyle, J.L. (1990). Isolation of plant DNA from fresh tissues. Focus **12**.

Elmowalid, G.A., Qiao, M., Jeong, S.H., Borg, B.B., Baumert, T.F., Sapp, R.K., Hu, Z.Y., Murthy, K., and Liang, T.J. (2007). Immunization with hepatitis C virus-like particles results in control of hepatitis C virus infection in chimpanzees. Proc. Natl. Acad. Sci. U. S. A. **104,** 8427-8432.

Eymery, F., and Rey, P. (1999). Immunocytolocalization of CDSP 32 and CDSP 34, two chloroplastic drought-induced stress proteins in Solanum tuberosum plants. Plant Physiology and Biochemistry **37,** 305-312.

Fitzpatrick, L.M., and Keegstra, K. (2001). A method for isolating a high yield of Arabidopsis chloroplasts capable of efficient import of precursor proteins. Plant J. **27,** 59-65.

Gaude, N., Brehelin, C., Tischendorf, G., Kessler, F., and Dormann, P. (2007). Nitrogen deficiency in Arabidopsis affects galactolipid composition and gene expression and results in accumulation of fatty acid phytyl esters. Plant J. **49,** 729-739.

Gillet, B., Beyly, A., Peltier, G., and Rey, P. (1998). Molecular characterization of CDSP 34, a chloroplastic protein induced by water deficit in Solanum tuberosum L. plants, and regulation of CDSP 34 expression by ABA and high illumination. Plant J. **16,** 257-262.

Gisby, M.F., Mellors, P., Madesis, P., Ellin, M., Laverty, H., O'Kane, S., Ferguson, M.W.J., and Day, A. (2011). A synthetic gene increases TGF beta 3 accumulation by 75-fold intobacco chloroplasts enabling rapid purification and folding into a biologically active molecule. Plant Biotechnol. J. **9,** 618-628.

Glenz, K., Bouchon, B., Stehle, T., Wallich, R., Simon, M.M., and Warzecha, H. (2006). Production of a recombinant bacterial lipoprotein in higher plant chloroplasts. Nat. Biotechnol. **24,** 76-77.

Gonzalez-Rabade, N., McGowan, E.G., Zhou, F., McCabe, M.S., Bock, R., Dix, P.J., Gray, J.C., and Ma, J.K.C. (2011). Immunogenicity of chloroplast-derived HIV-1 p24 and a p24-Nef fusion protein following subcutaneous and oral administration in mice. Plant Biotechnol. J. **9,** 629-638.

Guarente, L., and Mason, T. (1983). Heme regulates transcription of the CYC1 gene of S. cerevisiae via an upstream activation site. Cell **32,** 1279-1286.

Hanke, T., and McMichael, A.J. (2000). Design and construction of an experimental HIV-1 vaccine for a year-2000 clinical trial in Kenya. Nat. Med. **6,** 951-955.

Hiltbrunner, A., Bauer, J., Vidi, P.A., Infanger, S., Weibel, P., Hohwy, M., and Kessler, F. (2001). Targeting of an abundant cytosolic form of the protein import receptor at Toc159 to the outer chloroplast membrane. J. Cell Biol. **154,** 309-316.

Hortensteiner, S. (2006). Chlorophyll degradation during senescence. In Annual Review of Plant Biology (Palo Alto: Annual Reviews), pp. 55-77.

Hortensteiner, S., and Krautler, B. (2011). Chlorophyll breakdown in higher plants. Biochim. Biophys. Acta-Bioenerg. **1807,** 977-988.

Huang, F.C., Molnar, P., and Schwab, W. (2009). Cloning and functional characterization of carotenoid cleavage dioxygenase 4 genes. J. Exp. Bot. **60,** 3011-3022.

Humbert, N., Zocchi, A., and Ward, T.R. (2005). Electrophoretic behavior of streptavidin complexed to a biotinylated probe: A functional screening assay for biotin-binding proteins. Electrophoresis **26,** 47-52.

Inoue, H., Nojima, H., and Okayama, H. (1990). High-efficiency transformation of escherichia-coli with plasmids. Gene **96,** 23-28.

Ischebeck, T., Zbierzak, A.M., Kanwischer, M., and Dormann, P. (2006). A salvage pathway for phytol metabolism in Arabidopsis. J. Biol. Chem. **281,** 2470-2477.

Jaquinod, M., Villiers, F., Kieffer-Jaquinod, S., Hugouvieu, V., Bruley, C., Garin, J., and Bourguignon, J. (2007). A proteomics dissection of Arabidopsis thaliana vacuoles isolated from cell culture. Mol. Cell. Proteomics **6,** 394-412.

Jarvis, P., Dormann, P., Peto, C.A., Lutes, J., Benning, C., and Chory, J. (2000). Galactolipid deficiency and abnormal chloroplast development in the Arabidopsis MGD synthase 1 mutant. Proc. Natl. Acad. Sci. U. S. A. **97,** 8175-8179.

Joensuu, J.J., Conley, A.J., Lienemann, M., Brandle, J.E., Linder, M.B., and Menassa, R. (2010). Hydrophobin Fusions for High-Level Transient Protein Expression and Purification in Nicotiana benthamiana. Plant Physiol. **152,** 622-633.

Jones, A.M.E., Bennett, M.H., Mansfield, J.W., and Grant, M. (2006). Analysis of the defence phosphoproteome of Arabidopsis thaliana using differential mass tagging. Proteomics **6,** 4155-4165.

Joshi, B., Morley, S.J., Rhoads, R.E., and Pain, V.M. (1995). Inhibition of protein-synthesis by the heme-controlled eIF-2-alpha kinase leads to the appearance of mRNA-containing 48S complexes that contain eIF-4E but lack methionyl-tRNA(f). Eur. J. Biochem. **228,** 31-38.

Kabeya, Y., Nakanishi, H., Suzuki, K., Ichikawa, T., Kondou, Y., Matsui, M., and Miyagishima, S. (2010). The YlmG protein has a conserved function related to the distribution of nucleoids in chloroplasts and cyanobacteria. Bmc Plant Biology **10**.

Kazan, K., and Manners, J.M. (2011). The interplay between light and jasmonate signalling during defence and development. J. Exp. Bot. **62,** 4087-4100.

Kessler, F., and Schnell, D. (2009). Chloroplast biogenesis: diversity and regulation of the protein import apparatus. Curr. Opin. Cell Biol. **21,** 494-500.

Kessler, F., Schnell, D., and Blobel, G. (1999). Identification of proteins associated with plastoglobules isolated from pea (Pisum sativum L.) chloroplasts. Planta **208,** 107-113.

Khanna, R., Shen, Y., Toledo-Ortiz, G., Kikis, E.A., Johannesson, H., Hwang, Y.S., and Quail, P.H. (2006). Functional profiling reveals that only a small number of phytochrome-regulated early-response genes in Arabidopsis are necessary for optimal deetiolation. Plant Cell **18,** 2157-2171.

Kikuchi, S., Hirohashi, T., and Nakai, M. (2006). Characterization of the preprotein translocon at the outer envelope membrane of chloroplasts by blue native PAGE. Plant Cell Physiol. **47,** 363-371.

Kim, H.U., Wu, S.S.H., Ratnayake, C., and Huang, A.H.C. (2001). Brassica rapa has three genes that encode proteins associated with different neutral lipids in plastids of specific tissues. Plant Physiol. **126,** 330-341.

Kohchi, T., Mukougawa, K., Frankenberg, N., Masuda, M., Yokota, A., and Lagarias, J.C. (2001). The arabidopsis HY2 gene encodes phytochromobilin synthase, a ferredoxin-dependent biliverdin reductase. Plant Cell **13,** 425-436.

Kuroda, H., and Maliga, P. (2001). Complementarity of the 16S rRNA penultimate stem with sequences downstream of the AUG destabilizes the plastid mRNAs. Nucleic Acids Research **29,** 970-975.

Landy, A. (1989). Dynamic, structural, and regulatory aspects of lambda-site-specific recombination. Annu. Rev. Biochem. **58,** 913-949.

Langenkamper, G., Manac'h, N., Broin, M., Cuine, S., Becuwe, N., Kuntz, M., and Rey, P. (2001). Accumulation of plastid lipid-associated proteins (fibrillin/CDSP34) upon oxidative stress, ageing and biotic stress in Solanaceae and in response to drought in other species. J. Exp. Bot. **52,** 1545-1554.

Larkin, R.M., Alonso, J.M., Ecker, J.R., and Chory, J. (2003). GUN4, a regulator of chlorophyll synthesis and intracellular signaling. Science **299,** 902-906.

Lathrop, J.T., and Timko, M.P. (1993). Regulation by heme of mitochondrial protein-transport through a conserved amino-acid motif. Science **259,** 522-525.

Lichtenthaler, Hk. (1968). Distribution and relative concentrations of lipophilic plastid quinones in green plants. Planta **81,** 140-&.

Lichtenthaler, H.K. (2007). Biosynthesis, accumulation and emission of carotenoids, alpha-tocopherol, plastoquinone, and isoprene in leaves under high photosynthetic irradiance. Photosynth. Res. **92,** 163-179.

Lin, C.T. (2000). Plant blue-light receptors. Trends Plant Sci. **5,** 337-342.

Lippold, F., vom Dorp, K., Abraham, M., Hölzl, G., Wewer, V., Yilmaz, J.L., Lager, I., Montandon, C., Besagni, C., Kessler, F., Stymne, S., and Dörmann, P. (2012). Fatty Acid Phytyl Ester Synthesis in Chloroplasts of Arabidopsis. The Plant Cell Online.

Locy, R.D., Chang, C.C., Nielsen, B.L., and Singh, N.K. (1996). Photosynthesis in salt-adapted heterotrophic tobacco cells and regenerated plants. Plant Physiol. **110,** 321-328.

Lopez-Juez, E., and Pyke, K.A. (2005). Plastids unleashed: their development and their integration in plant development. Int. J. Dev. Biol. **49,** 557-577.

Lorrain, S., Allen, T., Duek, P.D., Whitelam, G.C., and Fankhauser, C. (2008). Phytochrome-mediated inhibition of shade avoidance involves degradation of growth-promoting bHLH transcription factors. Plant J. **53,** 312-323.

Lundquist, P., Poliakov, A., Bhuiyan, N.H., Zybailov, B., Sun, Q., and van Wijk, K.J. (2012). The functional network of the Arabidopsis thaliana plastoglobule proteome based on quantitative proteomics and genome-wide co-expression analysis. Plant Physiol.

Ma, J.K.C., Barros, E., Bock, R., Christou, P., Dale, P.J., Dix, P.J., Fischer, R., Irwin, J., Mahoney, R., Pezzotti, M., Schillberg, S., Sparrow, P., Stoger, E., Twyman, R.M., and European Union Framework, P. (2005). Molecular farming for new drugs and vaccines - Current perspectives on the production of pharmaceuticals in transgenic plants. Embo Reports **6,** 593-599.

Madesis, P., Osathanunkul, M., Georgopoulou, U., Gisby, M.F., Mudd, E.A., Nianiou, I., Tsitoura, P., Mavromara, P., Tsaftaris, A., and Day, A. (2010). A hepatitis C virus core polypeptide expressed in chloroplasts detects anti-core antibodies in infected human sera. Journal of Biotechnology **145,** 377-386.

Maliga, P. (2004). Plastid transformation in higher plants. Annual Review of Plant Biology **55,** 289-313.

Maliga, P., and Bock, R. (2011). Plastid Biotechnology: Food, Fuel, and Medicine for the 21st Century. Plant Physiol. **155,** 1501-1510.

Matsumoto, F., Obayashi, T., Sasaki-Sekimoto, Y., Ohta, H., Takamiya, K., and Masuda, T. (2004). Gene expression profiling of the tetrapyrrole metabolic pathway in Arabidopsis with a mini-array system. Plant Physiol. **135,** 2379-2391.

McCabe, M.S., Klaas, M., Gonzalez-Rabade, N., Poage, M., Badillo-Corona, J.A., Zhou, F., Karcher, D., Bock, R., Gray, J.C., and Dix, P.J. (2008). Plastid transformation of high-biomass tobacco variety Maryland Mammoth for production of human immunodeficiency virus type 1 (HIV-1) p24 antigen. Plant Biotechnol. J. **6,** 914-929.

Menassa, R., Nguyen, V., Jevnikar, A., and Brandle, J. (2001). A self-contained system for the field production of plant recombinant interleukin-10. Molecular Breeding **8,** 177-185.

Merchant, S.S., Prochnik, S.E., Vallon, O., Harris, E.H., Karpowicz, S.J., Witman, G.B., Terry, A., Salamov, A., Fritz-Laylin, L.K., Marechal-Drouard, L., Marshall, W.F., Qu, L.H., Nelson, D.R., Sanderfoot, A.A., Spalding, M.H., Kapitonov, V.V., Ren, Q.H., Ferris, P., Lindquist, E., Shapiro, H., Lucas, S.M., Grimwood, J., Schmutz, J., Cardol, P., Cerutti, H., Chanfreau, G., Chen, C.L., Cognat, V., Croft, M.T., Dent, R., Dutcher, S., Fernandez, E., Fukuzawa, H., Gonzalez-Ballester, D., Gonzalez-Halphen, D., Hallmann, A., Hanikenne, M., Hippler, M., Inwood, W., Jabbari, K., Kalanon, M., Kuras, R., Lefebvre, P.A., Lemaire, S.D., Lobanov, A.V., Lohr, M., Manuell, A., Meir, I., Mets, L., Mittag, M., Mittelmeier, T., Moroney, J.V., Moseley, J., Napoli, C., Nedelcu, A.M., Niyogi, K., Novoselov, S.V., Paulsen, I.T., Pazour, G., Purton, S., Ral, J.P., Riano-Pachon, D.M., Riekhof, W., Rymarquis, L., Schroda, M., Stern, D., Umen, J., Willows, R., Wilson, N., Zimmer, S.L., Allmer, J., Balk, J., Bisova, K., Chen, C.J., Elias, M., Gendler, K., Hauser, C., Lamb, M.R., Ledford, H., Long, J.C., Minagawa, J., Page, M.D., Pan, J.M., Pootakham, W., Roje, S., Rose, A., Stahlberg, E., Terauchi, A.M., Yang, P.F., Ball, S., Bowler, C., Dieckmann, C.L., Gladyshev, V.N., Green, P., Jorgensen, R., Mayfield, S., Mueller-Roeber, B., Rajamani, S., Sayre, R.T., Brokstein, P., Dubchak, I., Goodstein, D., Hornick, L., Huang, Y.W., Jhaveri, J., Luo, Y.G., Martinez, D., Ngau, W.C.A., Otillar, B., Poliakov, A., Porter, A., Szajkowski, L., Werner, G., Zhou, K.M., Grigoriev, I.V., Rokhsar, D.S., Grossman, A.R., Chlamydomonas, A., and Team, J.G.I.A. (2007). The Chlamydomonas genome reveals the evolution of key animal and plant functions. Science **318,** 245-251.

Meskauskiene, R., Nater, M., Goslings, D., Kessler, F., den Camp, R.O., and Apel, K. (2001). FLU: A negative regulator of chlorophyll biosynthesis in Arabidopsis thaliana. Proc. Natl. Acad. Sci. U. S. A. **98,** 12826-12831.

Mochizuki, N., Tanaka, R., Grimm, B., Masuda, T., Moulin, M., Smith, A.G., Tanaka, A., and Terry, M.J. (2010). The cell biology of tetrapyrroles: a life and death struggle. Trends Plant Sci. **15,** 488-498.

Moradpour, D., Penin, F., and Rice, C.M. (2007). Replication of hepatitis C virus. Nature Reviews Microbiology **5,** 453-463.

Muramoto, T., Kohchi, T., Yokota, A., Hwang, I.H., and Goodman, H.M. (1999). The Arabidopsis photomorphogenic mutant hy1 is deficient in phytochrome chromophore biosynthesis as a result of a mutation in a plastid heme oxygenase. Plant Cell **11,** 335-347.

Murashige, T., and Skoog, F. (1962). A revised medium for rapid growth and bio assays with tobacco tissue cultures. Physiol. Plant. **15,** 473-497.

Mustilli, A.C., Fenzi, F., Ciliento, R., Alfano, F., and Bowler, C. (1999). Phenotype of the tomato high pigment-2 mutant is caused by a mutation in the tomato homolog of DEETIOLATED1. Plant Cell **11,** 145-157.

Nordby, H.E., and Yelenosky, G. (1985). Change in citrus leaf lipids during freeze-thaw stress. Phytochemistry **24,** 1675-1679.

Nott, A., Jung, H.S., Koussevitzky, S., and Chory, J. (2006). Plastid-to-nucleus retrograde signaling. In Annual Review of Plant Biology (Palo Alto: Annual Reviews), pp. 739-759.

Obregon, P., Chargelegue, D., Drake, P.M.W., Prada, A., Nuttall, J., Frigerio, L., and Ma, J.K.C. (2006). HIV-1 p24-immunoglobulin fusion molecule: a new strategy for plant-based protein production. Plant Biotechnol. J. **4,** 195-207.

Oey, M., Lohse, M., Kreikemeyer, B., and Bock, R. (2009). Exhaustion of the chloroplast protein synthesis capacity by massive expression of a highly stable protein antibiotic. Plant J. **57,** 436-445.

Ogrzewalla, K., Piotrowski, M., Reinbothe, S., and Link, G. (2002). The plastid transcription kinase from mustard (Sinapis alba L.) - A nuclear-encoded CK2-type chloroplast enzyme with redox-sensitive function. Eur. J. Biochem. **269,** 3329-3337.

Papenbrock, J., Mock, H.P., Kruse, E., and Grimm, B. (1999). Expression studies in tetrapyrrole biosynthesis: inverse maxima of magnesium chelatase and ferrochelatase activity during cyclic photoperiods. Planta **208,** 264-273.

Parmenter, D.L., Boothe, J.G., vanRooijen, G.J.H., Yeung, E.C., and Moloney, M.M. (1995). Production of biologically active hirudin in plant seeds using oleosin partitioning. Plant Mol.Biol. **29,** 1167-1180.

Peltier, J.B., Ytterberg, A.J., Sun, Q., and van Wijk, K.J. (2004). New functions of the thylakoid membrane proteome of Arabidopsis thaliana revealed by a simple, fast, and versatile fractionation strategy. J. Biol. Chem. **279,** 49367-49383.

Peltier, J.B., Cai, Y., Sun, Q., Zabrouskov, V., Giacomelli, L., Rudella, A., Ytterberg, A.J., Rutschow, H., and van Wijk, K.J. (2006). The oligomeric stromal proteome of Arabidopsis thaliana chloroplasts. Mol. Cell. Proteomics **5,** 114-133.

Perez-Filgueira, D.M., Brayfield, B.P., Phiri, S., Borca, M.V., Wood, C., and Morris, T.J. (2004). Preserved antigenicity of HIV-1 p24 produced and purified in high yields from plants inoculated with a tobacco mosaic virus (TMV)-derived vector. Journal of Virological Methods **121,** 201-208.

Pfannschmidt, T. (2010). Plastidial retrograde signalling - a true "plastid factor" or just metabolite signatures? Trends Plant Sci. **15,** 427-435.

Piffanelli, P., and Murphy, D.J. (1998). Novel organelles and targeting mechanisms in the anther tapetum. Trends Plant Sci. **3,** 250-253.

Piller, L.E., Besagni, C., Ksas, B., Rumeau, D., Brehelin, C., Glauser, G., Kessler, F., and Havaux, M. (2011). Chloroplast lipid droplet type II NAD(P)H quinone oxidoreductase is essential for prenylquinone metabolism and vitamin K-1 accumulation. Proc. Natl. Acad. Sci. U. S. A. **108,** 14354-14359.

Pogson, B.J., and Albrecht, V. (2011). Genetic Dissection of Chloroplast Biogenesis and Development: An Overview. Plant Physiol. **155,** 1545-1551.

Pogson, B.J., Woo, N.S., Forster, B., and Small, I.D. (2008). Plastid signalling to the nucleus and beyond. Trends Plant Sci. **13,** 602-609.

Poon, W.W., Davis, D.E., Ha, H.T., Jonassen, T., Rather, P.N., and Clarke, C.F. (2000). Identification of Escherichia coli ubiB, a gene required for the first monooxygenase step in ubiquinone biosynthesis. J. Bacteriol. **182,** 5139-5146.

Porfirova, S., Bergmuller, E., Tropf, S., Lemke, R., and Dormann, P. (2002). Isolation of an Arabidopsis mutant lacking vitamin E and identification of a cyclase essential for all tocopherol biosynthesis. Proc. Natl. Acad. Sci. U. S. A. **99,** 12495-12500.

PozuetaRomero, J., Rafia, F., Houlne, G., Cheniclet, C., Carde, J.P., Schantz, M.L., and Schantz, R. (1997). A ubiquitous plant housekeeping gene, PAP, encodes a major protein component of bell pepper chromoplasts. Plant Physiol. **115,** 1185-1194.

Protchenko, O., Shakoury-Elizeh, M., Keane, P., Storey, J., Androphy, R., and Philpott, C.C. (2008). Role of PUG1 in inducible porphyrin and heme transport in Saccharomyces cerevisiae. Eukaryot. Cell **7,** 859-871.

Pruvot, G., Massimino, J., Peltier, G., and Rey, P. (1996). Effects of low temperature, high salinity and exogenous ABA on the synthesis of two chloroplastic drought-induced proteins in Solanum tuberosum. Physiol. Plant. **97,** 123-131.

Quail, P.H. (2002). Phytochrome photosensory signalling networks. Nat. Rev. Mol. Cell Biol. **3,** 85-93.

Reiland, S., Messerli, G., Baerenfaller, K., Gerrits, B., Endler, A., Grossmann, J., Gruissem, W., and Baginsky, S. (2009). Large-Scale Arabidopsis Phosphoproteome Profiling Reveals Novel Chloroplast Kinase Substrates and Phosphorylation Networks. Plant Physiol. **150,** 889-903.

Rey, P., Gillet, B., Romer, S., Eymery, F., Massimino, J., Peltier, G., and Kuntz, M. (2000). Over-expression of a pepper plastid lipid-associated protein intobacco leads to changes in plastid ultrastructure and plant development upon stress. Plant J. **21,** 483-494.

Rigaut, G., Shevchenko, A., Rutz, B., Wilm, M., Mann, M., and Seraphin, B. (1999). A generic protein purification method for protein complex characterization and proteome exploration. Nat. Biotechnol. **17,** 1030-1032.

Robertson, B., Myers, G., Howard, C., Brettin, T., Bukh, J., Gaschen, B., Gojobori, T., Maertens, G., Mizokami, M., Nainan, O., Netesov, S., Nishioka, K., Shin-i, T., Simmonds, P., Smith, D., Stuyver, L., and Weiner, A. (1998). Classification, nomenclature, and database development for hepatitis C virus (HCV) and related viruses: proposals for standardization. Arch. Virol. **143,** 2493-2503.

Rockwell, N.C., Su, Y.S., and Lagarias, J.C. (2006). Phytochrome structure and signaling mechanisms. In Annual Review of Plant Biology (Palo Alto: Annual Reviews), pp. 837-858.

Ruf, S., Hermann, M., Berger, I.J., Carrer, H., and Bock, R. (2001). Stable genetic transformation of tomato plastids and expression of a foreign protein in fruit. Nat. Biotechnol. **19,** 870-875.

Salinas, P., Fuentes, D., Vidal, E., Jordana, X., Echeverria, M., and Holuigue, L. (2006). An extensive survey of CK2 alpha and beta subunits in Arabidopsis: Multiple isoforms exhibit differential subcellular localization. Plant Cell Physiol. **47,** 1295-1308.

Sambrook J, Russel D (2001). Molecular cloning: a laboratory manual, New-York.

Sato, E., Sagami, I., Uchida, T., Sato, A., Kitagawa, T., Igarashi, J., and Shimizu, T. (2004). SOUL in mouse eyes is a new hexameric heme-binding protein with characteristic optical absorption, resonance Raman spectral, and heme-binding properties. Biochemistry **43,** 14189-14198.

Schagger, H., Cramer, W.A., and Vonjagow, G. (1994). Analysis of molecular masses and oligomeric states of protein complexes by blue native electrophoresis and isolation of membrane-protein complexes by 2-dimensional native electrophoresis. Anal. Biochem. **217,** 220-230.

Schmidt, M., Gessner, G., Matthias, L., Heiland, I., Wagner, V., Kaminski, M., Geimer, S., Eitzinger, N., Reissenweber, T., Voytsekh, O., Fiedler, M., Mittag, M., and Kreimer, G. (2006). Proteomic analysis of the eyespot of Chlamydomonas reinhardtii provides novel insights into its components and tactic movements. Plant Cell **18,** 1908-1930.

Schneider, S., Marles-Wright, J., Sharp, K.H., and Paoli, M. (2007). Diversity and conservation of interactions for binding heme in b-type heme proteins. Nat. Prod. Rep. **24,** 621-630.

Shan, Y., Lambrecht, R.W., Ghaziani, T., Donohue, S.E., and Bonkovsky, H.L. (2004). Role of Bach-1 in regulation of heme oxygenase-1 in human liver cells - Insights from studies with small interfering RNAs. J. Biol. Chem. **279,** 51769-51774.

Shin, J., Kim, K., Kang, H., Zulfugarov, I.S., Bae, G., Lee, C.H., Lee, D., and Choi, G. (2009). Phytochromes promote seedling light responses by inhibiting four negatively-acting phytochrome-interacting factors. Proc. Natl. Acad. Sci. U. S. A. **106,** 7660-7665.

Singh, D.K., and McNellis, T.W. (2011). Fibrillin protein function: the tip of the iceberg? Trends Plant Sci. **16,** 432-441.

Singh, D.P., Cornah, J.E., Hadingham, S., and Smith, A.G. (2002). Expression analysis of the two ferrochelatase genes in Arabidopsis in different tissues and under stress conditions reveals their different roles in haem biosynthesis. Plant Mol.Biol. **50,** 773-788.

Singh, N.D., Li, M., Lee, S.B., Schnell, D., and Daniell, H. (2008). Arabidopsis Tic40 Expression intobacco Chloroplasts Results in Massive Proliferation of the Inner Envelope Membrane and Upregulation of Associated Proteins. Plant Cell **20,** 3405-3417.

Smith, A.G., Santana, M.A., Wallacecook, A.D.M., Roper, J.M., and Labbebois, R. (1994). Isolation of a cDNA-encoding chloroplast ferrochelatase from arabidopsis-thaliana by functional complementation of a yeast mutant. J. Biol. Chem. **269,** 13405-13413.

Smith, M.D., Hiltbrunner, A., Kessler, F., and Schnell, D.J. (2002). The targeting of the atToc159 preprotein receptor to the chloroplast outer membrane is mediated by its GTPase domain and is regulated by GTP. J. Cell Biol. **159,** 833-843.

Stephenson, P.G., and Terry, M.J. (2008). Light signalling pathways regulating the Mg-chelatase branchpoint of chlorophyll synthesis during de-etiolation in Arabidopsis thaliana. Photochem. Photobiol. Sci. **7,** 1243-1252.

Sun, J.Y., Brand, M., Zenke, Y., Tashiro, S., Groudine, M., and Igarashi, K. (2004). Heme regulates the dynamic exchange of Bach1 and NF-E2-related factors in the Maf transcription factor network. Proc. Natl. Acad. Sci. U. S. A. **101,** 1461-1466.

Susek, R.E., Ausubel, F.M., and Chory, J. (1993). Signal-transduction mutants of arabidopsis uncouple nuclear *CAB* and *RBCS* gene-expression from chloroplast development. Cell **74,** 787-799.

Suzuki, G., Yanagawa, Y., Kwok, S.F., Matsui, M., and Deng, X.W. (2002). Arabidopsis COP10 is a ubiquitin-conjugating enzyme variant that acts together with COP1 and the COP9 signalosome in repressing photomorphogenesis. Genes Dev. **16,** 554-559.

Svab, Z., and Maliga, P. (1993). High-frequency plastid transformation intobacco by selection for a chimeric *aadA* gene. Proc. Natl. Acad. Sci. U. S. A. **90,** 913-917.

Svab, Z., Hajdukiewicz, P., and Maliga, P. (1990). Stable transformation of plastids in higher-plants. Proc. Natl. Acad. Sci. U. S. A. **87,** 8526-8530.

Takahashi, S., Ogawa, T., Inoue, K., and Masuda, T. (2008). Characterization of cytosolic tetrapyrrole-binding proteins in Arabidopsis thaliana. Photochem. Photobiol. Sci. **7,** 1216-1224.

Tanaka, R., and Tanaka, A. (2007). Tetrapyrrole biosynthesis in higher plants. In Annual Review of Plant Biology (Palo Alto: Annual Reviews), pp. 321-346.

Tanaka, R., Kobayashi, K., and Masuda, T. (2011). Tetrapyrrole Metabolism in Arabidopsis thaliana. The Arabidopsis book / American Society of Plant Biologists **9,** e0145.

Tang, X.D., Xu, R., Reynolds, M.F., Garcia, M.L., Heinemann, S.H., and Hoshi, T. (2003). Haem can bind to and inhibit mammalian calcium-dependent Slo1 BK channels. Nature **425,** 531-535.

Targett-Adams, P., Chambers, D., Gledhill, S., Hope, R.G., Coy, J.F., Girod, A., and McLauchlan, J. (2003). Live cell analysis and targeting of the lipid droplet-binding adipocyte differentiation-related protein. J. Biol. Chem. **278,** 15998-16007.

Tepperman, J.M., Hwang, Y.S., and Quail, P.H. (2006). phyA dominates in transduction of red-light signals to rapidly responding genes at the initiation of Arabidopsis seedling de-etiolation. Plant J. **48,** 728-742.

Terry, M.J. (1997). Phytochrome chromophore-deficient mutants. Plant Cell Environ. **20,** 740-745.

Terry, M.J., Linley, P.J., and Kohchi, T. (2002). Making light of it: the role of plant haem oxygenases in phytochrome chromophore synthesis. Biochem. Soc. Trans. **30,** 604-609.

Tissot, G., Canard, H., Nadai, M., Martone, A., Botterman, J., and Dubald, M. (2008). Translocation of aprotinin, a therapeutic protease inhibitor, into the thylakoid lumen of genetically engineered tobacco chloroplasts. Plant Biotechnol. J. **6,** 309-320.

Tregoning, J.S., Nixon, P., Kuroda, H., Svab, Z., Clare, S., Bowe, F., Fairweather, N., Ytterberg, J., van Wijk, K.J., Dougan, G., and Maliga, P. (2003). Expression of tetanus toxin Fragment C intobacco chloroplasts. Nucleic Acids Research **31,** 1174-1179.

Vanhee, C., Zapotoczny, G., Masquelier, D., Ghislain, M., and Batoko, H. (2011). The Arabidopsis Multistress Regulator TSPO Is a Heme Binding Membrane Protein and a Potential Scavenger of Porphyrins via an Autophagy-Dependent Degradation Mechanism. Plant Cell **23,** 785-805.

Vanrooijen, G.J.H., and Moloney, M.M. (1995). Plant seed oil-bodies as carriers for foreign proteins. Bio-Technology **13,** 72-77.

Vidi, P.A., Kessler, F., and Brehelin, C. (2007). Plastoglobules: a new address for targeting recombinant proteins in the chloroplast. Bmc Biotechnology **7**.

Vidi, P.A., Kanwischer, M., Baginsky, S., Austin, J.R., Csucs, G., Dormann, P., Kessler, F., and Brehelin, C. (2006). Tocopherol cyclase (VTE1) localization and vitamin E accumulation in chloroplast plastoglobule lipoprotein particles. J. Biol. Chem. **281,** 11225-11234.

Vinti, G., Fourrier, N., Bowyer, J.R., and Lopez-Juez, E. (2005). Arabidopsis cue mutants with defective plastids are impaired primarily in the photocontrol of expression of photosynthesis-associated nuclear genes. Plant Mol.Biol. **57,** 343-357.

Vishnevetsky, M., Ovadis, M., and Vainstein, A. (1999). Carotenoid sequestration in plants: the role of carotenoid-associated proteins. Trends Plant Sci. **4,** 232-235.

von Gromoff, E.D., Alawady, A., Meinecke, L., Grimm, B., and Beck, C.F. (2008). Heme, a plastid-derived regulator of nuclear gene expression in Chlamydomonas. Plant Cell **20,** 552-567.

Voss, B., Meinecke, L., Kurz, T., Al-Babili, S., Beck, C.F., and Hess, W.R. (2011). Hemin and Magnesium-Protoporphyrin IX Induce Global Changes in Gene Expression in Chlamydomonas reinhardtii. Plant Physiol. **155,** 892-905.

Waters M, Pyke K. (2004). Plastid development and differentiation. In Plastids, S.G. Møller, ed. Plastids, ed (Oxford, UK, Blackwell Publishing), pp. 30–59.

Wagner, V., Ullmann, K., Mollwo, A., Kaminski, M., Mittag, M., and Kreimer, G. (2008). The phosphoproteome of a Chlamydomonas reinhardtii eyespot fraction includes key proteins of the light signaling pathway. Plant Physiol. **146,** 772-788.

Weston, E.L., and Pyke, K.A. (1999). Developmental ultrastructure of cells and plastids in the petals of wallflower (Erysimum cheiri). Ann. Bot. **84,** 763-769.

WHO (2009) World Health Organization statistics. http://www.who.int/gho/en/. last accessed: 16 March 2011.

Wroblewski, T., Tomczak, A., and Michelmore, R. (2005). Optimization of Agrobacterium-mediated transient assays of gene expression in lettuce, tomato and Arabidopsis. Plant Biotechnol. J. **3,** 259-273.

Wurbs, D., Ruf, S., and Bock, R. (2007). Contained metabolic engineering intomatoes by expression of carotenoid biosynthesis genes from the plastid genome. Plant J. **49,** 276-288.

Yamasato, A., Nagata, N., Tanaka, R., and Tanaka, A. (2005). The N-terminal domain of chlorophyllide a oxygenase confers protein instability in response to chlorophyll b accumulation in Arabidopsis. Plant Cell **17,** 1585-1597.

Yang, Y., Sulpice, R., Himmelbach, A., Meinhard, M., Christmann, A., and Grill, E. (2006). Fibrillin expression is regulated by abscisic acid response regulators and is involved in abscisic acid-mediated photoprotection. Proc. Natl. Acad. Sci. U. S. A. **103,** 6061-6066.

Youssef, A., Laizet, Y., Block, M.A., Marechal, E., Alcaraz, J.P., Larson, T.R., Pontier, D., Gaffe, J., and Kuntz, M. (2010). Plant lipid-associated fibrillin proteins condition jasmonate production under photosynthetic stress. Plant J. **61,** 436-445.

Ytterberg, A.J., Peltier, J.B., and van Wijk, K.J. (2006). Protein profiling of plastoglobules in chloroplasts and chromoplasts. A surprising site for differential accumulation of metabolic enzymes. Plant Physiol. **140,** 984-997.

Zhang, G.G., Rodrigues, L., Rovinski, B., and White, K.A. (2002). Production of HIV-1 p24 protein in transgenic tobacco plants. Molecular Biotechnology **20,** 131-136.

Zhou, F., Badillo-Corona, J.A., Karcher, D., Gonzalez-Rabade, N., Piepenburg, K., Borchers, A.-M.I., Maloney, A.P., Kavanagh, T.A., Gray, J.C., and Bock, R. (2008). High-level expression of human immunodeficiency virus antigens from the tobacco and tomato plastid genomes. Plant Biotechnol. J. **6,** 897-913.

Zylka, M.J., and Reppert, S.M. (1999). Discovery of a putative heme-binding protein family (SOUL/HBP) by two-tissue suppression subtractive hybridization and database searches. Brain research. Molecular brain research **74,** 175-181.

ACKNOWLEDGEMENTS

I would like to thank Prof. Dr. Felix Kessler for giving me the opportunity to perform my PhD thesis in his group at the Laboratory of Plant Physiology, University of Neuchatel. Notably, I am deeply grateful for his support and encouragement throughout my thesis work, as well as his enthusiasm, constructive criticism and interesting collaborations.

I would also like to acknowledge Prof. Dr. Jean-Marc Neuhaus, Prof. Dr. Sacha Baginsky and Prof. Dr. Stefan Hörtensteiner as members of my thesis committee.

Special thanks to Dr. Céline Besagni-Andrès and Lucia Eugeni-Piller for grateful discussion and sharing the ideas. I am obliged to for Douet Véronique for technical assistance and taking care of general laboratory things. I am also thankful to Dr. Birgit Agne for her inspiring discussion. I would like to express my gratitude to Dr. Charles Andrès, Meryll, Cyrille, Ashok, and all past and present lab members of LPV for friendly and helpful atmosphere.

I am grateful, too, to Prof. Dr. Ralph bock, Dr. Stephanie Ruf, Dr. Roger Kuhn, Prof. Dr. Jerry Kaplan, Prof. Dr. Bernhard Grimm and Prof. Dr. Christian Fankhauser for kindly providing a space for plastid transformation, strains, plasmid constructs, tetrapyrroles measurement and photomorphogenetic study.

Raghu, Jas, Theju, Pradyu, Rajes, Mathi, Vimal, Justin, Ashok, Senthil, IMBINAS and all my friends for their support and encouragement. Last but not least, I would like to thank my parents, family and Heidi for their love, patience and support in all situations.